

A STATISTICAL AND MECHANICAL
ANALYSIS OF THE MARSHALL SANDSTONE
IN WESTERN MICHIGAN TO DETERMINE
THE ENVIRONMENTAL PATTERN OF THE
DEPOSIT

Thesis for the Degree of M. S.
MICHIGAN STATE COLLEGE
Norbert Wilhelm O'Hara
1954

THESIS



This is to certify that the

thesis entitled

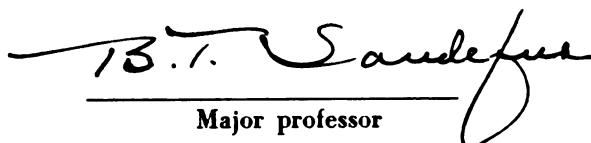
A STATISTICAL AND MECHANICAL ANALYSIS OF
THE MARSHALL SANDSTONE IN WESTERN MICHIGAN TO
DETERMINE THE ENVIRONMENTAL PATTERN OF
THE DEPOSIT

presented by

Norbert W. O'Hara

has been accepted towards fulfillment
of the requirements for

Masters degree in Geology


Major professor

Date June 14, 1954

A STATISTICAL AND MECHANICAL ANALYSIS OF THE MARSHALL
SANDSTONE IN WESTERN MICHIGAN TO DETERMINE THE
ENVIRONMENTAL PATTERN OF THE DEPOSIT

By

NORBERT WILHELM O'HARA

A THESIS

Submitted to the School of Graduate Studies of Michigan
State College of Agriculture and Applied Science
in partial fulfillment of the requirements
for the degree of

MASTER OF SCIENCE

Department of Geology and Geography

1954

THESIS

///

1-23-66
86

ACKNOWLEDGMENTS

The author wishes to express his most sincere thanks to Dr. B. T. Sandefur for his direction, aid, and helpful suggestions throughout this investigation. Also to Dr. W. A. Kelly for his suggestions concerning the choice of the lithologic unit analyzed in this problem.

The writer greatly appreciates the critical and constructive editing of the manuscript by Dr. S. G. Bergquist.

Sincere thanks are also due to Dr. Justin Zinn and Dr. J. W. Trow for their critical review of the manuscript and general assistance. Messrs. R. M. Acker and R. M. Ives of the Michigan State Geological Survey generously helped the author obtain many of the well samples used in this study. Dr. A. D. Perejda is also to be sincerely thanked for his valuable assistance in the preparation of the maps and figures.

ABSTRACT

The use of statistical and mechanical methods of analysis appears to be a means of determining the environmental pattern of a sandstone formation. In attempting to reconstruct the directions of sedimentation and conditions of deposition within the Marshall formation in western Michigan, composite samples from forty wells completely penetrating the formation were analyzed with respect to their roundness, sphericity, and size distributions.

Numerical pictures in the form of isopleth maps, a relatively new tool in determining environmental patterns of ancient deposits, were constructed from the values obtained in the various statistical analyses. The environmental pattern of the Marshall formation was derived from these maps and general similarities in the trends of deposition are shown. Interpretation of these relationships is attempted to determine the conditions of deposition.

From the results obtained in this investigation, the author has concluded that during the period of deposition, the Marshall sea was regressing and deltaic deposits were being formed. With the increased wave action, much of the material carried to the sea by

streams appears to have been reworked and deposited between these delta areas to form beaches. The statistical relationships existing in various parts of the area are therefore directly dependent upon the agent and method of deposition.

TABLE OF CONTENTS

	Page
INTRODUCTION	1
General Information	1
Purpose of Study	3
SAMPLE SELECTION	5
Source of Samples	5
Selection of Lithologic Unit	5
LOCATION AND WELL DISTRIBUTION	8
Location of Area	8
Distribution of Wells	8
LABORATORY PROCEDURE	15
General	15
Method of Sampling	15
Disaggregation	15
Removal of Iron Oxide Stain	16
Shale Extraction	17
Heavy Mineral Analysis	18
Decantation	18
Sieving	19
Mounting of Slides	20

	Page
Measurements and Calculations of Roundness and Sphericity	29
STATISTICAL ANALYSIS	34
Methods of Approach	34
Cumulative Curve Analysis	35
COMPARISON AND PRESENTATION OF DATA	87
Introduction	87
Analysis of Size Distribution	91
Analysis of Roundness Distribution	98
Analysis of Sphericity Distribution	118
Summary Comparison	124
INTERPRETATIONS	128
Method of Deposition	128
Shape of Sand Grains	129
Rounding of Sand Grains	131
Effect of Grain Size	131
Summary Interpretation	132
CONCLUSION	136
Sequence of Events	137
REFERENCES	140

LIST OF TABLES

TABLE	Page
I. Well Description	13
II. Data from Sieve Analysis	21
III. Roundness Calculations from Cumulative Curves	43
IV. Sphericity Calculations from Cumulative Curves	45
V. Quartile Calculations from Sieve Analysis	89
VI. Arithmetic Averages of Roundness and Sphericity	99

LIST OF FIGURES

FIGURE	Page
1. Generalized Stratigraphic Section of the Mississippian and Pennsylvanian, for Lower Peninsula of Michigan	6
2. Methods Used for Determining Shape and Roundness	30
3. Cumulative Curves of Roundness and Sphericity	40

LIST OF MAPS

MAP	Page
1. Areal Extent of the Marshall Sandstones Under Investigation	9
2. Well Locations	10
3. Numbering of Wells	12
4. Median Size Distribution, Sieve Analysis	92
5. Sorting (S_o) Distribution, Sieve Analysis	93
6. Skewness (Sk_g) Distribution, Sieve Analysis	94
7. Kurtosis (Kq_a) Distribution, Sieve Analysis	95
8. Average Roundness Distribution	102
9. Median ($Md\phi$) Roundness Distribution	103
10. Sorting ($QD\phi$) Distribution Roundness	104
11. Sorting (S_o) Distribution, Roundness	105
12. Skewness (Sk) Distribution, Roundness	106
13. Average Shape Distribution	119
14. Median ($Md\phi$) Shape Distribution	120
15. Sorting ($QD\phi$) Distribution, Sphericity	121
16. Sorting (S_o) Distribution, Sphericity	122
17. Sand Thickness Distribution	125

LIST OF GRAPHS

Well No.		Page
1 - 40	Cumulative Curves of Size Distribution	47-86
1 - 40	Histograms of Roundness and Sphericity Distribution	108-117

INTRODUCTION

General Information

Much use has been made of statistical and mechanical methods of analysis in correlating sandstones, determining stratigraphic horizons, and classifying the various types of sediments. Little work, however, has been done with these methods to determine either the manner in which formations were deposited or the gradational correlation between subsurface formations.

The increasing significance of marine geology in the last few years has greatly influenced the study of sedimentation. Many professional papers and texts have been published concerning the deposition of marine sediments and the factors controlling this deposition. Some of the country's best-known sedimentologists and oceanographers have taken advantage of the many electronic instruments developed by the Navy during World War II. These instruments are being employed to gain a better understanding of the influence of current and wave action on marine deposition. From this increased knowledge, new methods for analyzing ancient marine deposits may be developed.

One of the most recent methods to determine the conditions of deposition in ancient seas is to study the environmental pattern of the area. From this pattern the general areas of extreme deposition can be determined and more-specific directions in which to carry on drilling operations may be determined. W. C. Krumbein stated that:

Environmental patterns provide a means of reconstructing ancient environments. The localization of high-energy areas, the prevailing directions of currents, the average depth of water, and other features may be inferred, especially if the faunal elements are included in the analysis. Environmental patterns also permit the segregations of closely related environments, as beach and dune, which cannot be distinguished by individual samples.

R. A. Hobbs (1949, p. 30) has shown that the possibility of determining the main direction of sedimentation may be positive when directed toward a small area. By using sedimentary methods of analysis, he was able to show a difference in the physical properties of rounding, sorting, skewness, and kurtosis of the samples. However, only three wells were considered, and whether these indicate the main directions of deposition or simply the result of local conditions, cannot be determined without more extensive investigation.

The Marshall formation was chosen for this study because of the excellent supply of sandstone present in Michigan. C. Rominger (1876, p. 98) described the Marshall formation as a shore deposit,

because "the stratification often becomes discordant and frequent changes in the material are induced by local influence; while in one place a shale bed forms, in another near by a sand-rock ledge may be accumulated." In the first attempt to describe the history of Marshall time, C. W. Cook (1941, p. 64) suggested that the red shales found in the lower Marshall indicate periods of stability in which the finer material is transported seaward and that the main feature of this geologic history was the isolation of the Michigan basin during Marshall time. V. B. Monnett (1948, p. 629) made an extensive study of the Marshall formation and concluded that there is both a dominant eastern and western source of sediments. Source areas responsible for the materials deposited in the Michigan basin, according to G. W. Pirtle (1932, p. 32), are the Wisconsin arch on the west, the Kankakee arch to the southwest, the Findlay arch to the southeast, the Algonquin arch on the east, and the pre-Cambrian complex to the north.

Purpose of Study

One purpose of this investigation is to determine the possibility of reconstructing the main directions of sedimentation within a specific subsurface horizon. With this information, it may be possible

to reconstruct ancient shore lines of deposition which would be of economic value in the search for petroleum. Another purpose is to show how the material forming the Marshall formation was distributed in the Marshall sea and from this information to determine the conditions of deposition during that period. Both purposes may be regarded as an attempt to determine the environmental pattern of the deposit.

SAMPLE SELECTION

Source of Samples

The well samples used in this study were obtained from the Department of Geology, Michigan State College, and the Michigan Geological Survey, Lansing, Michigan.

Selection of Lithologic Unit

The sands chosen for analysis in this investigation are from the Marshall sandstone formation of the Mississippian period (Figure 1).

The sample used from each well depends upon the thickness of the sands between the oldest nonclastic bed in the Michigan formation and the first showing of the Coldwater shale. This choice was suggested by Dr. W. A. Kelly, Professor of Geology at Michigan State College. Using these boundaries, it is possible to obtain the most uniform horizon throughout the area. Another reason for this choice is that it eliminates all doubts whether to include or exclude the so-called "stray" sands which appear from place to place within the area. Many geologists include the "stray" sandstones with the

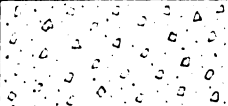
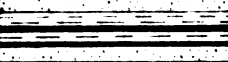
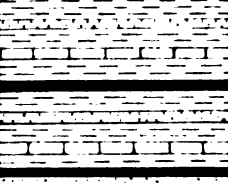

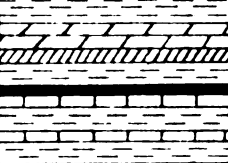
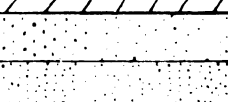
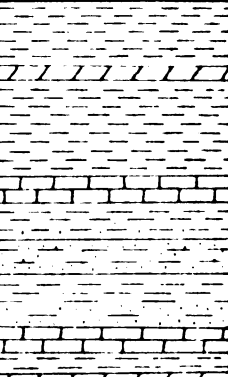
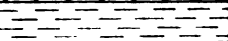

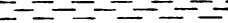
SERIES	FORMATION	LITHOLOGY	DESCRIPTION	THICKNESS
Quaternary	Wisconsin		gravel, sand and clay	0-860'
Pennsylvanian	Grand River		sand, shale and coal	80-95'
	Saginaw		sand, shale, coal and limestone	400-535'
Mississippian	Bayport		sand, and limestone	40-100'
	Michigan		gypsum, sand, shale, dolomite and limestone	0-500'
	Marshall		sand, shale, and siltstone	160-320'
	Coldwater		sand, shale, and siltstone	500-1000'
	Sunbury		shale	10-90'
	Berea		sand and shale	0-210'
	Bedford		shale	10-300'

Figure 1.- Generalized Stratigraphic Section of the Mississippian and Pennsylvanian, for Lower Peninsula of Michigan. (After Monnett, 1948)

Michigan formation, while others place them in the Marshall. One group of geologists thinks that the Michigan "stray" sandstones were deposited as bars in the Michigan sea following erosion of the top of the Marshall formation. The other group, however, considers the "stray" sandstones to be reworked and redeposited Marshall sediments. The writer agrees with the latter group that these sands should be included within the Marshall formation and that by using the boundaries stated above, these "stray" sands will be included in all samples in which they occur.

LOCATION AND WELL DISTRIBUTION

Location of Area

The area selected for this investigation is confined to the west-central section of the Lower Peninsula of Michigan. The western limit is confined to the area where the Marshall formation crops out beneath the overlying drift. The northern, eastern, and southern boundaries are arbitrarily set to form a semicircular pattern toward the center of the basin (Map 1). Within these boundaries is an area approximately 55 miles wide and 110 miles long, covering all or part of the following counties:

Clare	Muskegon
Ionia	Newaygo
Kent	Oceana
Lake	Osceola
Mecosta	Ottawa
Missaukee	Wexford
Montcalm	

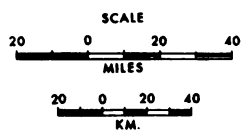
Distribution of Wells

Forty wells were selected, all of which are located in different townships within the above-listed counties (Map 2).

MICHIGAN

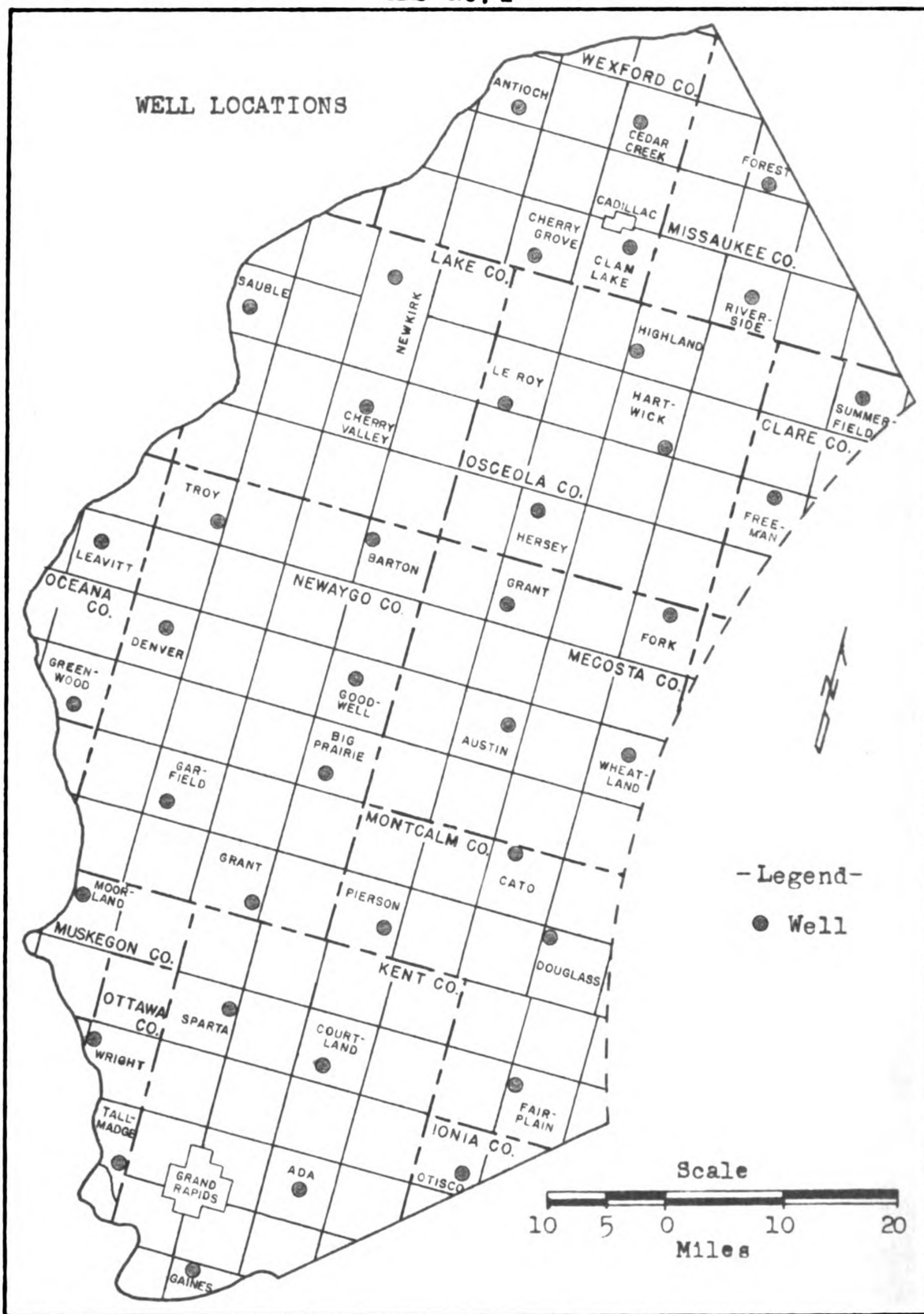
MAP No. 1

**AREAL EXTENT OF THE
MARSHALL SANDSTONES
UNDER INVESTIGATION**



Compiled & Drawn by Andrew B. Porcjo
Mich. State College, Dep't. of Geol. & Geog.

MAP No. 2



The total area under investigation was divided into seven east-west sections, each having dimensions of approximately 20 by 50 miles. Each section forms a wedge-shaped area which greatly simplifies later discussion and presentation of the final results. Four to eight wells were selected from each section. It is not possible to divide the total area in such manner that each section has the same number of wells and still obtain a complete coverage.

Wells are designated by numbers from one through forty, by a method such that the wells in each section, beginning with the southernmost section, are completely numbered from west to east before progressing northward into the next section (Map 3).

Table I lists the wells plotted on Maps 2 and 3, the permit number and location of each well, along with the thickness of the sandstone being investigated.

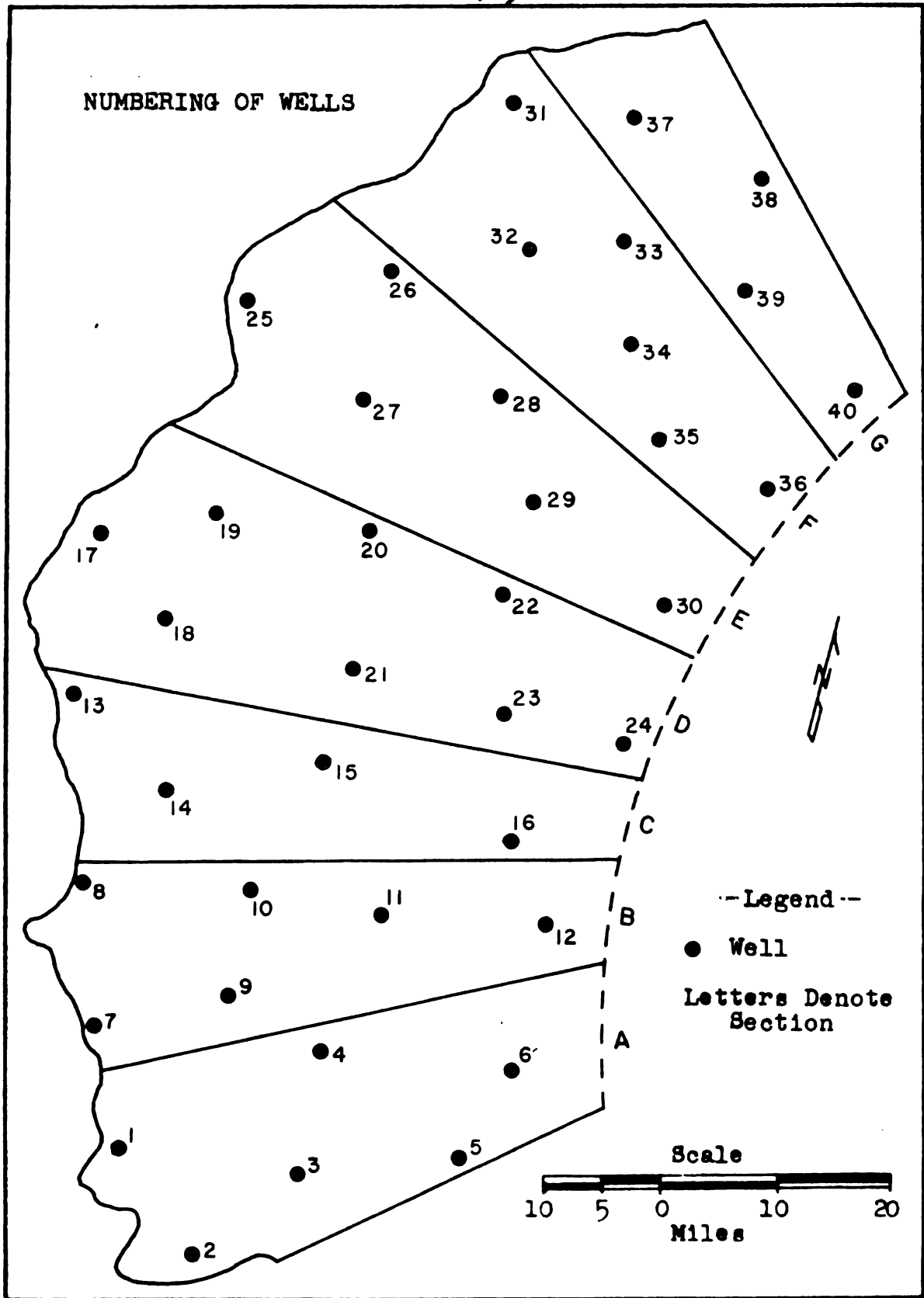


TABLE I
WELL DESCRIPTION

Well No.	Permit No.	County	Township	Land Description	Thickness of Sand (in feet)
1	6624	Ottawa	Tallmadge	36-T7N-R13W	160
2	14587	Kent	Gaines	5-T5N-R11W	269
3	7453	Kent	Ada	8-T7N-R10W	312
4	3144	Kent	Courtland	29-T9N-R10W	248
5	11472	Ionia	Otisco	26-T8N-R8W	163
6	13554	Montcalm	Fairplain	7-T9N-R7W	119
7	7099	Ottawa	Wright	7-T8N-R13W	278
8	15241	Muskegon	Moorland	9-T10N-R14W	270
9	14577	Kent	Sparta	12-T9N-R12W	258
10	13168	Newaygo	Grant	25-T11N-R12W	243
11	8149	Montcalm	Pierson	23-T11N-R10W	128
12	12254	Montcalm	Douglass	1-T11N-R7W	225
13	9946	Oceana	Greenwood	27-T13N-R15W	159
14	12952	Newaygo	Garfield	29-T12N-R13W	130
15	14886	Newaygo	Big Prairie	28-T13N-R11W	145
16	12365	Montcalm	Cato	5-T12N-R8W	125
17	13380	Oceana	Leavitt	17-T15N-R15W	123
18	13890	Newaygo	Denver	10-T14N-R14W	145
19	9697	Newaygo	Troy	24-T16N-R14W	242
20	4460	Newaygo	Barton	7-T16N-R11W	235
21	10419	Newaygo	Goodwell	8-T14N-R11W	165

TABLE I (Continued)

Well No.	Permit No.	County	Township	Land Description	Thickness of Sand (in feet)
22	13965	Mecosta	Grant	20-T16N-R9W	195
23	1440	Mecosta	Austin	11-T14N-R9W	255
24	12883	Mecosta	Wheatland	9-T14N-R7W	280
25	9394	Lake	Sauble	16-T19N-R14W	181
26	13013	Lake	Newkirk	16-T20N-R12W	265
27	14960	Lake	Cherry Valley	15-T18N-R12W	270
28	12379	Osceola	Leroy	33-T19N-R10W	290
29	16343	Osceola	Hersey	8-T17N-R9W	255
30	16329	Mecosta	Fork	3-T16N-R7W	100
31	1177	Wexford	Antiock	26-T23N-R11W	230
32	12515	Wexford	Cherry Grove	28-T21N-R10W	275
33	12590	Wexford	Clam Lake	11-T21N-R9W	170
34	15934	Osceola	Highland	19-T20N-R8W	160
35	14533	Osceola	Hartwick	36-T19N-R8W	200
36	5418	Clare	Freeman	3-T18N-R6W	180
37	14307	Wexford	Cedar Creek	16-T23N-R9W	225
38	12977	Missaukee	Forest	32-T23N-R7W	105
39	7357	Missaukee	Riverside	22-T21N-R7W	155
40	11444	Clare	Summerfield	7-T20N-R5W	110

LABORATORY PROCEDURE

General

This investigation involves physical and statistical methods of study, using such descriptive methods of analysis as weight percentages and quartile measures of sorted sieve sizes, roundness and sphericity measurements of quartz grains.

Method of Sampling

Each sample consists of eight to twenty-five vials of sand, with each vial representing a specific interval, usually 5 or 10 feet, of formation. The samples were considered as individual composite units, and the material from each vial was sampled according to the interval it represented. One-tenth gram was selected for each foot of Marshall formation, and weighed to the nearest 0.005 gram.

Disaggregation

Each sample studied was either partly or wholly consolidated. To remove the cement, which for the most part was calcareous, the samples were treated with a solution of 1:1 hydrochloric acid and a

30 per cent solution of hydrogen peroxide for a period of 24 hours, and then heated over a burner for one hour. While heating, a solution of 50 per cent hydrochloric acid was added so that the sample would not dry out and thus cause fracturing of the grains or baking of any cement which was still present.

The above reaction, however, did not completely disaggregate the sandstone, and although the coherence was not strong, it was found necessary to separate these grains with the use of a porcelain plate and a cork, held in the vial. This method consists of placing the aggregates on the porcelain plate, soaking them with water, and then subjecting them to a rubbing process, using the cork and a twisting motion of the wrist. This action was found adequate to almost completely disaggregate the quartz grains. No fracturing or other wearing effects were observable when the grains were examined under a binocular microscope.

Removal of Iron Oxide Stain

The hydrogen peroxide employed in disaggregation was used also for the purpose of removing the iron oxide stain which occurs in lenses ranging between 5 and 150 feet in thickness in most of the wells used in this study (Hobbs, 1949, p. 7). This method of removal

was highly successful in most instances; however, in those cases in which it was not, no serious consequences resulted because, as noted by Hobbs, this stain had no appreciable effect upon the roundness and sphericity values.

Shale Extraction

With the material now mostly unconsolidated, it was found necessary to remove a large amount of shale which, during drilling, had fallen into the Marshall samples from the overlying Michigan formation. This was accomplished with bromoform, a heavy liquid having a specific gravity of 2.87 at 20° C. Alcohol was mixed with the bromoform to lower the specific gravity to the point where the shale would float and the quartz grains sink (Kropschot, 1953, p. 25). A large funnel, with a piece of rubber tubing attached and closed with a wire clamp, was filled with the diluted bromoform. The sand and shale was sprinkled upon the bromoform and time was allotted for the sand to settle to the bottom. The clamp was then released and quickly replaced after allowing the sand and some liquid to flow into a lower funnel containing a filter paper. The sand was finally washed with alcohol and allowed to dry.

Heavy Mineral Analysis

Heavy mineral separations were conducted by the same method performed in the shale extraction, the only difference being in the specific gravity of the bromoform, which, in this case, had a gravity of pure bromoform. The sand fractions used for the heavy mineral studies was that between the sieve sized 65 and 100 mesh per inch. M. D. Stearns (1933) stated that few heavy minerals are present in the Marshall sands. This statement was checked in ten of the well samples obtained in this investigation and found to be correct.

In as much as very small amounts of muscovite, garnet, and opaque minerals were found, it was decided that the heavy mineral study would not be extended.

Decantation

Prior to the sieving analysis, all material finer than $1/32$ mm. was decanted from each sample. Decantation was accomplished by filling the beakers, containing the forty samples, with water, to a height of 10 cm., and allowing them to stand for a period of 1 minute and 56 seconds. At this instant all water and sediment finer than $1/32$ mm. was poured off, since all larger particles had settled to the bottom. This rate of settling was computed according to Stokes'

law for sediments with a specific gravity of 2.65 (Krumbein, 1938, p. 166).

Sieving

Each sample was examined for traces of gypsum and shale, which were extracted with a pair of tweezers. The samples were then weighed to the nearest milligram. Tyler sieve sizes 35, 48, 65, 100, 150, and 200 mesh per inch were first employed to divide the sample into seven different fractions. It was later found in many samples that the sand below sieve size 35 contained too large a percentage of material to make accurate cumulative curves below the ten percentile. This material, therefore, was passed through sieve size 28, thus establishing another point for plotting the curve below the ten percentile. These sieve sizes, when compared with the Wentworth grade scale, include coarse, medium, fine, and very fine sand. During the initial sieving operation, the sample was placed in the top Tyler sieve, size 35, which allowed all material finer than this size to pass through. That which remained on this sieve was found to consist mostly of sand aggregates. These aggregates were then dispersed by rubbing them over the sieve with a piece of rubber hose. The next grade size, between sieves 35 and 48, was then examined

to determine the aggregates still present. A surprisingly small amount was found, and it was felt by the author that any aggregates still prevailing would have little effect upon the end results. The sieving was finally completed by placing the individual samples in the ro-tap automatic shaking machine for a period of ten minutes. Each grade size was then weighed, recorded (Table II), and placed in ten-gram vials for possible future reference.

Mounting of Slides

It was found that the sand between Tyler sieve sizes 65 and 100 mesh per inch was the most desirable grade for projecting and measuring roundness and sphericity values.

Airaform (n-1.66) was used as the mounting medium in order that the quartz grains (n-1.544-1.553) would have greater relief when projected, and thus produce more distinct outlines. Approximately one gram of airaform was placed on each glass slide. These slides were then placed on a metal plate and warmed with a bunsen burner. Continued heating of the airaform for three minutes drove off all air bubbles. Approximately 150 sand grains were flicked from the vial onto the airaform; cover glasses were added and the airaform permitted to harden. Xylol served as the cleaning agent to remove any excess airaform from the slide.

TABLE II

DATA FROM SIEVE ANALYSIS

Well	Tyler Sieve Sizes							Loss	Total
	-28	28-35	35-48	48-65	65- 100	100- 150	150- 200		
#1									
Wt.(g)	0.065	0.113	1.270	2.389	3.218	6.718	3.565	0.837	18.250
Wt. %	0.36	0.62	6.99	13.14	17.70	36.96	19.61	4.61	100.40
Cum.%	0.36	0.98	7.97	21.11	38.81	75.77	95.38	99.99	99.99
#2									
Wt.(g)	0.087	0.185	1.645	3.495	4.276	3.620	2.885	1.156	17.421
Wt. %	0.50	1.07	9.48	20.15	24.65	20.87	16.63	6.66	100.42
Cum.%	0.50	1.57	11.05	31.20	55.85	76.72	93.35	100.01	100.01
#3									
Wt.(g)	0.170	0.715	3.975	6.440	4.915	4.550	3.350	0.510	24.730
Wt. %	0.69	2.90	16.14	26.15	19.96	18.48	13.60	2.07	100.41
Cum.%	0.69	3.59	19.73	45.88	65.84	84.32	97.92	99.99	99.99
#4									
Wt.(g)	0.088	0.307	2.660	5.795	7.140	2.820	0.835	0.240	19.941
Wt. %	0.44	1.55	13.38	29.14	35.91	14.18	4.20	1.21	100.29
Cum.%	0.44	1.99	15.37	44.51	80.42	94.60	98.80	100.01	100.01
#5									
Wt.(g)	0.062	0.372	1.995	3.040	3.933	2.845	1.387	0.395	14.108
Wt. %	0.44	2.65	14.22	21.67	28.03	20.28	9.89	2.82	100.56
Cum.%	0.44	3.09	17.31	38.98	67.01	87.29	97.18	100.00	100.00

TABLE II (Continued)

Well	Tyler Sieve Sizes							Loss	Total
	-28	28-35	35-48	48-65	65-100	100-150	150-200		
#6									
Wt.(g)	0.026	0.154	2.177	3.449	2.895	1.575	0.635	0.230	0.066 11.207
Wt. %	0.23	1.39	19.54	30.96	25.99	14.14	5.70	2.06	0.59 100.60
Cum.%	0.23	1.62	21.16	52.12	78.11	92.25	97.95	100.01	- 100.01
#7									
Wt.(g)	0.185	0.560	3.232	4.742	4.113	4.383	2.188	1.292	0.182 20.877
Wt. %	0.89	2.71	15.62	22.91	19.87	21.18	10.97	6.24	0.87 100.86
Cum.%	0.89	3.60	19.22	42.13	62.00	83.18	93.75	99.99	- 99.99
#8									
Wt.(g)	0.044	0.491	4.838	6.848	5.631	3.050	1.417	0.578	0.146 23.043
Wt. %	0.19	2.15	21.13	29.91	24.59	13.32	6.19	2.52	0.63 100.63
Cum.%	0.19	2.34	23.47	53.38	77.97	91.29	97.48	100.00	- 100.00
#9									
Wt.(g)	0.192	0.810	4.710	6.599	5.638	2.790	0.973	0.268	0.040 22.020
Wt. %	0.87	3.69	21.43	30.02	25.65	12.69	4.43	1.22	0.18 100.18
Cum.%	0.87	4.56	25.99	56.01	81.66	94.35	98.78	100.00	- 100.00
#10									
Wt.(g)	0.143	0.147	0.878	2.460	5.657	6.575	3.148	0.852	0.148 20.008
Wt. %	0.72	0.74	4.42	12.39	28.48	33.11	15.85	4.29	0.74 100.74
Cum.%	0.72	1.46	5.88	18.27	46.75	79.86	95.71	100.00	- 100.00

TABLE II (Continued)

Well	Tyler Sieve Sizes							Loss	Total
	-28	28-35	35-48	48-65	65-100	100-150	150-200		
#11									
Wt.(g)	0.031	0.220	2.157	2.977	2.407	1.498	0.807	0.449	0.072 10.618
Wt. %	0.29	2.09	20.45	28.23	22.82	14.20	7.65	4.26	0.68 100.67
Cum.%	0.29	2.38	22.83	51.06	73.88	88.08	95.73	99.99	- 99.99
#12									
Wt.(g)	0.560	1.557	6.984	5.502	2.255	0.845	0.477	0.470	0.167 18.817
Wt. %	3.00	8.35	37.45	29.50	12.09	4.53	2.56	2.52	0.90 100.90
Cum.%	3.00	11.35	48.80	78.30	90.39	94.92	97.48	100.00	- 100.00
#13									
Wt.(g)	0.032	0.193	1.718	4.125	3.390	1.705	1.435	0.780	0.081 13.459
Wt. %	0.24	1.44	12.84	30.83	25.34	12.74	10.73	5.83	0.60 100.59
Cum.%	0.24	1.68	14.52	45.35	70.69	83.43	94.16	99.99	- 99.99
#14									
Wt.(g)	0.082	0.223	1.275	1.510	2.110	2.278	1.129	0.635	0.068 9.310
Wt. %	0.89	2.41	13.80	16.34	22.83	24.65	12.22	6.87	0.73 100.74
Cum.%	0.89	3.30	17.10	33.44	56.27	80.92	93.14	100.01	- 100.01
#15									
Wt.(g)	0.255	0.482	2.593	2.532	1.719	0.659	0.278	0.510	0.113 9.141
Wt. %	2.82	5.34	28.72	28.05	19.04	7.30	3.08	5.65	1.23 101.23
Cum.%	2.82	8.16	36.88	64.93	83.97	91.27	94.35	100.00	- 100.00

TABLE II (Continued)

Well	Tyler Siever Sizes							Loss	Total
	-28	28-35	35-48	48-65	65-100	100-150	150-200		
#16									
Wt.(g)	0.553	1.072	3.180	2.983	1.765	0.494	0.226	0.107	0.032 10.412
Wt. %	5.33	10.33	30.64	28.74	17.00	4.76	2.18	1.03	0.31 100.32
Cum.%	5.33	15.66	46.30	75.04	92.04	96.80	98.98	100.00	- 100.00
#17									
Wt.(g)	0.215	0.320	1.355	2.050	2.070	1.300	1.070	0.680	0.065 9.125
Wt. %	2.37	3.54	14.96	22.63	22.85	14.35	11.81	7.51	0.71 100.73
Cum.%	2.37	5.91	20.87	43.50	66.35	80.70	92.51	100.02	- 100.02
#18									
Wt.(g)	0.134	0.398	2.271	2.839	2.565	2.043	1.307	0.576	0.117 12.250
Wt. %	1.10	3.28	18.72	23.40	21.14	16.84	10.77	4.75	0.96 100.96
Cum.%	1.10	4.38	23.10	46.50	67.64	84.48	95.25	100.00	- 100.00
#19									
Wt.(g)	0.203	0.787	2.640	1.250	0.525	0.737	1.305	1.360	0.083 8.890
Wt. %	2.30	8.94	29.98	14.19	5.96	8.37	14.82	15.44	0.93 100.93
Cum.%	2.30	11.24	41.22	55.41	61.37	69.74	84.56	100.00	- 100.00
#20									
Wt.(g)	0.245	1.037	3.868	3.968	2.664	3.213	2.464	1.040	0.091 18.590
Wt. %	1.32	5.61	20.91	21.45	14.40	17.37	13.32	5.62	0.49 100.49
Cum.%	1.32	6.93	27.84	49.29	63.69	81.06	94.38	100.00	- 100.00

TABLE II (Continued)

Well	Tyler Sieve Sizes							Loss	Total
	-28	28-35	35-48	48-65	65-100	100-150	150-200		
#21									
Wt.(g)	0.233	0.342	1.255	2.143	3.025	2.013	0.942	0.494	10.475
Wt. %	2.24	3.29	12.06	20.59	29.07	19.34	9.05	4.36	100.65
Cum.%	2.24	5.53	17.59	38.18	67.25	86.59	95.64	100.00	100.00
#22									
Wt.(g)	0.211	0.357	2.190	2.548	2.590	0.959	0.423	0.500	9.847
Wt. %	2.15	3.65	22.40	26.06	26.49	9.81	4.33	5.11	100.70
Cum.%	2.15	5.80	28.20	54.26	80.75	90.56	94.89	100.00	100.00
#23									
Wt.(g)	0.298	0.750	3.008	4.630	5.157	3.443	2.300	1.095	20.815
Wt. %	1.44	3.63	14.54	22.39	24.94	16.65	11.12	5.29	100.64
Cum.%	1.44	5.07	19.61	42.00	66.94	83.59	94.71	100.00	100.00
#24									
Wt.(g)	0.818	1.673	7.105	4.895	2.933	1.351	0.624	0.830	20.360
Wt. %	4.04	8.27	35.12	24.20	14.50	6.68	3.08	4.10	100.63
Cum.%	4.04	12.31	47.43	71.63	86.13	92.81	95.89	99.99	99.99
#25									
Wt.(g)	0.158	0.430	2.625	2.917	3.215	2.220	1.210	0.450	13.259
Wt. %	1.19	3.26	19.85	22.06	24.31	16.79	9.15	3.40	100.27
Cum.%	1.19	4.45	24.30	46.36	70.67	87.46	96.61	100.01	100.01

TABLE II (Continued)

Well	Tyler Sieve Sizes							Loss	Total
	-28	28-35	35-48	48-65	65-100	100-150	150-200		
#26									
Wt.(g)	0.121	0.311	2.166	2.812	4.477	4.448	2.302	0.893	0.120 17.650
Wt. %	0.69	1.77	12.36	16.04	25.54	25.37	13.13	5.09	0.68 100.67
Cum.%	0.69	2.46	14.82	30.86	56.40	81.77	94.90	99.99	- 99.99
#27									
Wt.(g)	0.182	0.790	4.347	4.771	4.072	3.678	3.100	1.057	0.133 22.130
Wt. %	0.83	3.59	19.76	21.69	18.51	16.72	14.09	4.81	0.60 100.60
Cum.%	0.83	4.42	24.18	45.87	64.38	81.10	95.19	100.00	- 100.00
#28									
Wt.(g)	0.606	0.561	2.605	2.818	2.758	2.275	1.677	1.597	0.089 14.986
Wt. %	4.06	3.77	17.49	18.92	18.51	15.27	11.26	10.72	0.59 100.59
Cum.%	4.06	7.83	25.32	44.24	62.75	78.02	89.28	100.00	- 100.00
#29									
Wt.(g)	0.244	0.573	2.683	3.846	4.585	2.798	1.536	1.455	0.158 17.878
Wt. %	1.38	3.23	15.14	21.70	25.87	15.79	8.67	8.21	0.88 100.87
Cum.%	1.38	4.61	19.75	41.45	67.32	83.11	91.78	99.99	- 99.99
#30									
Wt.(g)	0.100	0.280	1.270	2.480	2.595	1.012	0.428	0.412	0.055 8.632
Wt. %	1.17	3.26	14.81	28.91	30.26	11.80	4.99	4.80	0.64 100.64
Cum.%	1.17	4.43	19.24	48.15	78.41	90.21	95.20	100.00	- 100.00

TABLE II (Continued)

Well	Tyler Sieve Sizes							Loss	Total
	-28	28-35	35-48	48-65	65-100	100-150	150-200		
#31									
Wt.(g)	0.138	0.702	3.348	4.245	3.360	1.520	0.784	0.470	0.171 14.738
Wt. %	0.95	4.82	22.98	29.14	23.07	10.43	5.38	3.23	1.16 101.16
Cum.%	0.95	5.77	28.75	57.89	80.96	91.39	96.77	100.00	- 100.00
#32									
Wt.(g)	0.525	1.130	3.205	3.700	4.850	2.670	0.985	0.350	0.110 17.525
Wt. %	3.01	6.49	18.40	21.25	27.85	15.33	5.66	2.01	0.63 100.63
Cum.%	3.01	9.50	27.90	49.15	77.00	92.33	97.99	100.00	- 100.00
#33									
Wt.(g)	0.343	0.615	1.836	1.688	1.380	0.783	0.292	0.282	0.049 7.268
Wt. %	4.75	8.52	25.43	23.38	19.12	10.85	4.04	3.91	0.67 100.67
Cum.%	4.75	13.27	38.70	62.08	81.20	92.05	96.09	100.00	- 100.00
#34									
Wt.(g)	0.088	0.293	1.805	2.280	3.643	2.908	1.410	0.943	0.083 13.493
Wt. %	0.66	2.19	13.50	17.05	27.25	21.75	10.55	7.05	0.62 100.62
Cum.%	0.66	2.85	16.35	33.40	60.65	82.40	92.95	100.00	- 100.00
#35									
Wt.(g)	0.452	1.518	4.483	2.307	1.538	0.771	0.328	0.486	0.102 11.985
Wt. %	3.80	12.78	37.73	19.41	12.94	6.49	2.76	4.09	0.85 100.85
Cum.%	3.80	16.58	54.31	73.72	86.66	93.15	95.91	100.00	- 100.00

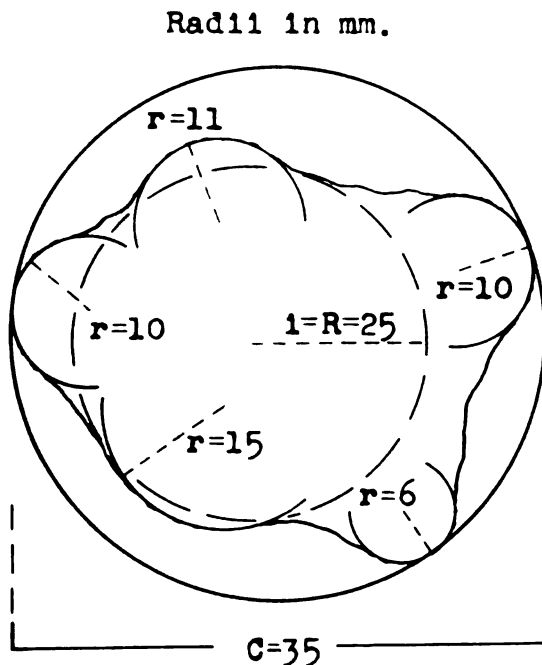
TABLE II (Continued)

Well	Tyler Sieve Sizes							Loss	Total
	-28	28-35	35-48	48-65	65-100	100-150	150-200		
#36									
Wt.(g)	1.049	1.403	3.520	3.093	2.675	2.012	1.398	0.276	0.104 15.530
Wt. %	6.80	9.10	22.82	20.05	17.34	13.04	9.06	1.79	0.67 100.67
Cum.%	6.80	15.90	38.72	58.77	76.11	89.15	98.21	100.00	- 100.00
#37									
Wt.(g)	0.288	0.610	2.153	2.455	2.828	1.595	0.587	0.272	0.087 10.875
Wt. %	2.67	5.65	19.96	22.76	26.21	14.78	5.44	2.52	0.80 100.79
Cum.%	2.67	8.32	28.28	51.04	77.25	92.03	97.47	99.99	- 99.99
#38									
Wt.(g)	0.090	0.395	1.547	2.418	2.722	1.182	0.255	0.108	0.023 8.740
Wt. %	1.03	4.53	17.75	27.74	31.23	13.56	2.93	1.24	0.26 100.27
Cum.%	1.03	5.56	23.31	51.05	82.28	95.84	98.77	100.01	- 100.01
#39									
Wt.(g)	0.050	0.285	1.606	2.399	3.240	1.760	0.687	0.328	0.055 10.410
Wt. %	0.48	2.75	15.51	23.17	31.29	17.00	6.63	3.17	0.53 100.53
Cum.%	0.48	3.23	18.74	41.91	73.20	90.20	96.83	100.00	- 100.00
#40									
Wt.(g)	0.636	0.701	1.385	0.903	0.537	0.207	0.117	0.128	0.029 4.643
Wt. %	13.78	15.20	30.02	19.57	11.64	4.49	2.54	2.77	0.62 100.63
Cum.%	13.78	28.98	59.00	78.57	90.21	94.70	97.24	100.01	- 100.01

Measurements and Calculations of Roundness and Sphericity

The most time-consuming portion of this study was involved in measuring the quartz grains for roundness and sphericity. This was accomplished by mounting a petrographic microscope in a horizontal position, removing the lower prism and reflection mirror, and directing the beam of light, from a 500-watt lamp, through the slide. A prism attached to the ocular of the microscope projected the grain images onto a concentric circle protractor, where they were measured. The method devised by Wadell and modified by Schmitt (1949, p. 47) was used to measure roundness and sphericity. This method employs the use of a concentric circle protractor drawn on white paper, rather than on plexiglass as suggested by Wadell. Measurements are made directly from the grain images, and therefore it is not necessary to draw each grain before measuring it.

The roundness of a sand grain, as defined by Wadell (1935), is a measure of the angularity of its corners, and may be expressed as the arithmetic average of the radii of curvature of its individual corners, divided by the maximum inscribed circle (Figure 2). As roundness increases, the radius of curvature of the corners also increases. This may be stated mathematically by the formula used in this investigation to determine roundness.



Wadell's Roundness (P):

$$P = \frac{\sum r/n}{R} = \frac{10.5}{25} = .420$$

Riley's Sphericity (S):

$$S = \sqrt{\frac{l}{C}} = \sqrt{\frac{25}{35}} = .833$$

where:

- R = radius of maximum inscribed circle.
- r = radius of curvature of individual corners.
- n = number of corners measured.
- l = radius of largest inscribed circle.
- C = radius of smallest circumscribed circle.

Figure 2.- Methods Used for Determining Shape and Roundness

$$P = (\Sigma r/n)/R$$

where: P = degree of roundness;
 R = radius of maximum inscribed circle;
 r = radius of curvature of individual corners;
 n = number of corners measured.

Roundness, therefore, is a function of the sharpness of the corners, and is entirely independent of shape which has to do with the form of the grain.

Although Wentworth (1922) recognized the difference between flatness (shape) and roundness, it was Wadell (1932) who first pointed out these two geometrically independent variables included in the general shape concept. Since a sphere has the smallest surface area in proportion to volume of any other shape, Wadell defined this as the unit measurement, and referred to the shape of a particle as having a specific "degree of sphericity." Wadell's original formula for determining sphericity may be expressed:

$$\phi = d/D$$

where: ϕ = degree of sphericity;
 d = diameter of circle equal in area to that of the grain obtained by planimeter measurements;
 D = diameter of smallest circle circumscribing the grain.

In the above formula it may be seen that in order to determine sphericity, it is necessary first to measure the exact area of the grain. This proved a most time-consuming procedure. Therefore, Wadell

developed a more practical formula which gives satisfactory results closely approaching those obtained when planimetric measurements are made. Wadell's short-method formula is:

$$S = R/D$$

where: S = degree of sphericity;
 R = radius of largest inscribed circle;
 D = diameter of smallest circumscribed circle.

From this short-method formula, N. A. Riley (1941) has derived another formula using the diameter of the largest inscribed circle, and dividing this by the diameter of the smallest circumscribed circle; the square root of the product is then taken as the degree of sphericity (Figure 2). Riley's short-method formula is:

$$S = i/C$$

where: S = degree of sphericity;
 i = radius of largest inscribed circle;
 C = radius of smallest circumscribed circle.

The writer selected the method of calculating sphericity derived by Riley, because it is believed to compare more closely with the true sphericity. Also, it proved to be the most rapid method. The writer found by using Riley's method with tables constructed from results computed with the aid of a slide rule, that considerably more speed was obtained than when the alignment diagram, suggested by Wadell (1934), was employed. Krumbein (1938, p. 294) allowed one-half

minute for each calculation with the alignment chart, whereas the writer made several calculations within this same period by using tables.

A total of four thousand quartz grains, one hundred from each of the forty wells under investigation, were measured to determine roundness and sphericity. Although Krumbein (1941, p. 69) suggested the measuring of fifty grains for each sample, R. C. Perry (1951, p. 10) stated: "After measuring 200 grains of the St. Peter sand the average sphericity and roundness were computed for the first 75 grains, the first 150 grains and the total 200 grains." In comparing the results, it was found that little, if any, additional accuracy was to be gained by counting more than 75: "It was decided therefore, that the measurement of 100 grains from each sample would result in a representative figure for the sample as a whole."

STATISTICAL ANALYSIS

Methods of Approach

Krumbein (1939, p. 559) described two main approaches to a statistical sedimentary analysis. The first and earliest method is that employed by workers who prefer to consider their data in terms of the original grade sizes used in the analysis. These investigators usually employ histograms in describing and comparing the modal class, number of grade sizes present, and the symmetry or asymmetry of the figures. This method, however, serves more as a picture to be compared visually than mathematically.

The second approach, which is far more popular and valuable, is to consider the data in terms of a continuous frequency distribution. This approach may be divided into two methods: using either cumulative curves or frequency curves as the basis of interpretation. The former is considered the most popular.

In this investigation, the author has endeavored to present mathematical results which could later be represented as isopleth maps and numerically comparable figures. For these reasons, cumulative curves were drawn, using the weight percentages of size

distribution (pp. 47-86) and the frequency distribution of roundness and sphericity measurements. Histograms were also drawn to represent more clearly a visual picture of the cumulative values obtained in the roundness and sphericity measurements (pp. 108-117).

Cumulative Curve Analysis

In order to obtain the geometrical ratios directly, cumulative curves representing the data secured from the sieve analysis (Table II) were drawn on semilogarithmic paper. The diameters of the grains in millimeters are plotted logarithmically along the horizontal axis and the cumulated weight percentages are plotted arithmetically along the vertical axis (pp. 47-86). The curve is drawn by erecting an ordinate at the first grade (Tyler sieve size 28), equal in height to the percentage of material in that class; at the end of the second grade, another ordinate is measured, equal in height to the sum of the percentages in the first two classes, and so on. The curve is then drawn through the upper limits of these ordinates. Krumbein (1938, p. 563) described a cumulative curve as, in effect, equivalent to setting a histogram block above and to the right of its predecessor, so that the base of each block is the total height of all preceding blocks.

Although many workers use cumulative curves purely in a descriptive manner, much the same as histograms, the greatest advantage of them is in obtaining statistical values. Five values may be obtained: the median, Md ; the first and third quartiles, Q_1 and Q_3 ; and the ten and ninety percentiles, P_{10} and P_{90} (pp. 47-86).

The median represents the value obtained at the point where the cumulative curve is intersected by the 50 per cent line, and is defined as that value which is larger than 50 per cent of the material and smaller than the other 50 percent. This value also is commonly used as the average.

The first and third quartiles lie on either side of the median and correspond to the intersections of the curve with the 25 per cent and 75 per cent lines, respectively. These may be considered similar to the median, depending upon their frequency values. In like manner, the ten and ninety percentiles yield values corresponding to the position of an ordinate projected downward at the intersection of the 10 and 90 per cent frequency lines and the cumulative curve.

The first use of quartile measures in sedimentary analysis was made by P. D. Trask (1930). With them, he was able to express three different relationships: the quartile deviation, quartile skewness, and quartile kurtosis. The quartile deviation or "sorting" of a

sample may be expressed as the measure of the spread of a cumulative curve. This may be expressed mathematically in any one of three forms. The first is the arithmetic quartile deviation:

$$QD_a = (Q_3 - Q_1)/2$$

The second is the geometric form introduced by Trask (1932) as the sorting coefficient, "So," and used here to represent the data obtained from both the sieve analysis and the roundness and sphericity calculations. This form may be defined as:

$$QD_g = So = \sqrt{Q_1/Q_3}$$

Trask has reversed the quartiles in the above relationship. By placing the largest quartile value in the numerator, positive values are obtained. The advantage of this form is that it eliminates the size factor and units of measurement.

The third form is logarithmic, and may be expressed:

$$\log QD_g = \log SO = (\log Q_3 - \log Q_1)/2$$

In a similar manner, the quartile skewness, used as a measure of the asymmetry of the curve or the departure of the quartiles from the median, may also be expressed in three forms:

$$SK_a = (Q_3 + Q_1 - 2Md)/2$$

$$SK_g = \sqrt{Q_3 Q_1 / Md^2}$$

$$\log SK_g = (\log Q_3 + \log Q_1 - 2 \log Md)/2$$

The subscripts "a" and "g" are used to distinguish between the arithmetic and geometric cases.

Geometric skewness has the same advantage as geometric quartile deviation in that size factors and units of measurement are eliminated. It was this independence of the size factor and the direct ratios between quartiles in the case of "So" and between quartiles and medians in the case of skewness, which prompted Trask to introduce geometric measures for sediments. Geometric measures, however, are not the best method of comparing data. In other words, it cannot be said that a sediment with a sorting of 2.0 is twice as well sorted as a sediment with a sorting of 4.0. When the logarithmic values of the above two sediments are found, however, they may be compared in such a manner. This is possible because as "So" increases geometrically, "log So" increases arithmetically.

Unlike the two previous quartile ratios considered, the quartile kurtosis is generally expressed only in the arithmetic form derived by Kelley (1924, p. 77):

$$Kq_a = (Q_1 - Q_3)/2(P_{10} - P_{90})$$

This measure is essentially a comparison of the spread of the central portion of a frequency curve to the spread of the curve as a whole. It is the measure of the degree of peakedness of a curve and

is similar in expression to that of sorting, in that a well sorted sand should form a more peaked curve than a poorly sorted one. Kurtosis, as defined here, yields values which decrease with increasing peakedness; this should be kept in mind when comparisons are made. At present, this method has received little attention in sedimentation.

Krumbein (1936) has developed another method, represented by what is known as the "phi" scale, to secure quartile measures. This method consists of plotting the cumulated weight percentages against the logarithmic values of the grain diameters to the base 2, rather than to the base 10, as is done to obtain geometric values. In this method, arithmetic graph paper may be used and will show directly, in the case of size frequency distribution, how many Wentworth grade scales are present between the various quartiles. Each Wentworth class limit is an integer and is plotted on the "phi" scale along the horizontal axis, size increasing to the right. The cumulated weight percentages are plotted along the vertical axis in the same manner. This method has been employed in the statistical analysis of the roundness and sphericity measurements made in this study by substituting for the Wentworth grade scale 0.05 intervals of roundness and sphericity values (Figure 3).

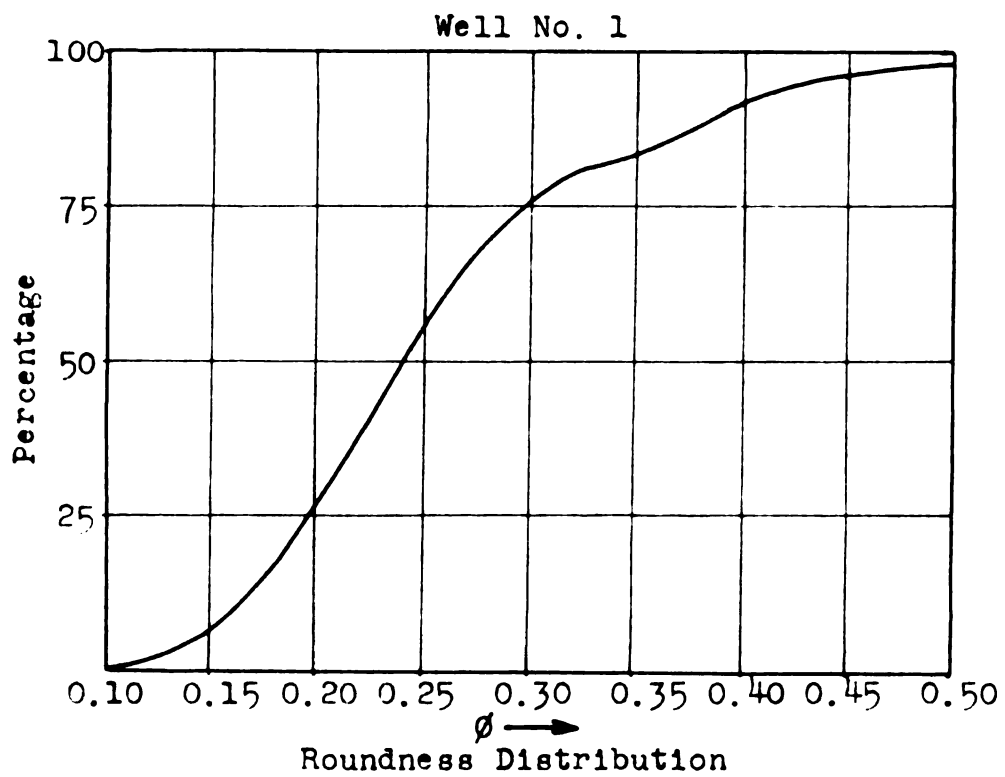
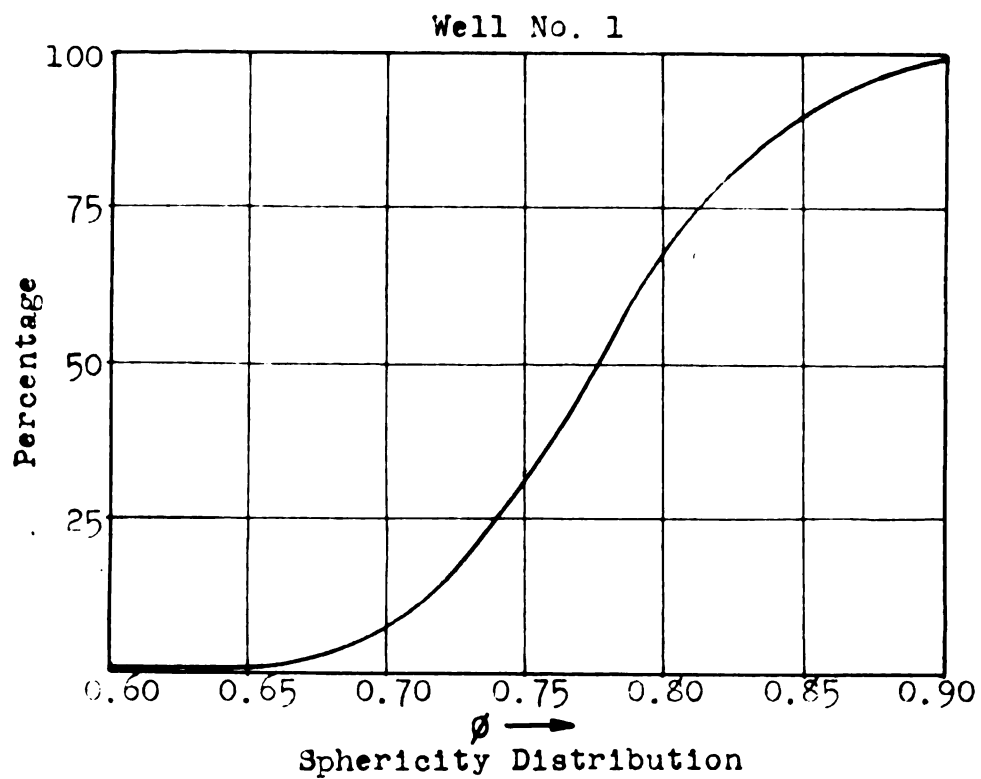


Figure 3.- Cumulative Curves of Roundness and Sphericity

The advantage of the "phi" scale is that quartile deviation, $QD\phi$, and quartile skewness, $Sk_g\phi$, may be compared both visually and logarithmically. However, when "phi" values are converted to geometric values based on the logarithmic scale to the base 10, a troublesome method of conversion must be employed. Although Krumbein (1938, p. 235) has provided conversion charts, these were not readable to the desired degree of accuracy. It was therefore found necessary to compute the So and Sk values in the following manner: In obtaining So from $QD\phi$, it was first necessary to find the $\log_{10} So$, the antilog then yields the So value. This means that $QD\phi$ equals $\log_2 QD_g$, and to find $\log_{10} QD_g$, one may use the relation $\log_{10} n$ equals $\log_{10} 2 \log_2 n$, where $\log_{10} 2$ equals 0.301. By substituting QD_g for n , and $QD\phi$ for $\log_2 QD_g$, there results $\log_{10} QD_g$ equals 0.301 $QD\phi$. Since $\log_{10} QD_g$ equals $\log_{10} So$, the antilog of $\log_{10} QD_g$ equals So .

In a manner similar to the above, the geometric skewness, or its square, which is Trask's skewness, Sk , may be found. The relationship used is $\log_{10} Sk$ equals $-0.602 Sk_g\phi$. The antilog of $\log_{10} Sk$ yields Sk . From Tables III and IV it may be noted that the sign before $Sk_g\phi$ is opposite to that before $\log_{10} Sk$. This is a convention in terms of the change of variables, and is consistent with the phi notation.

The curve, whether expressed in phi terms or in diameters, is, of course, skewed in the same direction; merely the sign given to the direction is changed. When the curve is symmetrical, the skewness is equal to unity. The values obtained, therefore, range from less than one to greater than one. The significance of this depends on the fact that numbers less than one present a reciprocal relation to the numbers greater than one. Reciprocal values, however, are not easily visualized; therefore, Trask introduced $\log_{10} S_k$, which is positive when S_k is greater than unity, and negative when S_k is less than unity.

TABLE III

ROUNDNESS CALCULATIONS FROM CUMULATIVE CURVES

Well No.	$Q_1\phi$	$Md\phi$	$Q_3\phi$	$QD\phi$	$\text{Log } S_o$	S_o	$S_{k_g}\phi$	$\text{Log } S_k$	S_k
1	1.97	2.37	2.97	0.500	0.151	1.416	+ .200	- .120	0.759
2	2.13	2.76	3.48	0.675	0.204	1.600	+ .090	- .054	0.883
3	2.14	2.61	3.40	0.625	0.188	1.542	+ .320	- .193	0.642
4	2.10	2.52	3.19	0.545	0.164	1.459	+ .250	- .150	0.708
5	2.08	2.48	2.93	0.425	0.128	1.343	+ .050	- .030	0.934
6	1.91	2.38	3.05	0.570	0.172	1.486	+ .200	- .120	0.759
7	2.82	3.16	3.78	0.480	0.144	1.393	+ .280	- .169	0.678
8	2.35	3.16	4.00	0.825	0.248	1.770	+ .030	- .018	0.960
9	1.98	2.33	3.03	0.525	0.158	1.439	+ .450	- .271	0.563
10	2.28	2.79	3.44	0.580	0.175	1.496	+ .140	- .084	0.825
11	2.20	2.75	3.56	0.680	0.205	1.603	+ .260	- .157	0.696
12	1.66	2.25	3.00	0.670	0.202	1.592	+ .160	- .096	0.802
13	1.87	2.24	2.85	0.490	0.148	1.406	+ .240	- .144	0.718
14	1.88	2.44	2.95	0.535	0.161	1.449	- .050	+ .030	1.072
15	1.96	2.43	3.07	0.555	0.167	1.469	+ .170	- .102	0.791
16	1.82	2.17	2.72	0.450	0.136	1.368	+ .200	- .120	0.759
17	2.25	2.80	3.73	0.740	0.223	1.671	+ .380	- .229	0.514
18	2.33	2.91	3.68	0.675	0.204	1.600	+ .190	- .114	0.770
19	2.00	2.41	2.89	0.445	0.134	1.361	+ .070	- .042	0.908
20	2.26	2.92	3.55	0.645	0.194	1.563	- .030	+ .018	1.042
21	2.35	2.77	3.37	0.510	0.154	1.426	+ .180	- .108	0.780
22	2.42	2.95	3.60	0.590	0.178	1.507	+ .120	- .072	0.847

TABLE III (Continued)

Well No.	$Q_1\phi$	$Md\phi$	$C_3\phi$	$QD\phi$	Log_{S_o}	S_o	$S_{k_g}\phi$	Log_{S_k}	S_k
23	2.17	2.65	3.20	0.515	0.155	1.429	+0.070	1.042	0.908
24	2.25	2.77	3.40	0.575	0.173	1.489	+0.110	-0.066	0.860
25	2.07	2.58	3.18	0.555	0.167	1.469	+0.090	-0.054	0.883
26	2.47	2.87	3.78	0.655	0.197	1.574	+0.510	-0.307	0.494
27	2.18	2.53	3.07	0.445	0.134	1.361	+0.190	-0.114	0.770
28	2.23	2.77	3.59	0.680	0.205	1.603	+0.280	-0.169	0.677
29	2.25	2.85	3.80	0.775	0.234	1.714	+0.350	-0.211	0.615
30	1.95	2.53	3.00	0.525	0.158	1.439	-0.090	+0.054	1.132
31	2.14	2.59	3.06	0.460	0.138	1.374	+0.020	-0.012	0.759
32	2.07	2.55	3.13	0.530	0.155	1.429	+0.100	-0.060	0.871
33	2.19	2.80	3.68	0.745	0.224	1.675	+0.270	-0.163	0.687
34	2.55	3.05	3.62	0.535	0.161	1.449	+0.070	-0.042	0.908
35	2.10	2.58	3.26	0.580	0.175	1.496	+0.200	-0.120	0.759
36	1.44	1.77	2.30	0.430	0.130	1.349	+0.200	-0.120	0.759
37	2.37	2.85	3.30	0.465	0.140	1.380	-0.030	+0.018	1.042
38	2.32	2.85	3.71	0.695	0.210	1.622	+0.330	-0.199	0.633
39	2.33	2.93	3.50	0.585	0.176	1.500	-0.030	+0.018	1.042
40	2.46	3.03	3.48	0.510	0.154	1.426	-0.100	+0.060	1.148

TABLE IV

SPHERICITY CALCULATIONS FROM CUMULATIVE CURVES

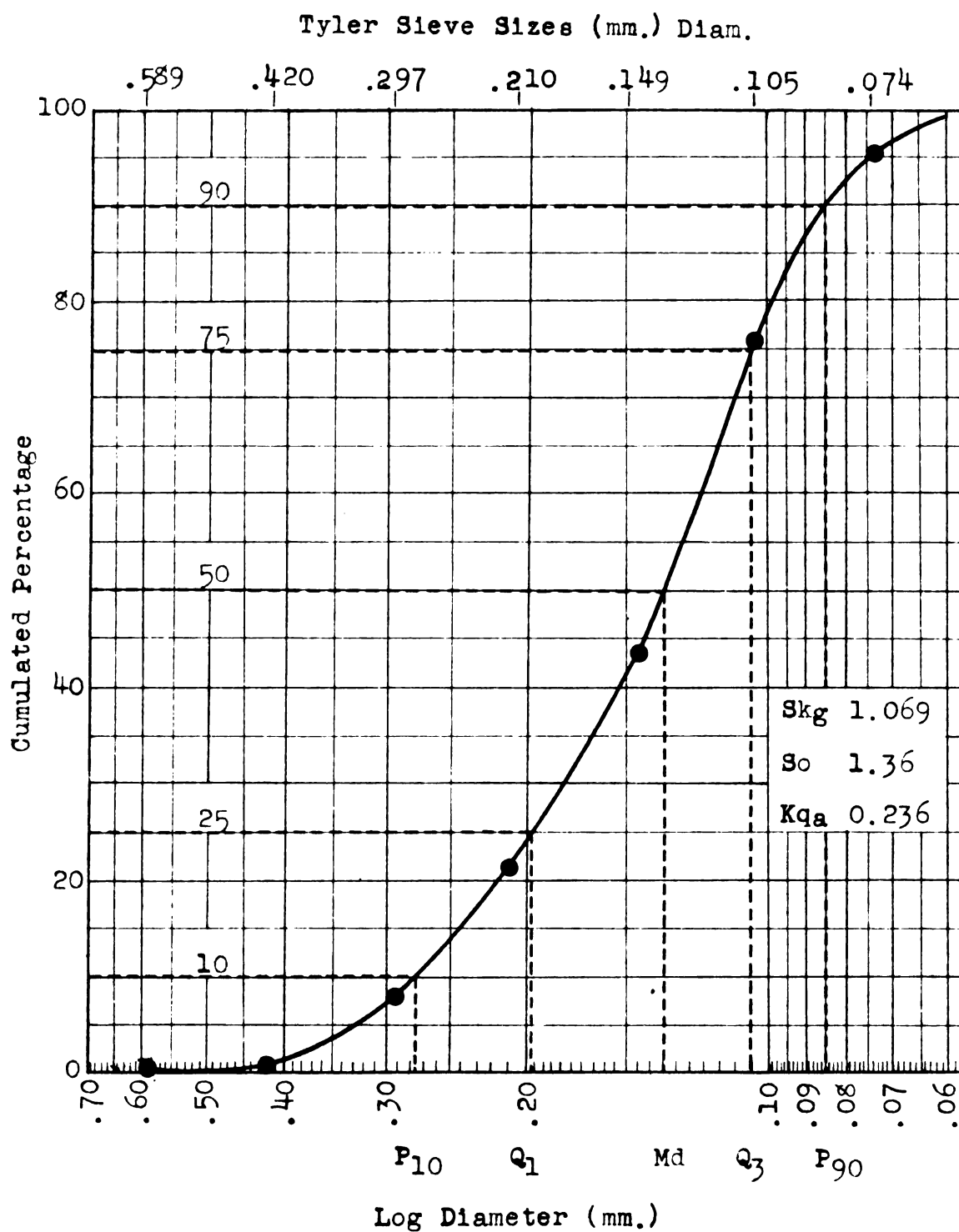
Well No.	$Q_1\phi$	$Md\phi$	$Q_3\phi$	$QD\phi$	$\text{Log } S_o$	S_o	$S_{k_g}\phi$	$\text{Log } S_k$	S_k
1	7.36	7.73	8.13	0.385	0.116	1.306	+0.030	-.018	0.960
2	7.52	8.02	8.48	0.480	0.145	1.396	-.040	+0.024	1.058
3	7.75	8.06	8.45	0.350	0.105	1.274	+0.080	-.048	0.895
4	7.26	7.87	8.35	0.445	0.134	1.361	-.130	+0.078	1.197
5	7.64	7.93	8.35	0.355	0.107	1.279	+0.130	-.078	0.836
6	7.50	7.91	8.28	0.390	0.118	1.312	-.040	+0.024	1.057
7	7.62	8.23	8.42	0.400	0.120	1.318	-.420	+0.253	1.791
8	7.53	8.07	8.34	0.405	0.122	1.324	-.270	+0.163	1.457
9	7.54	7.95	8.37	0.415	0.125	1.334	+0.010	-.006	0.986
10	7.58	7.92	8.36	0.390	0.117	1.309	+0.100	-.060	0.871
11	7.62	8.13	8.34	0.360	0.108	1.282	-.300	+0.180	1.515
12	7.54	8.06	8.48	0.470	0.142	1.387	-.100	+0.060	1.149
13	7.70	8.04	8.40	0.350	0.105	1.274	+0.020	-.012	0.974
14	7.39	7.86	8.24	0.425	0.128	1.343	-.090	+0.054	1.132
15	7.60	7.95	8.29	0.345	0.104	1.271	-.010	+0.006	1.014
16	7.50	7.96	8.34	0.420	0.126	1.337	-.080	+0.048	1.117
17	7.44	7.64	8.20	0.380	0.114	1.300	+0.360	-.217	0.606
18	7.67	8.00	8.43	0.380	0.114	1.300	+0.100	-.060	0.871
19	7.57	7.98	8.31	0.370	0.112	1.294	-.080	+0.048	1.117
20	7.78	8.20	8.37	0.295	0.089	1.227	-.250	+0.150	1.413
21	7.54	7.93	8.35	0.405	0.122	1.324	+0.030	-.018	0.960
22	7.61	8.04	8.31	0.350	0.105	1.274	-.160	+0.096	1.247

TABLE IV (Continued)

Well No.	$Q_1\phi$	$Md\phi$	$Q_3\phi$	$CD\phi$	$\text{Log } S_o$	S_o	$Sk_g\phi$	$\text{Log } Sk$	Sk
23	7.64	8.11	8.40	0.380	0.114	1.300	-.180	+.108	1.282
24	7.50	7.94	8.95	0.725	0.218	1.652	+.370	-.223	0.599
25	7.58	8.02	8.30	0.360	0.108	1.282	-.160	+.096	1.247
26	7.50	7.95	8.36	0.400	0.120	1.318	-.040	+.024	1.057
27	7.50	7.93	8.32	0.410	0.124	1.330	-.040	+.024	1.057
28	7.62	8.13	8.37	0.375	0.113	1.297	-.270	+.163	1.455
29	7.50	7.96	8.31	0.405	0.122	1.324	-.110	+.066	1.164
30	7.37	8.00	8.43	0.530	0.160	1.445	-.200	+.120	1.318
31	7.60	8.02	8.43	0.415	0.125	1.334	-.010	+.006	1.014
32	7.50	7.92	8.31	0.405	0.122	1.324	-.110	+.066	1.164
33	7.57	7.92	8.31	0.370	0.112	1.294	-.040	+.024	1.057
34	7.37	8.00	8.27	0.450	0.136	1.368	-.460	+.277	1.892
35	7.49	7.81	8.29	0.400	0.120	1.318	+.160	-.096	0.802
36	7.29	7.69	8.14	0.425	0.128	1.343	+.050	-.030	0.934
37	7.52	8.03	8.46	0.470	0.142	1.387	-.080	+.048	1.117
38	7.70	8.06	8.41	0.355	0.107	1.279	-.010	+.006	1.014
39	7.47	7.94	8.36	0.445	0.134	1.361	-.050	+.030	1.072
40	7.55	8.00	8.43	0.440	0.132	1.355	-.020	+.012	1.028

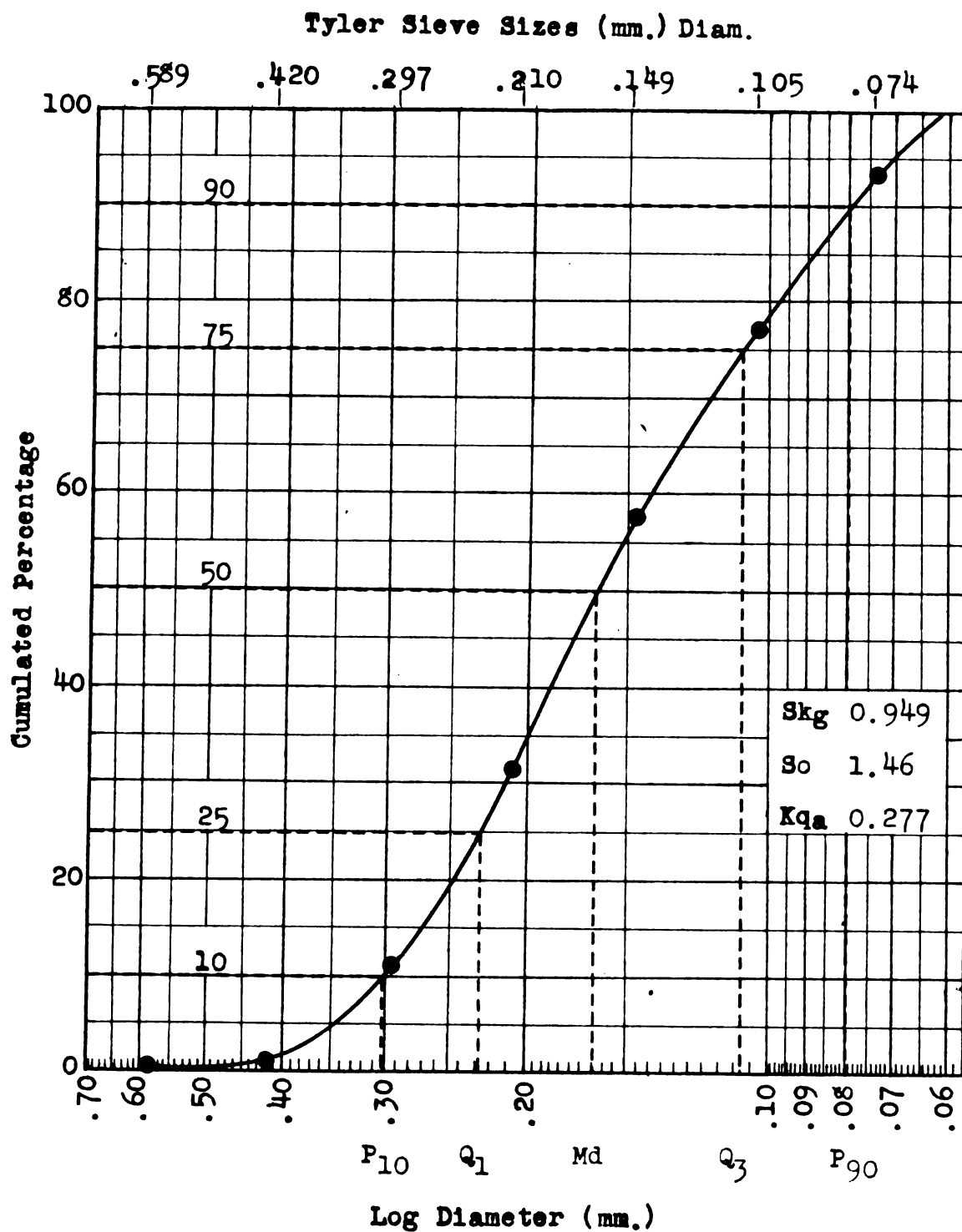
WELL #1, Sec. A

Cumulative Curve of Sieve Analysis Weights



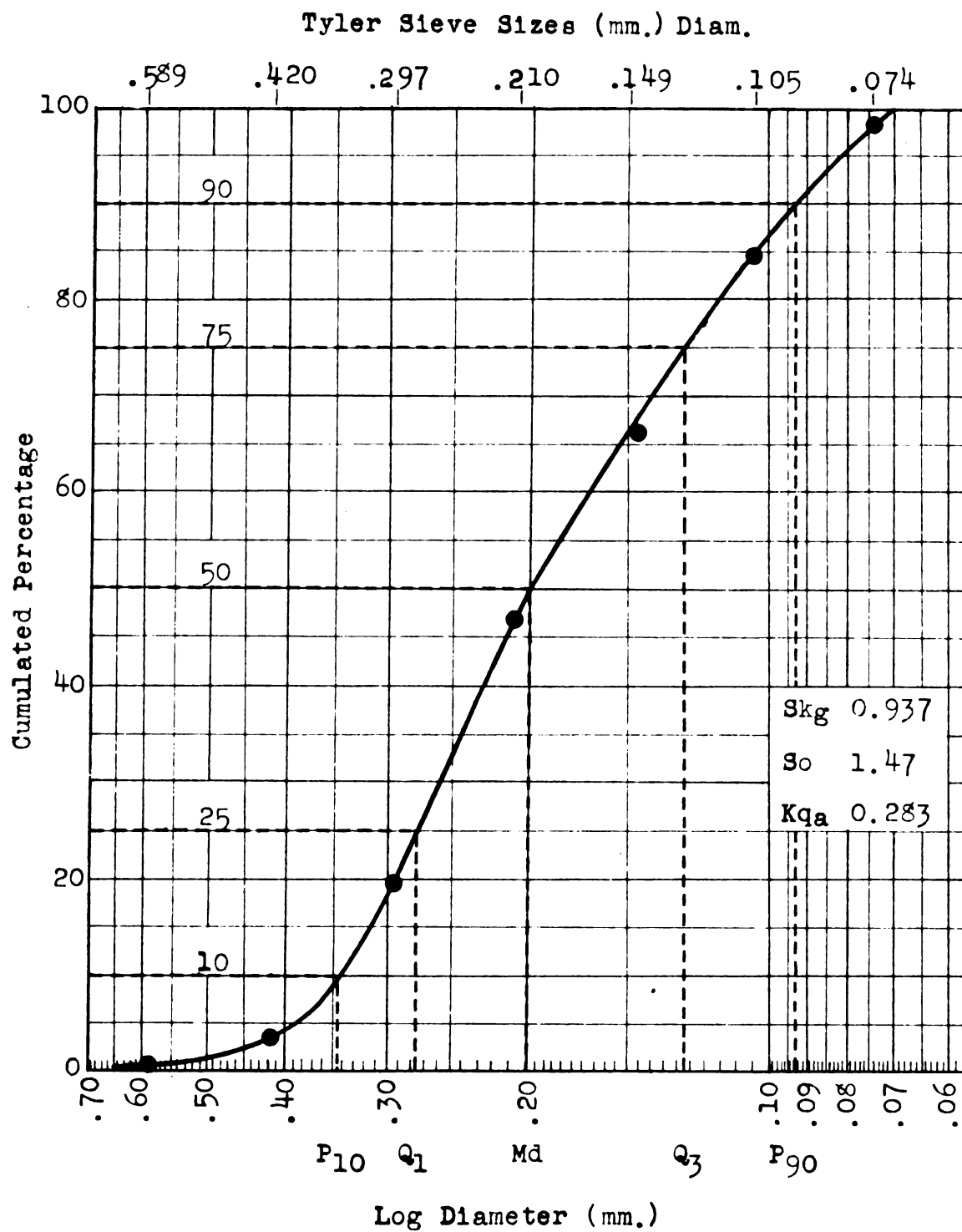
WELL #2, Sec. A

Cumulative Curve of Sieve Analysis Weights



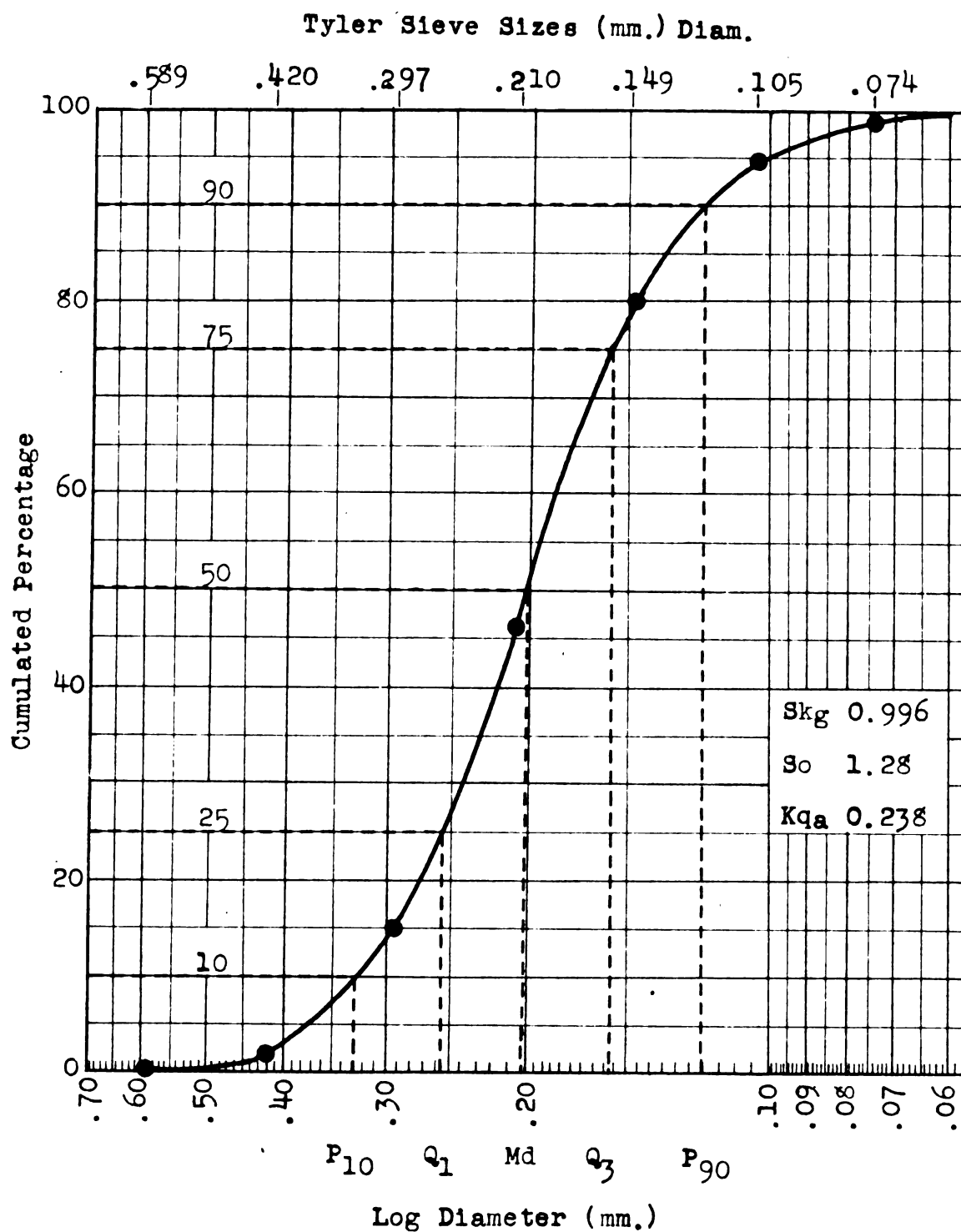
WELL #3, Sec. A

Cumulative Curve of Sieve Analysis Weights



WELL #4, Sec. A

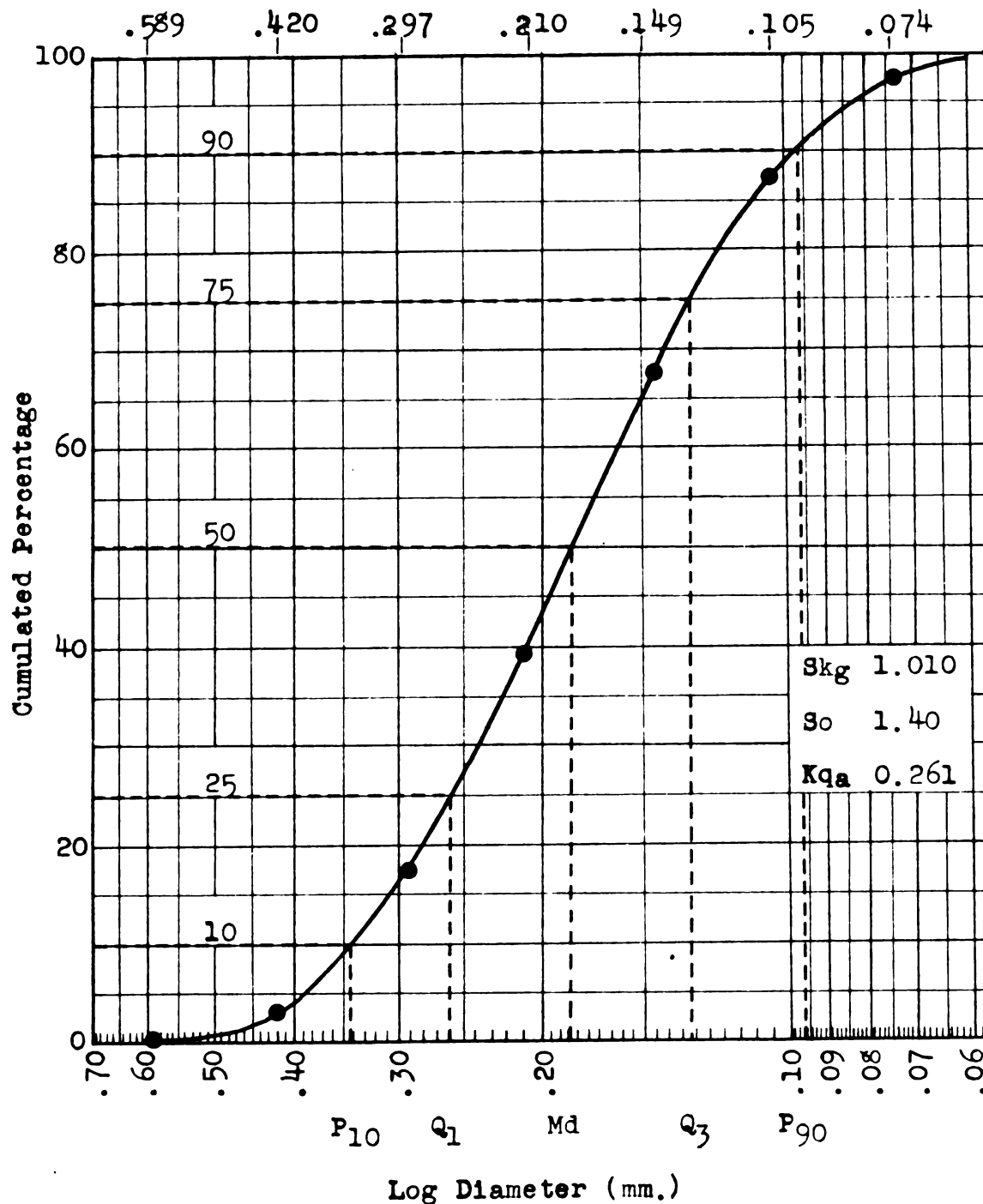
Cumulative Curve of Sieve Analysis Weights



WELL #5, Sec. A

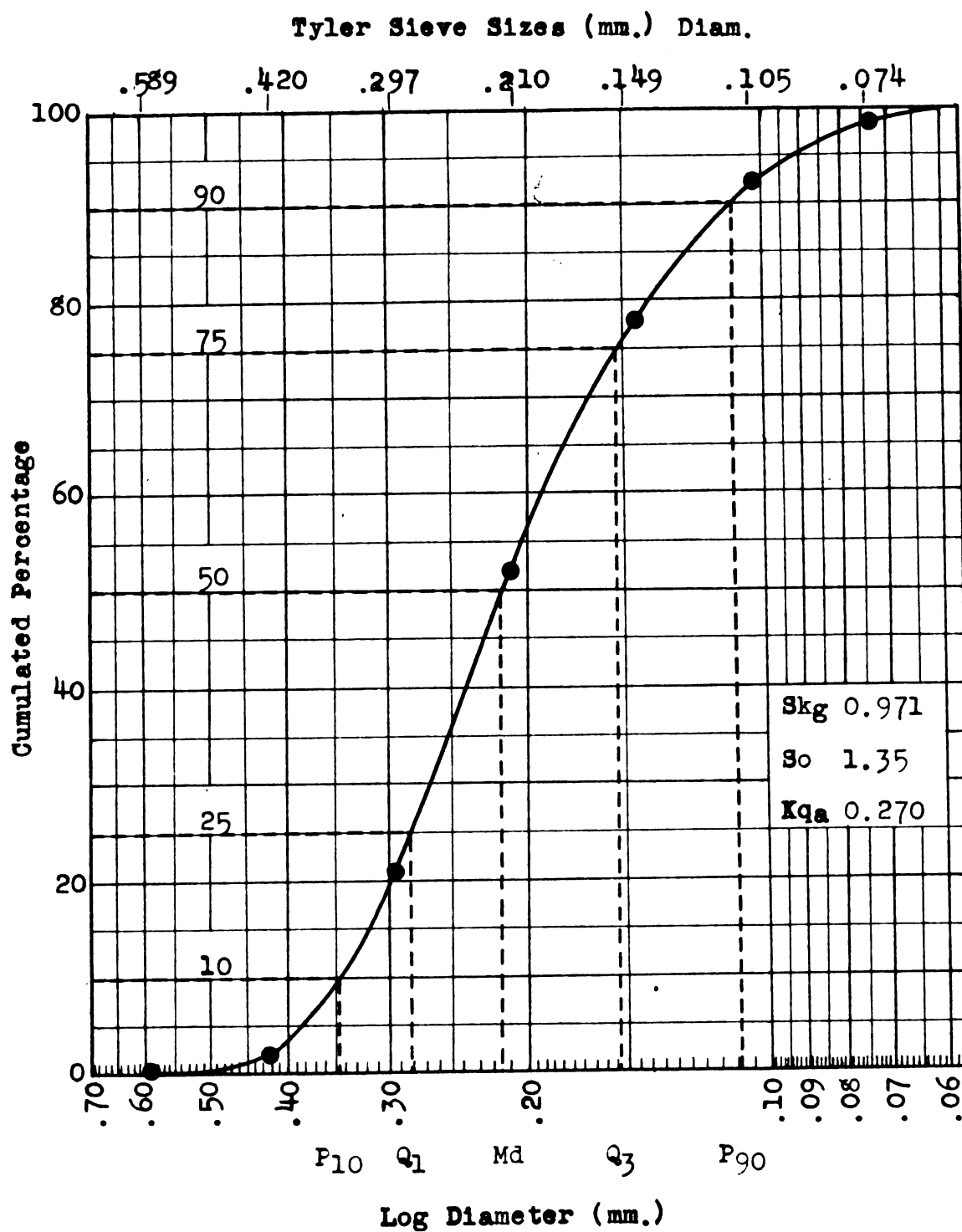
Cumulative Curve of Sieve Analysis Weights

Tyler Sieve Sizes (mm.) Diam.



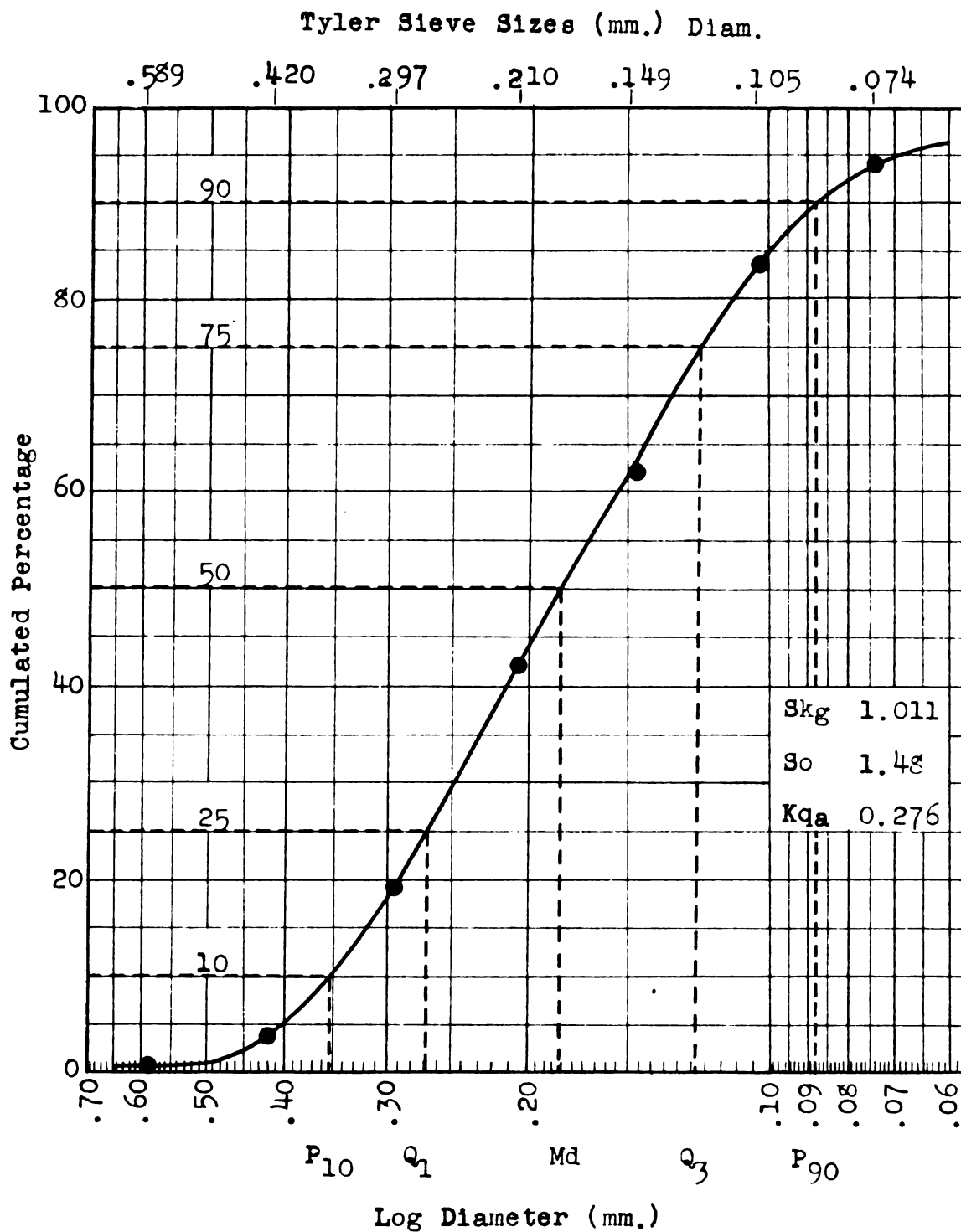
WELL #6, Sec. A

Cumulative Curve of Sieve Analysis Weights



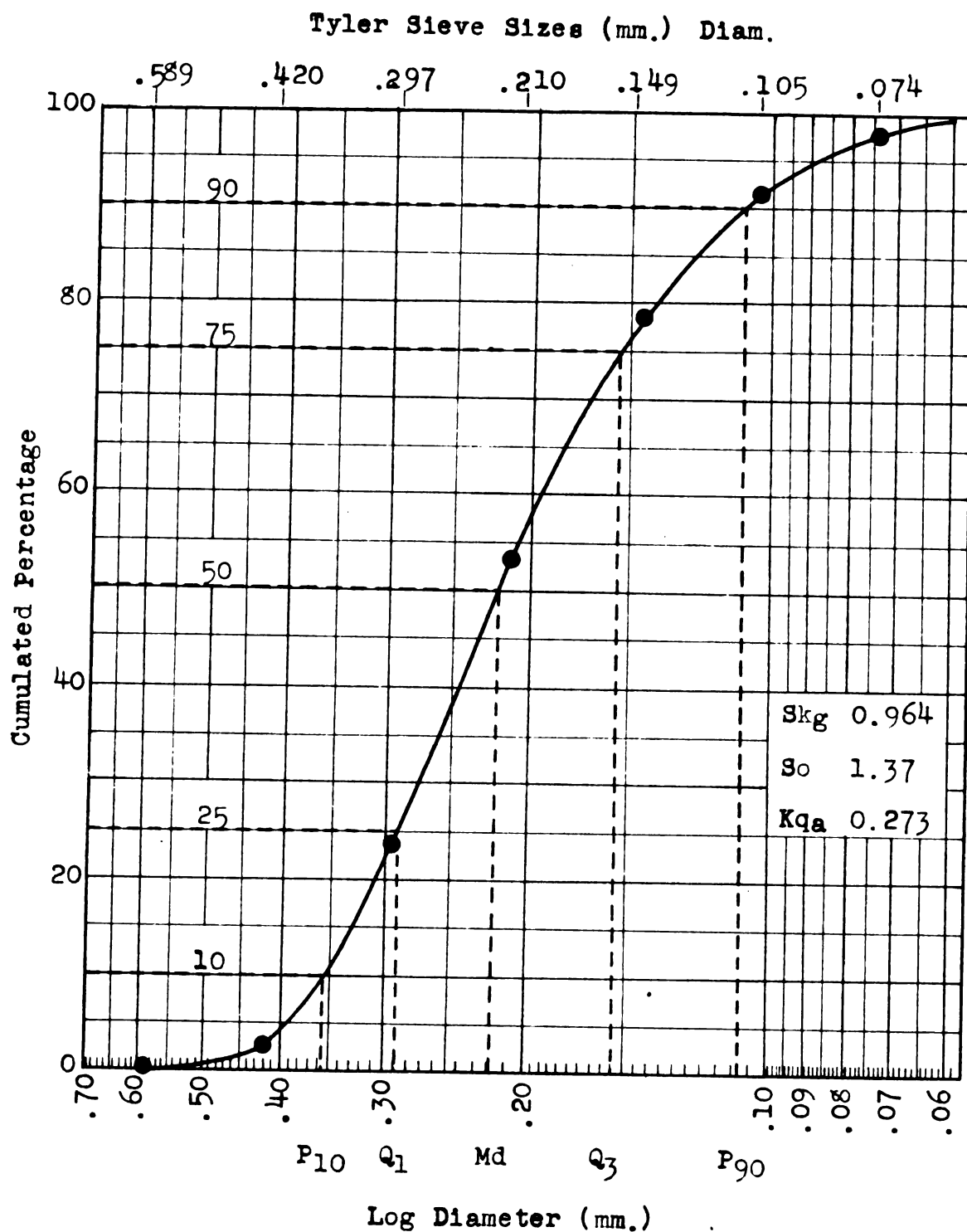
WELL #7, Sec. B

Cumulative Curve of Sieve Analysis Weights



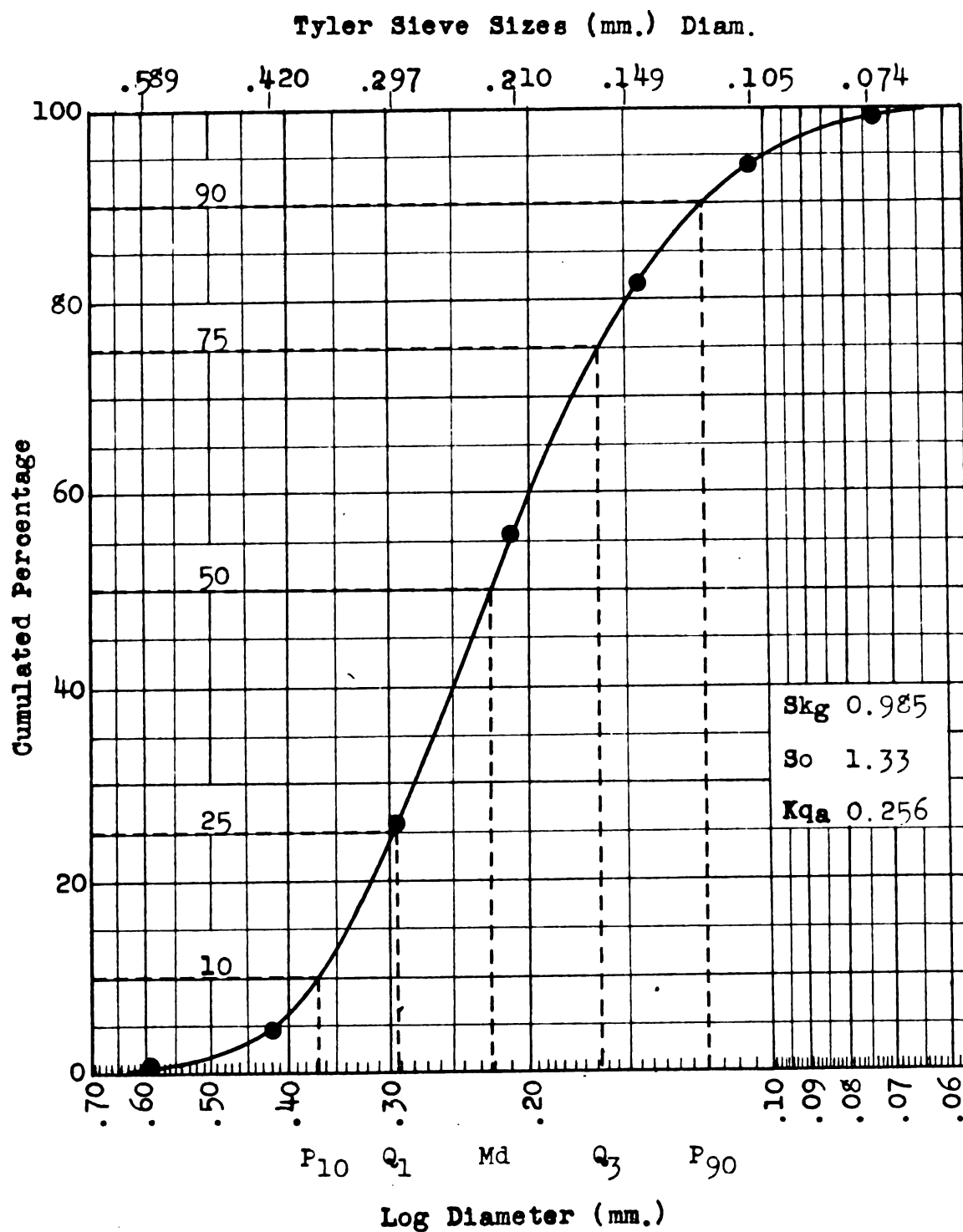
WELL #8, Sec. B

Cumulative Curve of Sieve Analysis Weights



WELL #9, Sec. B

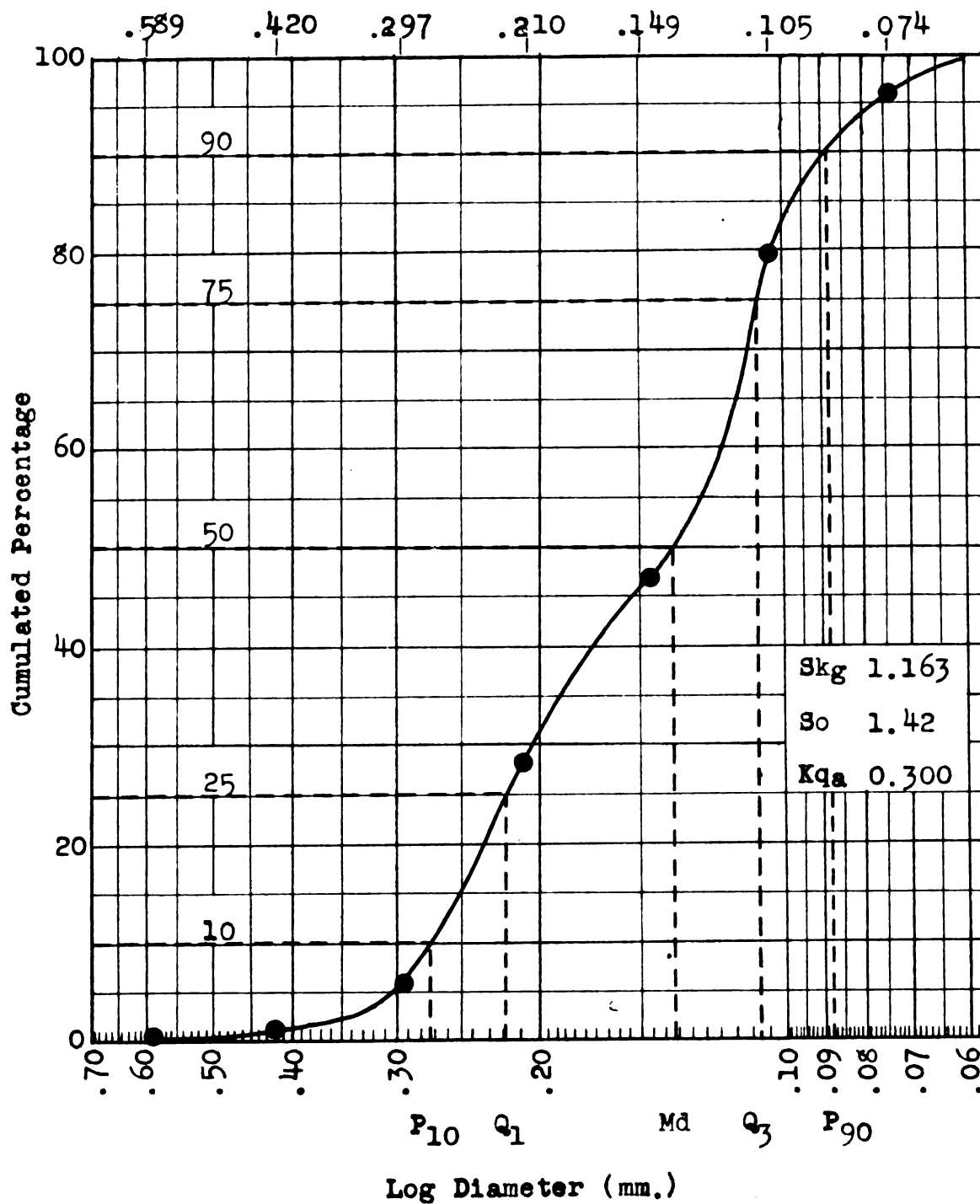
Cumulative Curve of Sieve Analysis Weights



WELL #10, Sec. B

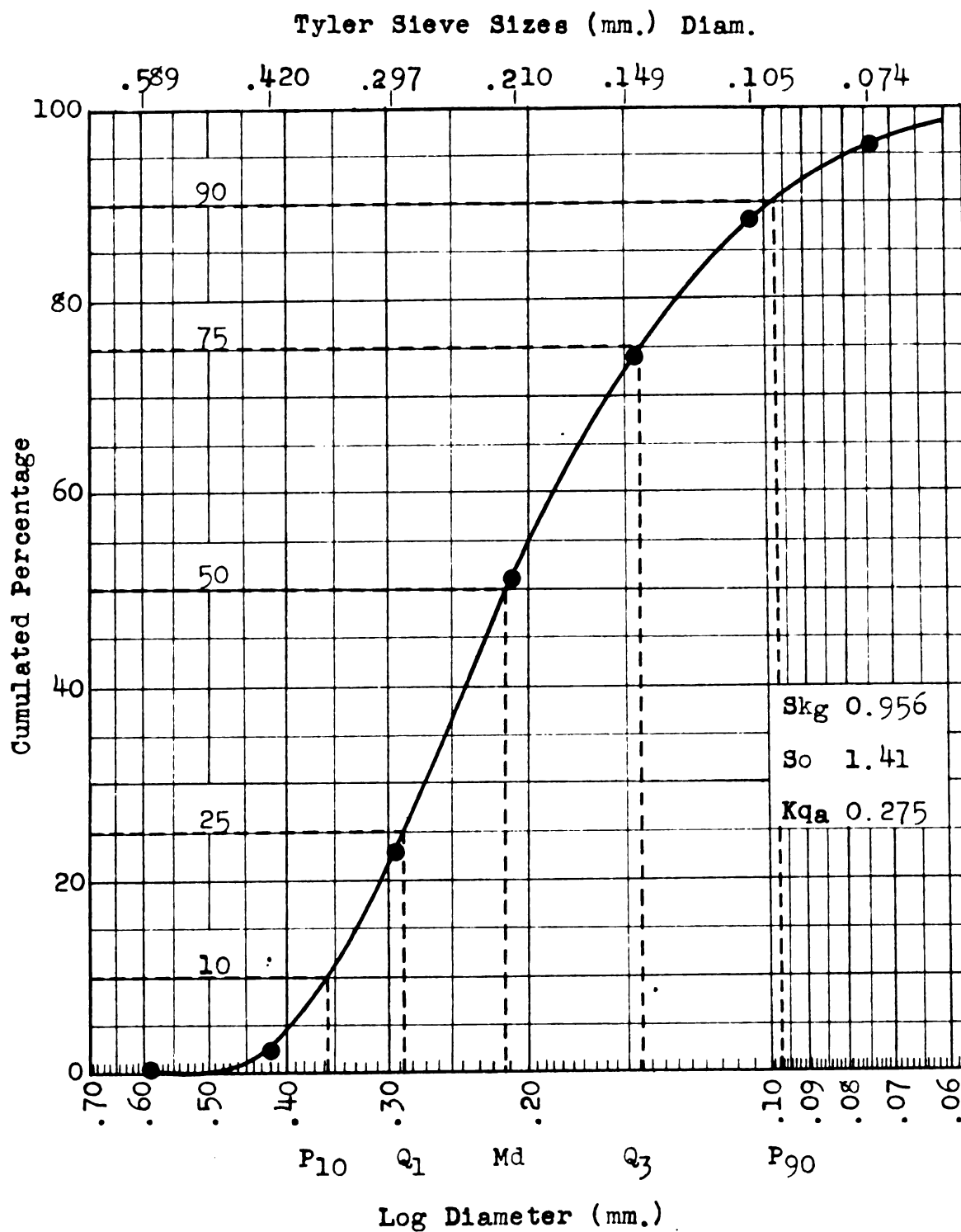
Cumulative Curve of Sieve Analysis Weights

Tyler Sieve Sizes (mm.) Diam.



WELL #11, Sec. B

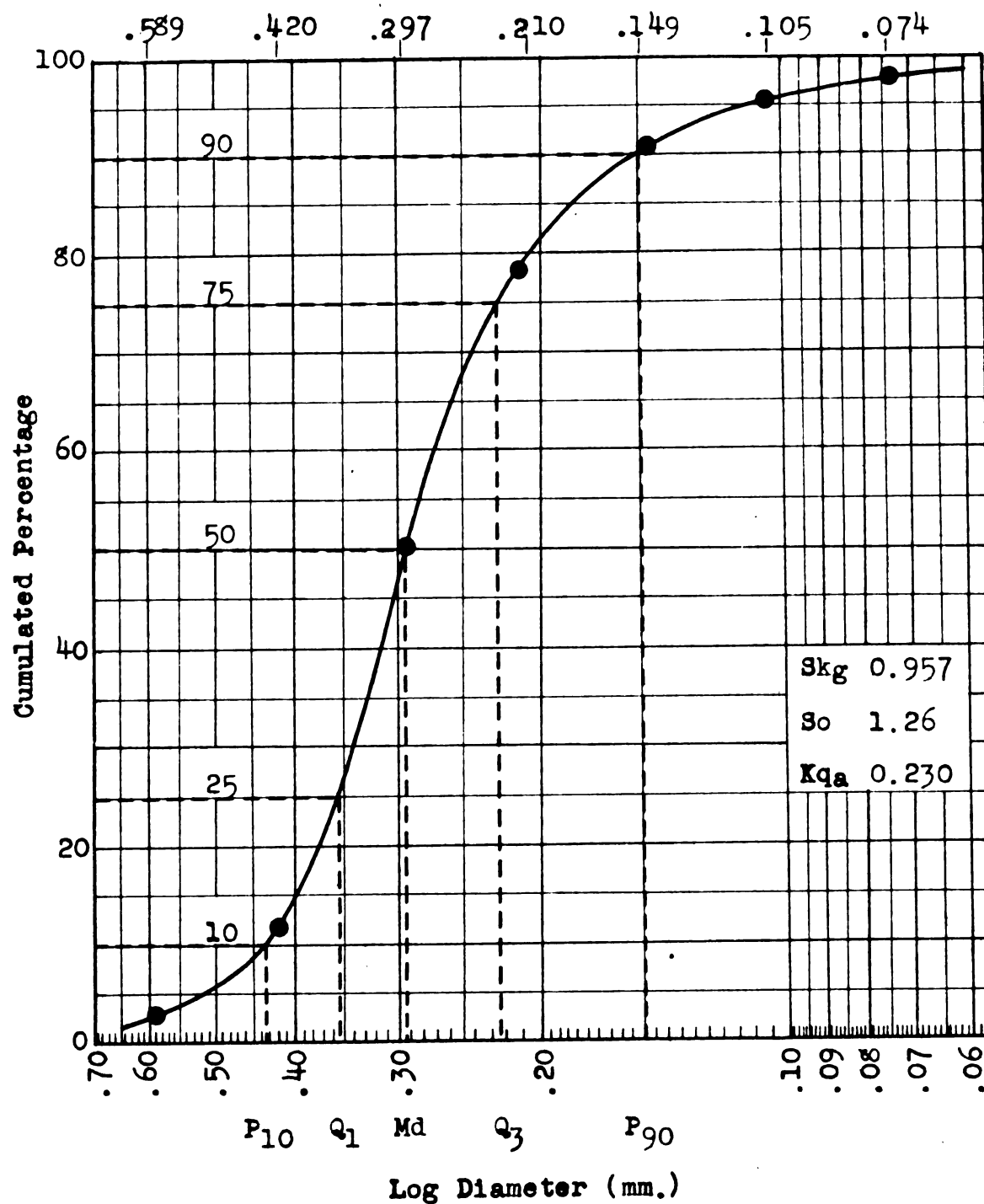
Cumulative Curve of Sieve Analysis Weights



WELL #12, Sec. B

Cumulative Curve of Sieve Analysis Weights

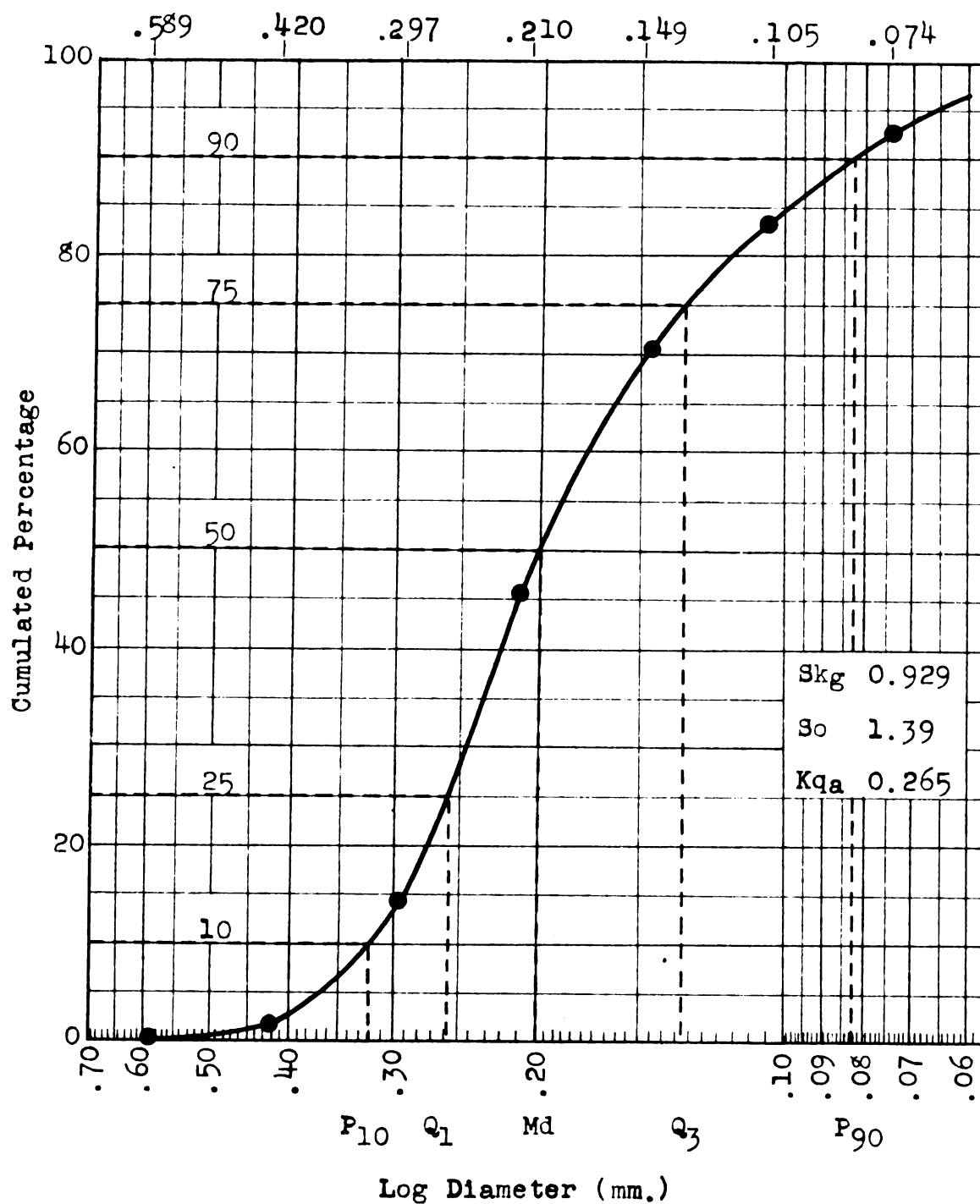
Tyler Sieve Sizes (mm.) Diam.



WELL #13, Sec. C

Cumulative Curve of Sieve Analysis Weights

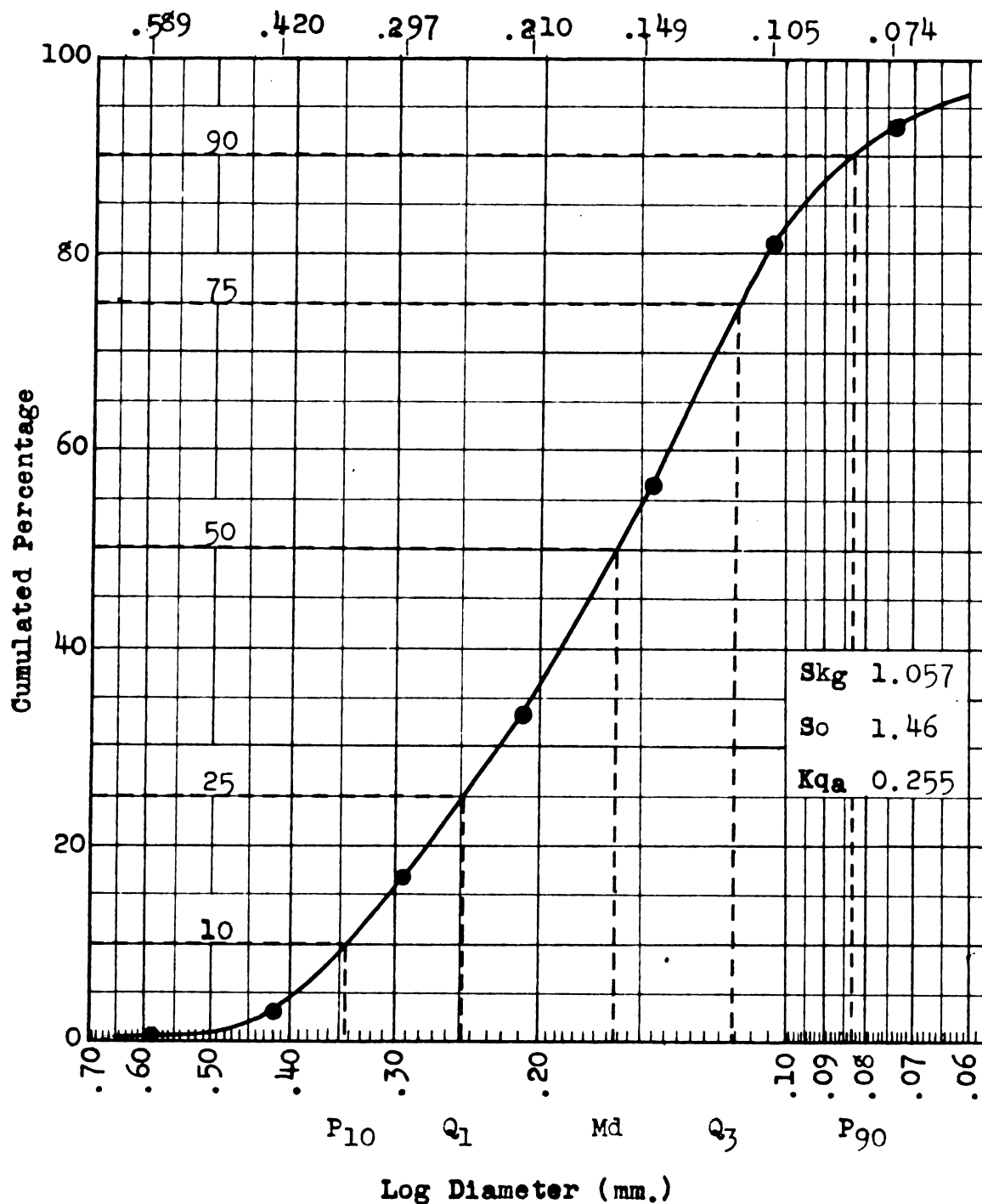
Tyler Sieve Sizes (mm.) Diam.



WELL #14, Sec. C

Cumulative Curve of Sieve Analysis Weights

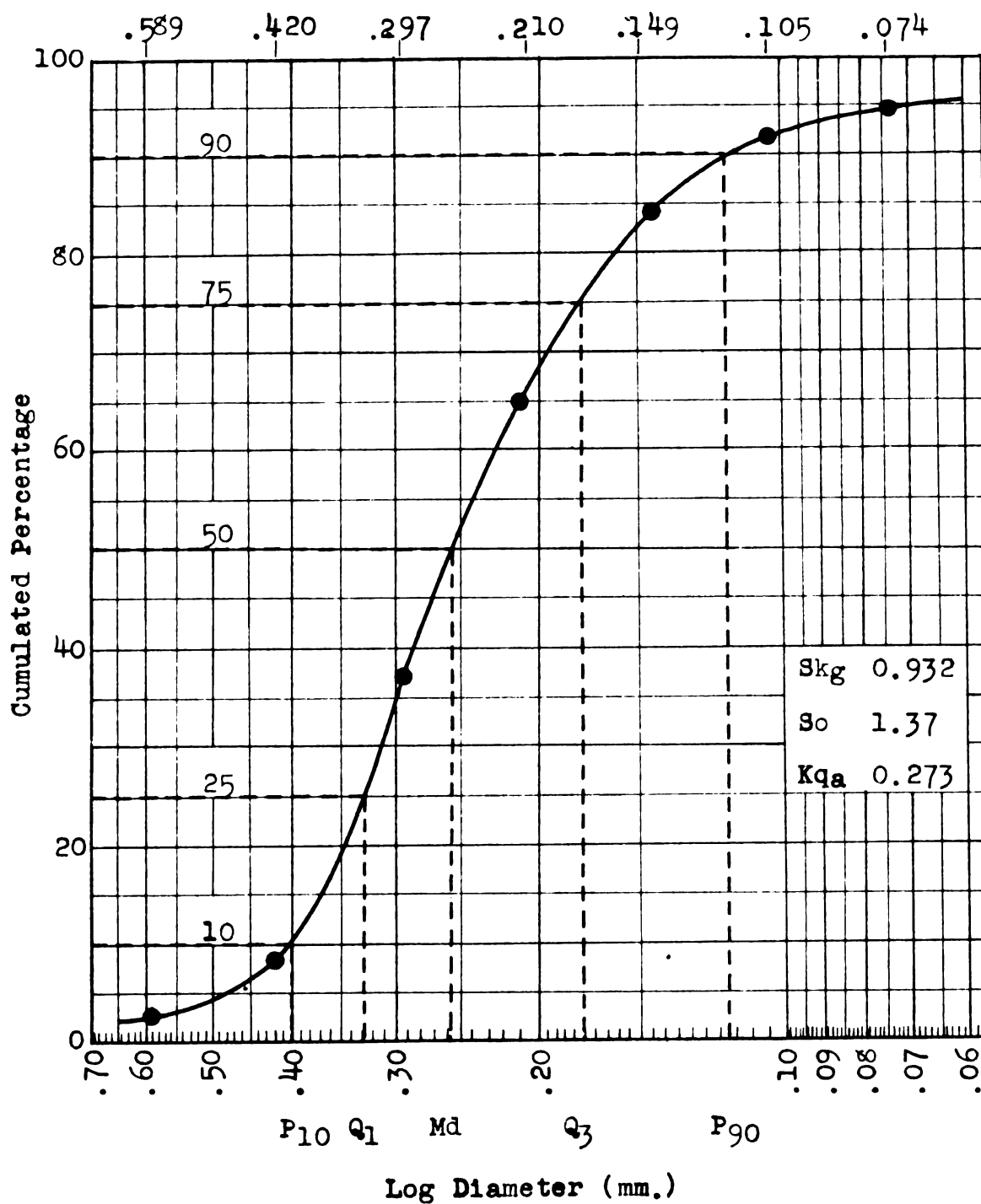
Tyler Sieve Sizes (mm.) Diam.



WELL #15, Sec. C

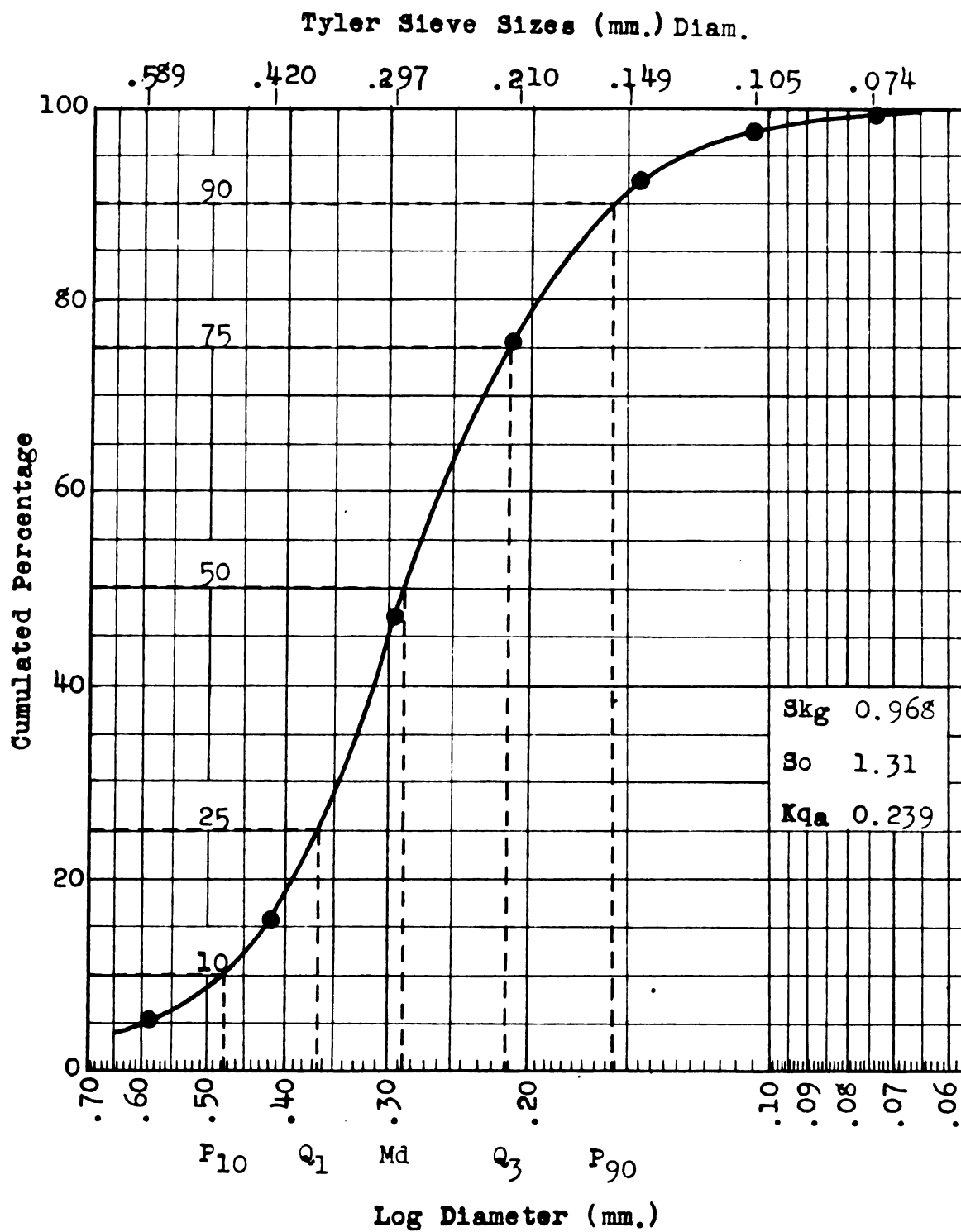
Cumulative Curve of Sieve Analysis Weights

Tyler Sieve Sizes (mm.) Diam.



WELL #16, Sec. C

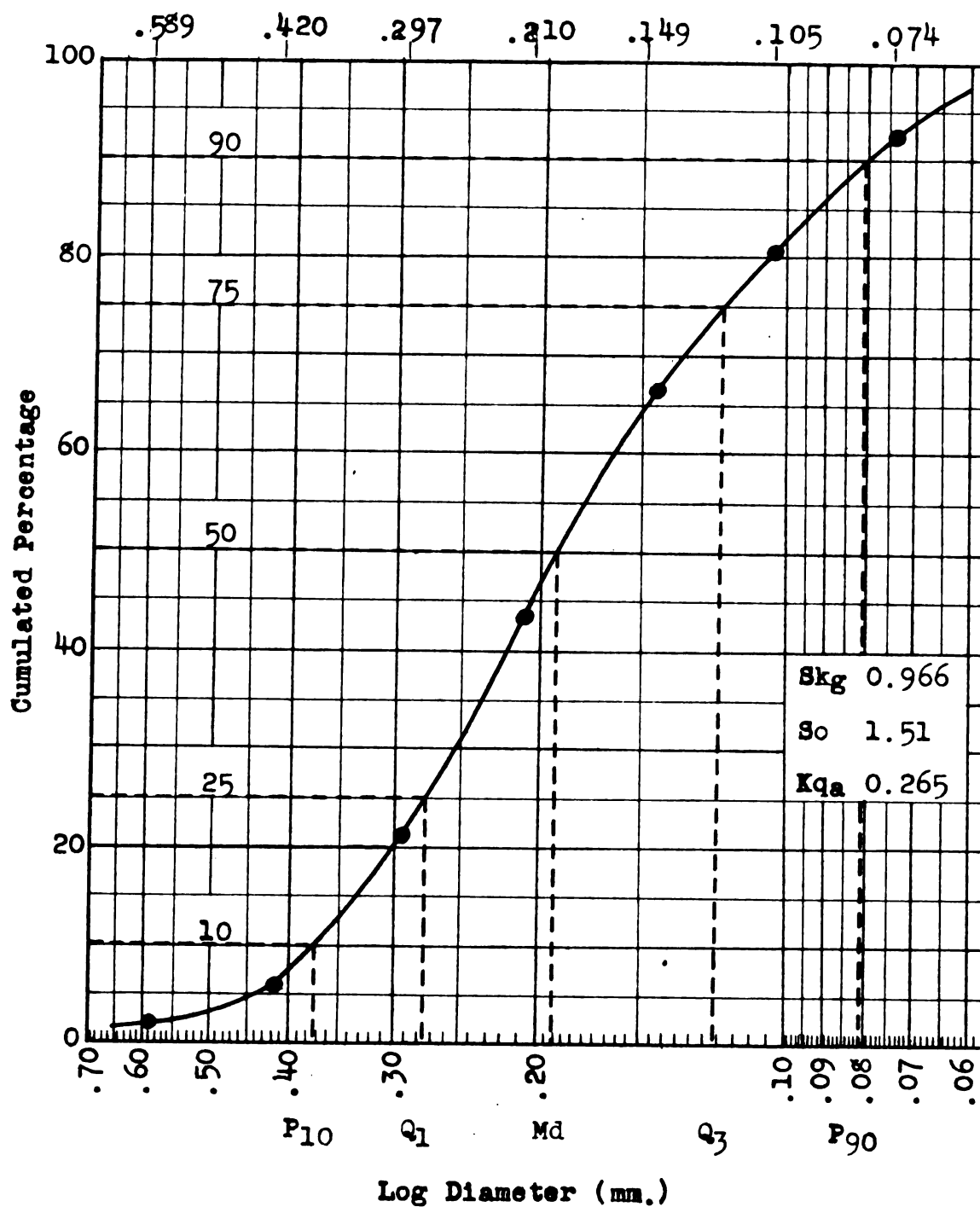
Cumulative Curve of Sieve Analysis Weights



WELL #17, Sec. D

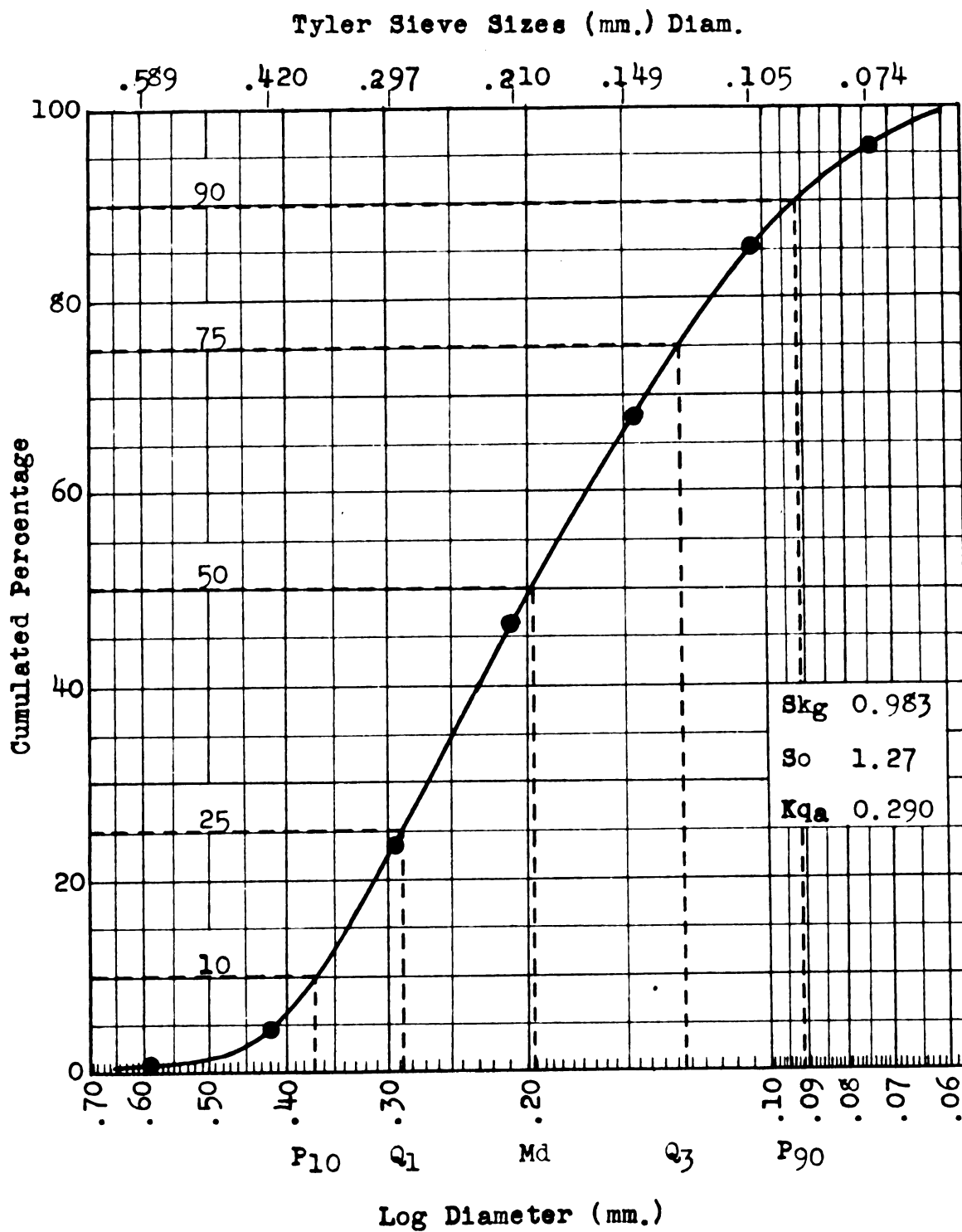
Cumulative Curve of Sieve Analysis Weights

Tyler Sieve Sizes (mm.) Diam.



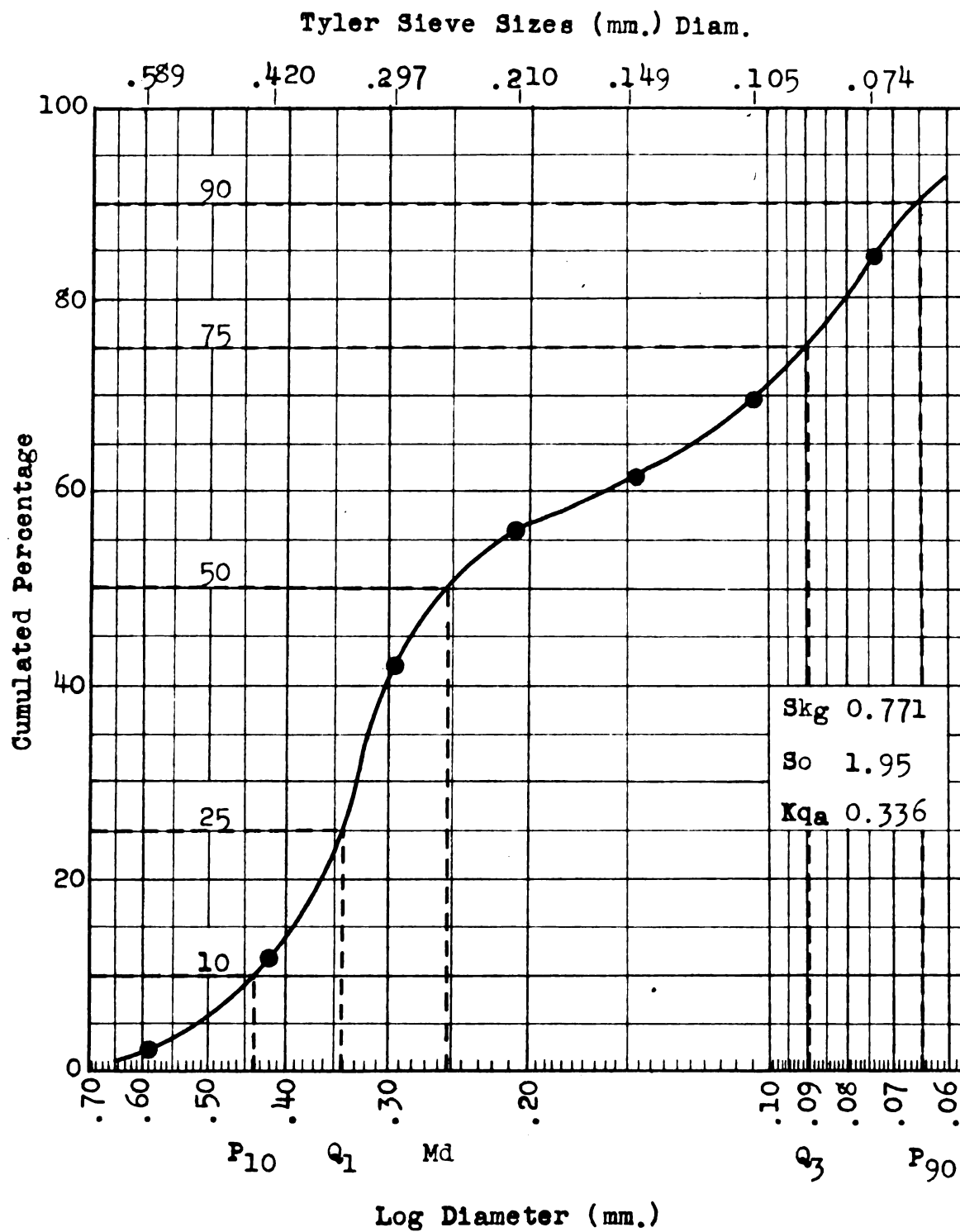
WELL #18, Sec. D

Cumulative Curve of Sieve Analysis Weights



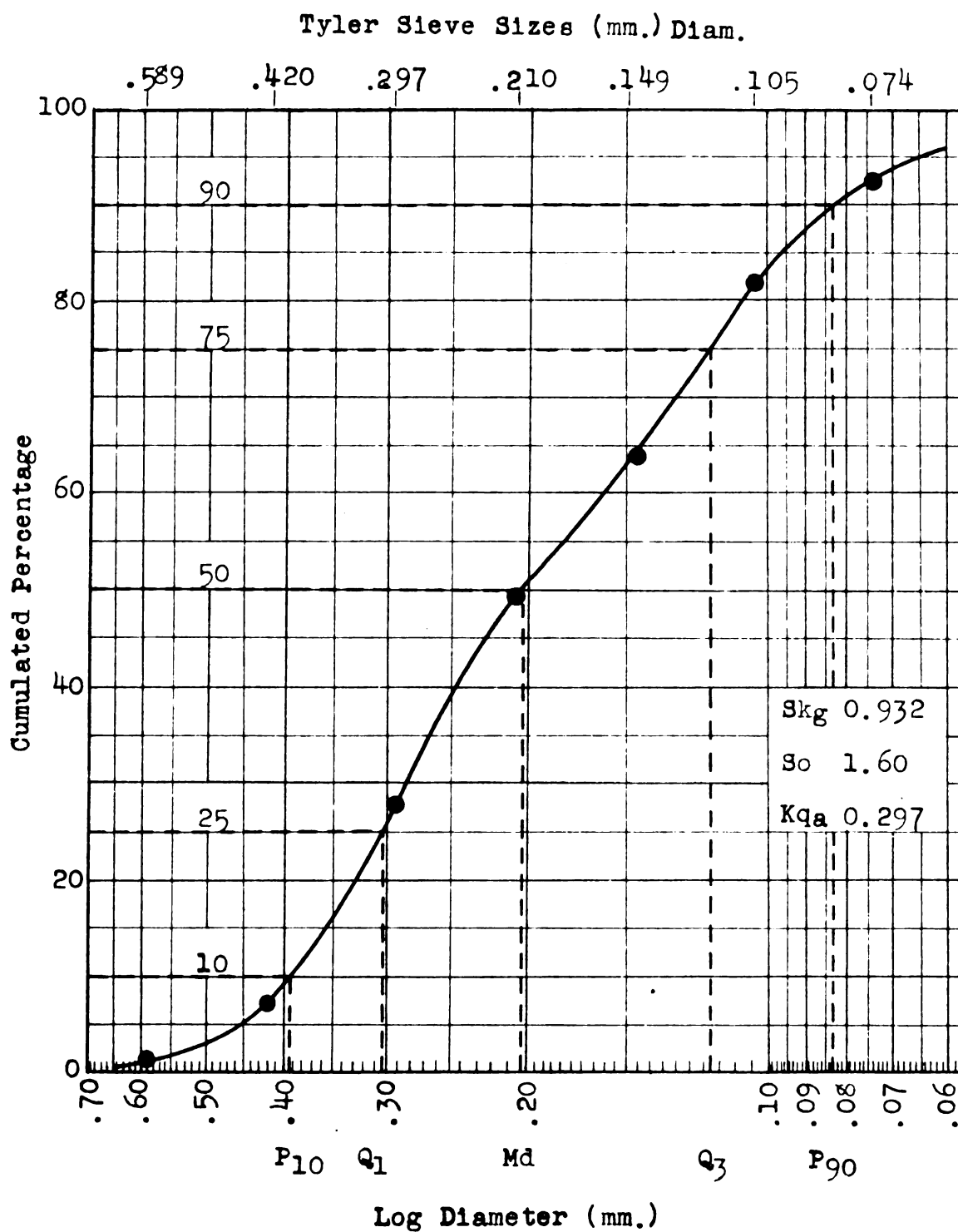
WELL #19, Sec. D

Cumulative Curve of Sieve Analysis Weights



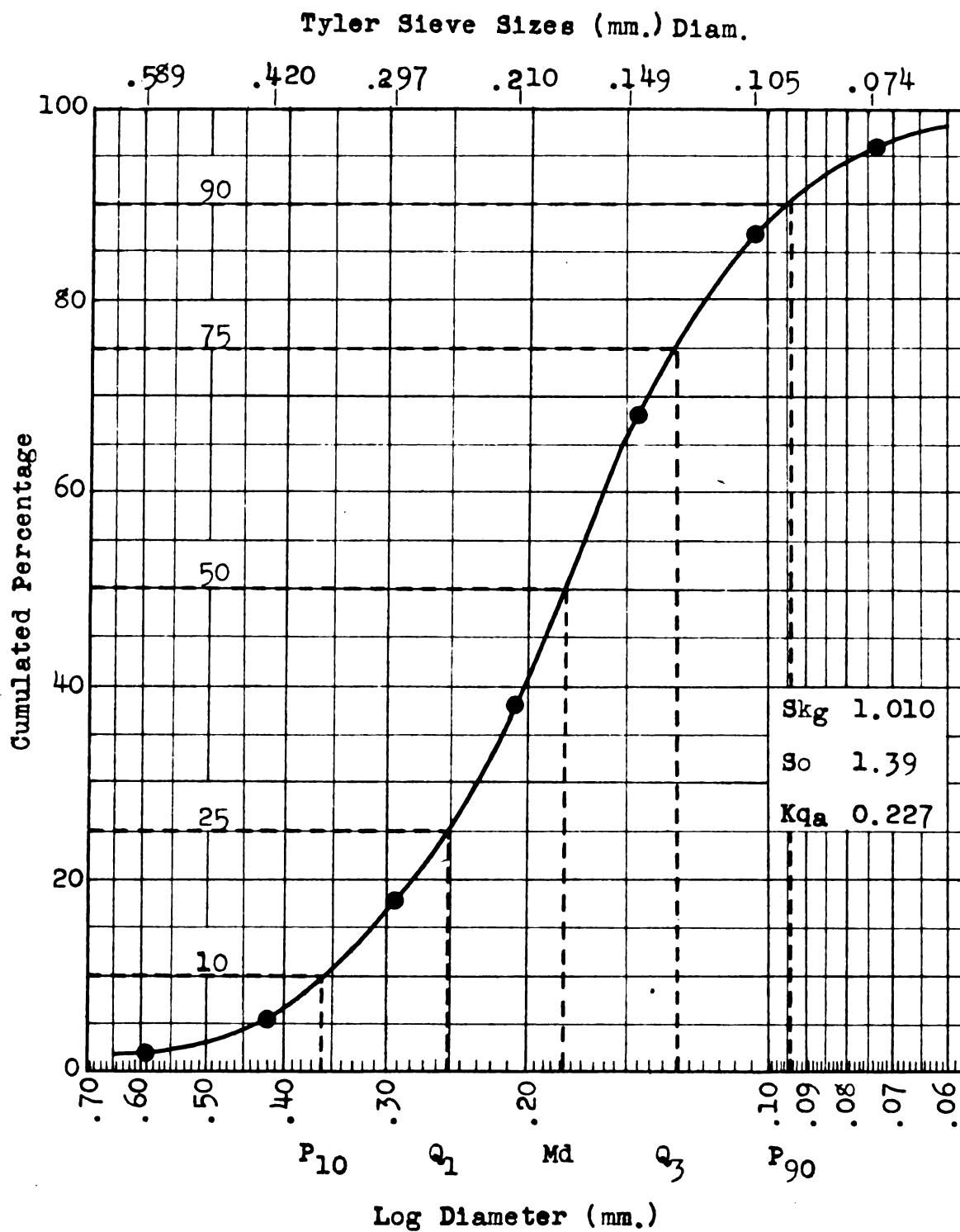
WELL #20, Sec. D

Cumulative Curve of Sieve Analysis Weights



WELL # 21, Sec. D

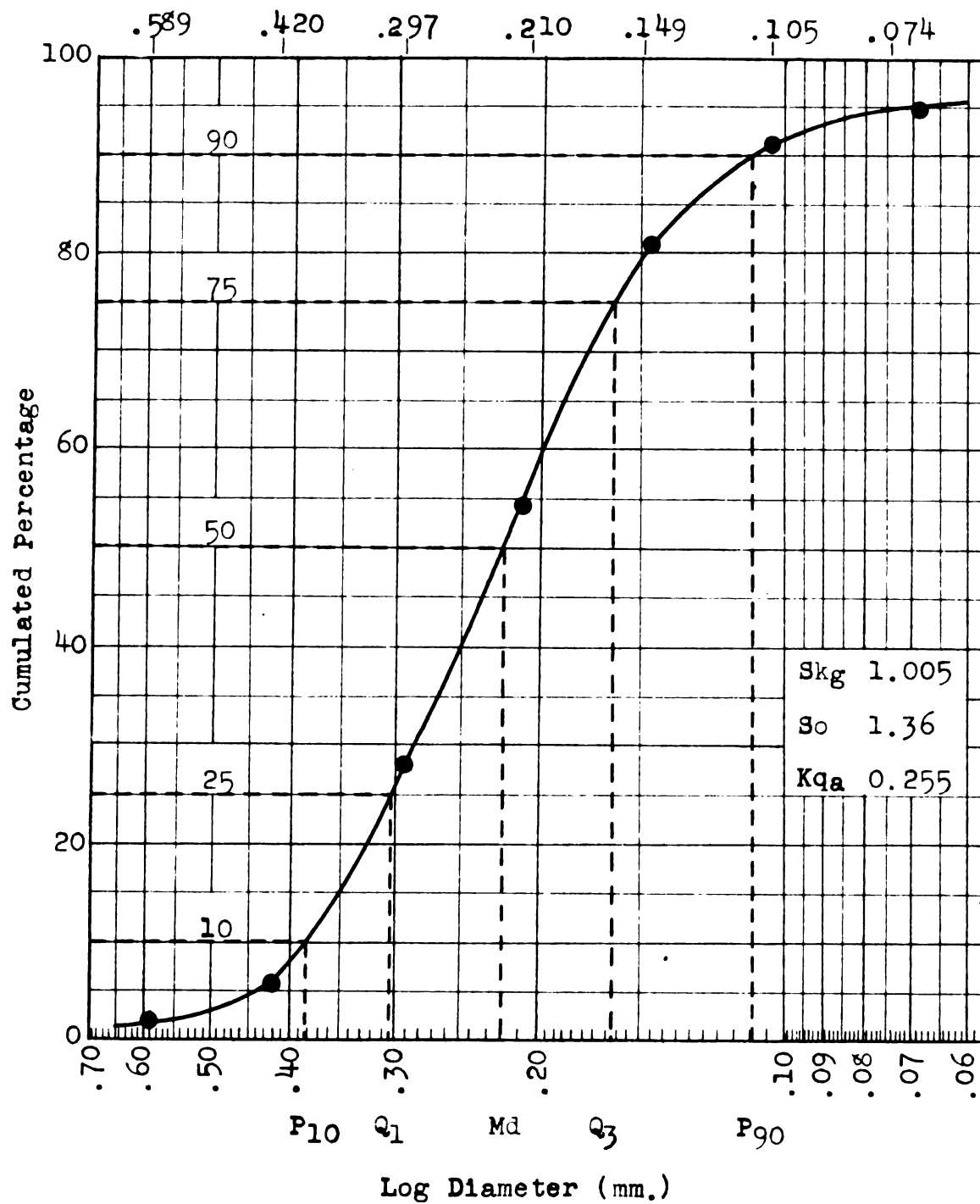
Cumulative Curve of Sieve Analysis Weights



WELL #22, Sec. D

Cumulative Curve of Sieve Analysis Weights

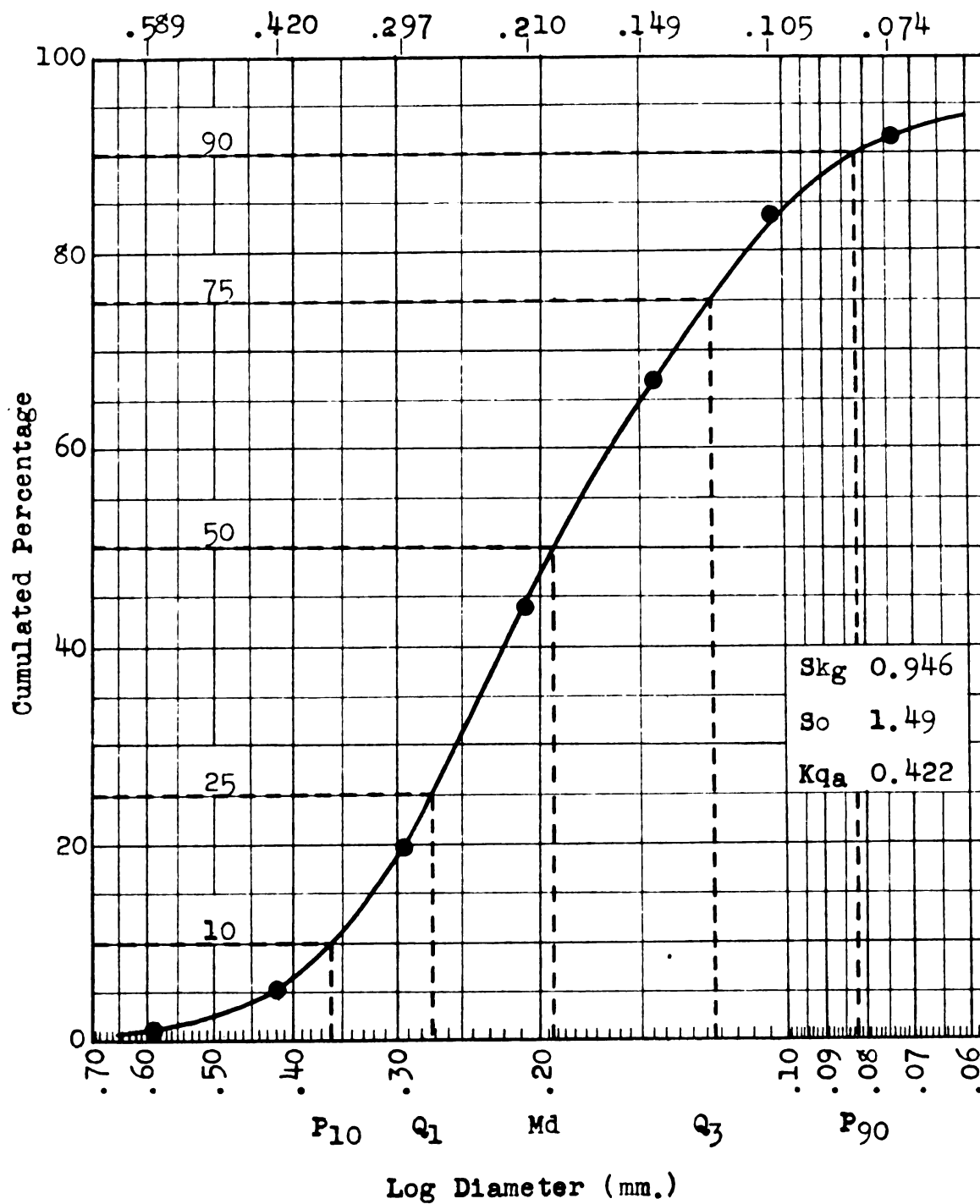
Tyler Sieve Sizes (mm.) Diam.



WELL #23, Sec. D

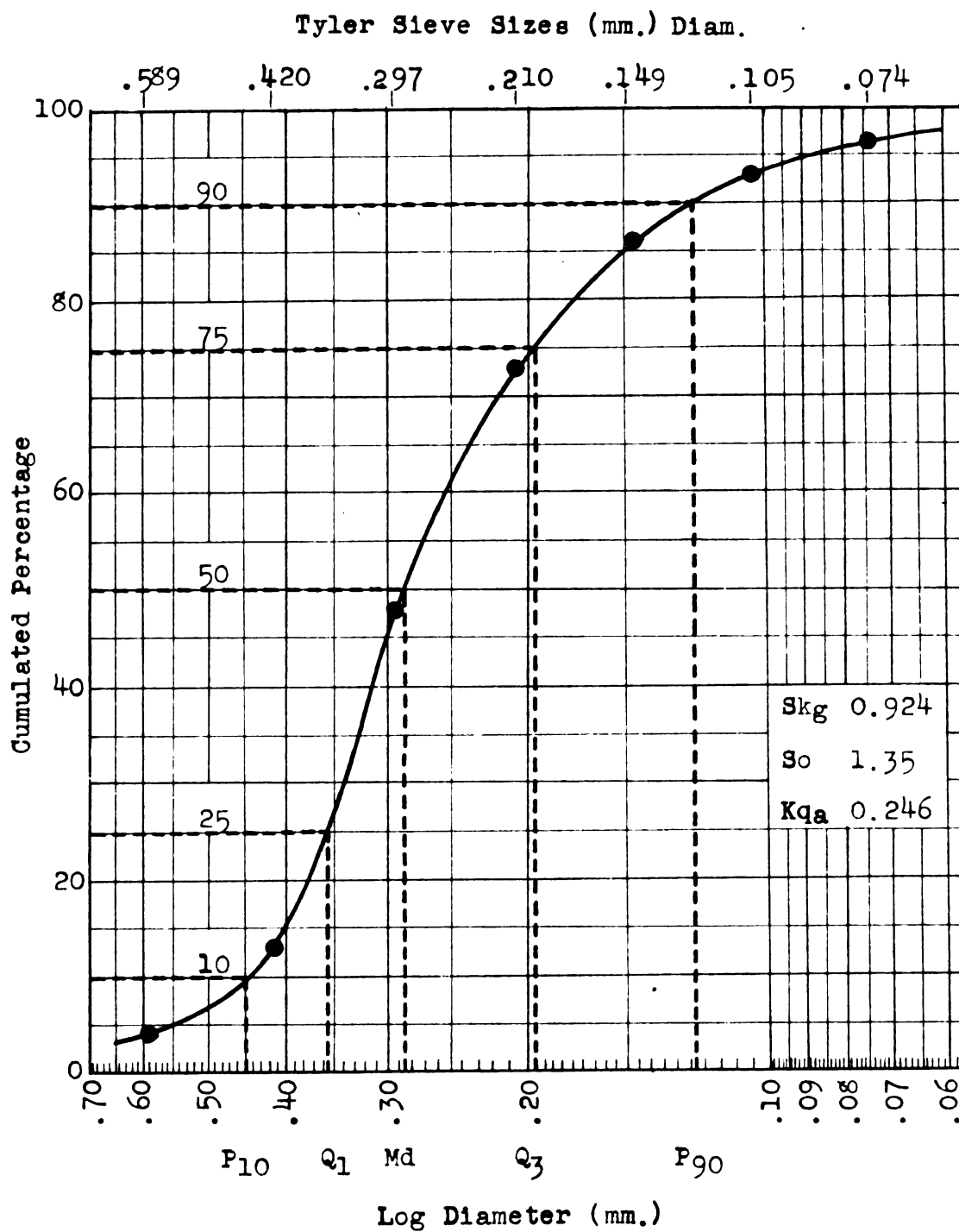
Cumulative Curve of Sieve Analysis Weights

Tyler Sieve Sizes (mm.) Diam.



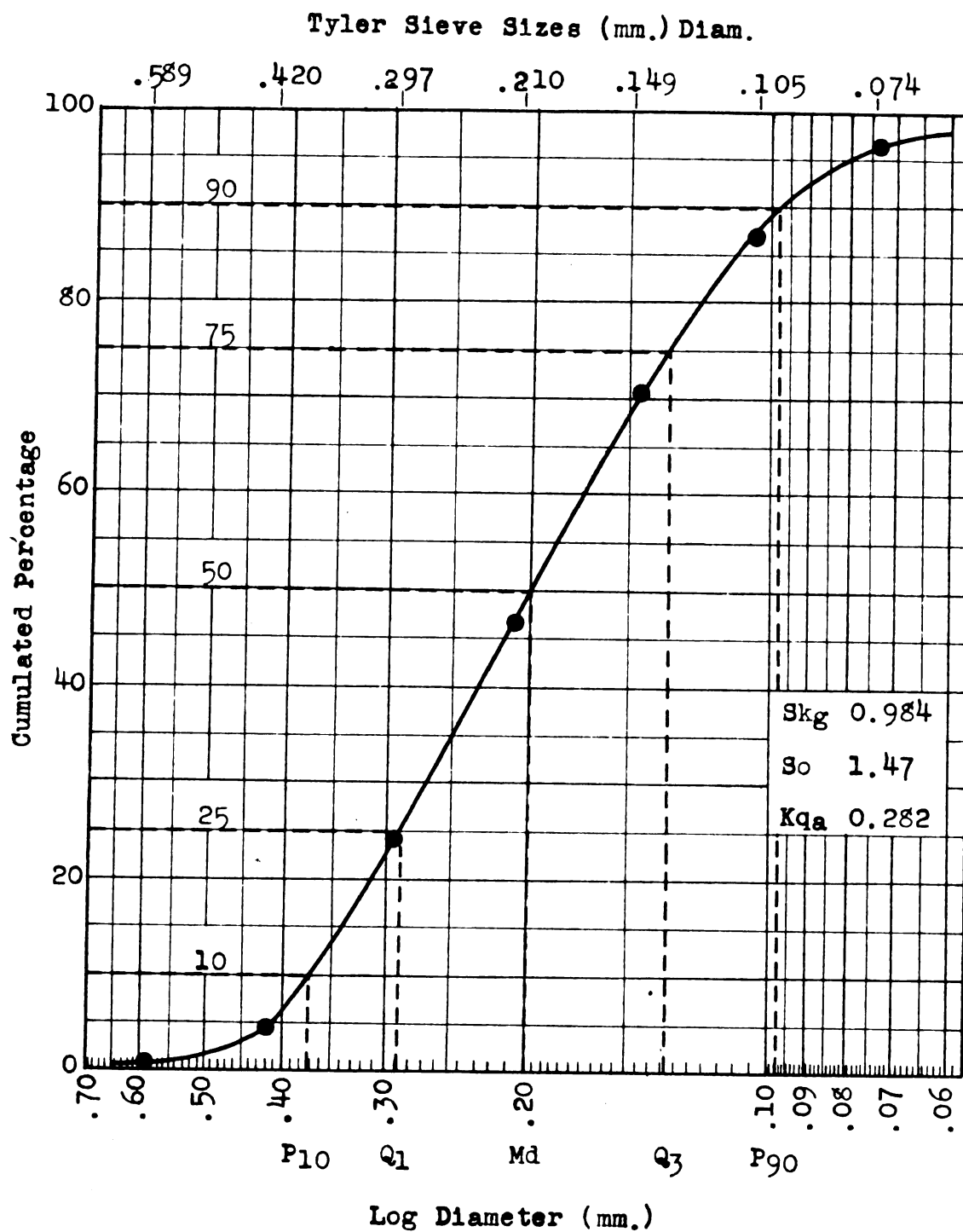
WELL #24, Sec. D

Cumulative Curve of Sieve Analysis Weights



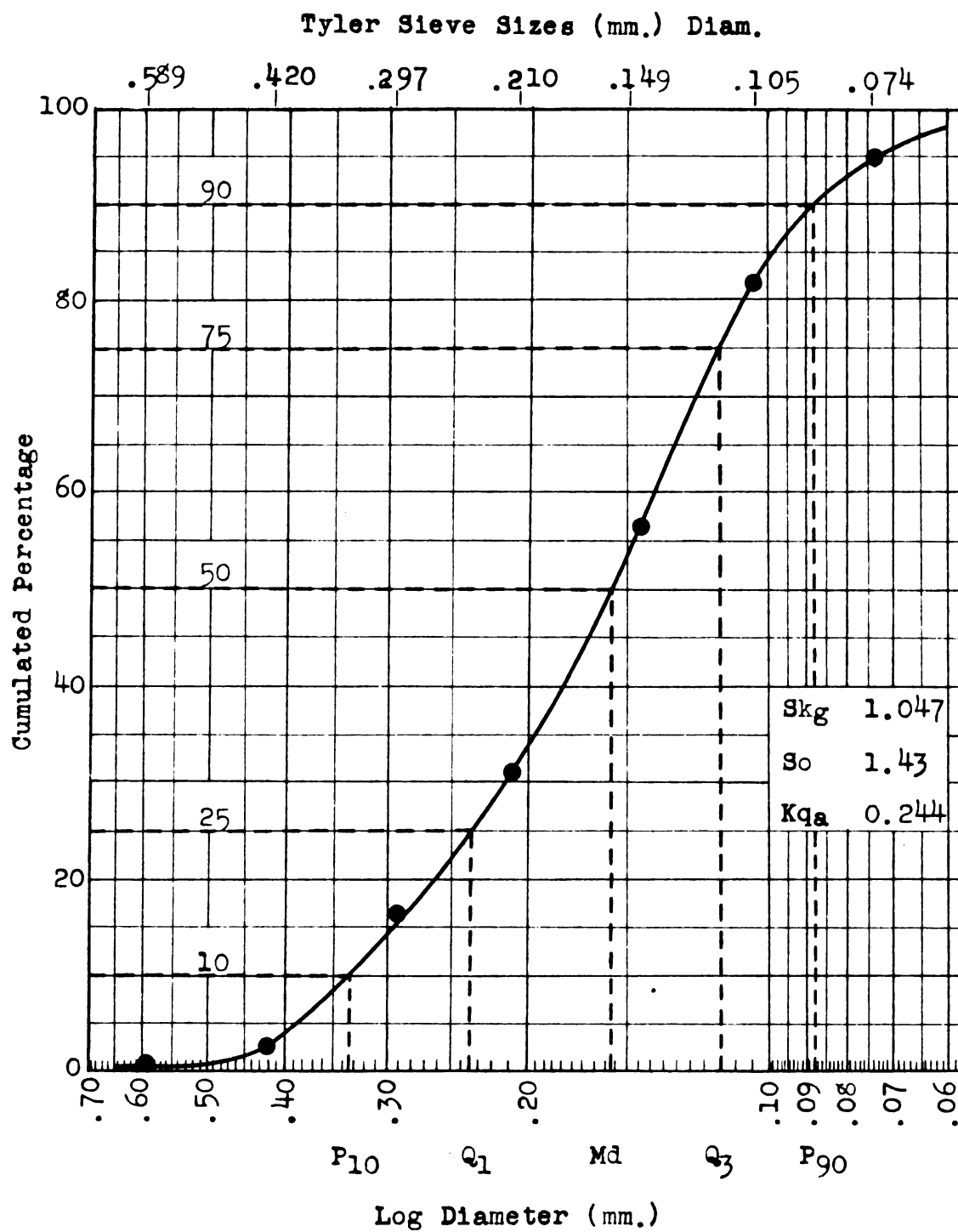
WELL #25, Sec. E

Cumulative Curve of Sieve Analysis Weights



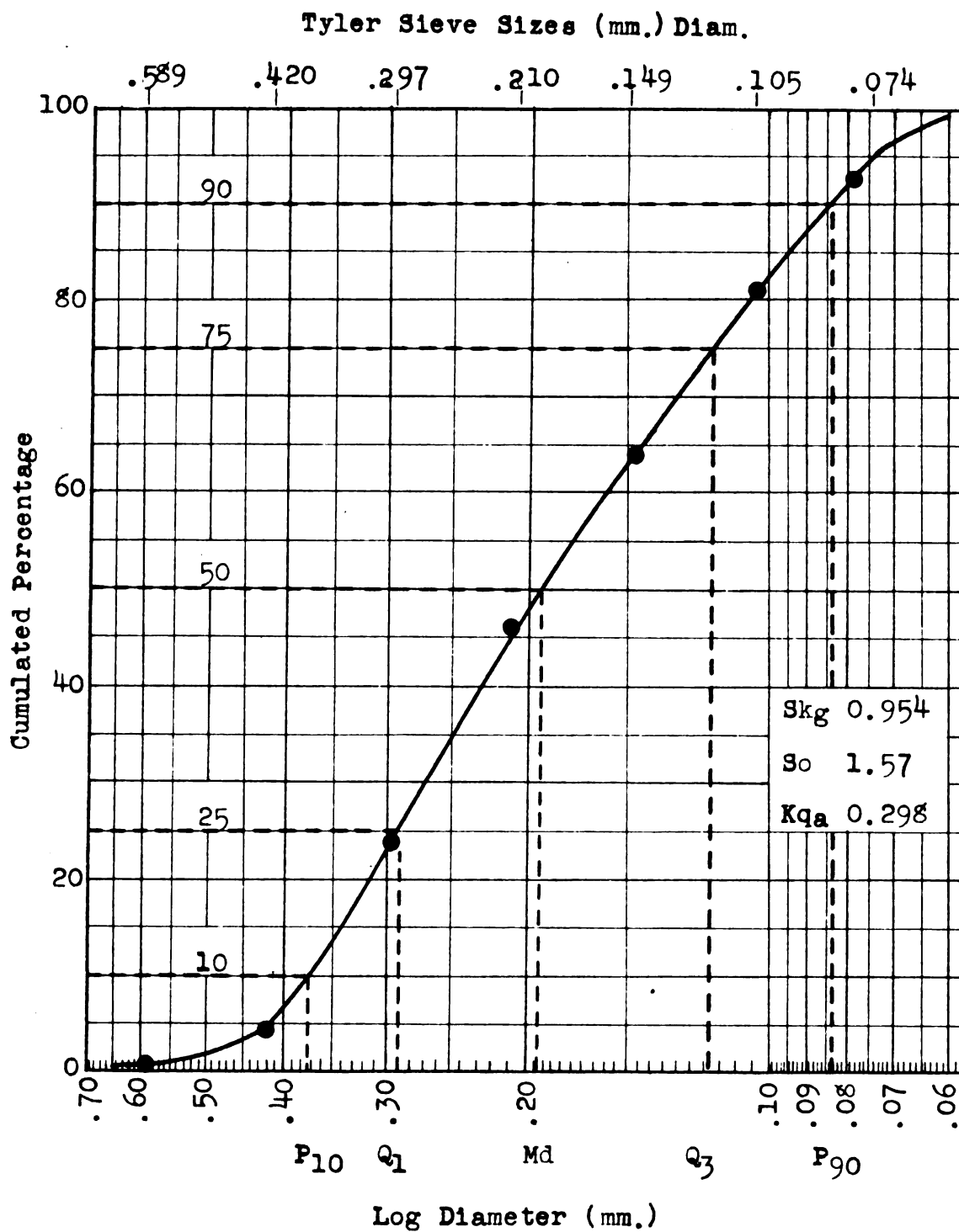
WELL #26, Sec. E

Cumulative Curve of Sieve Analysis Weights



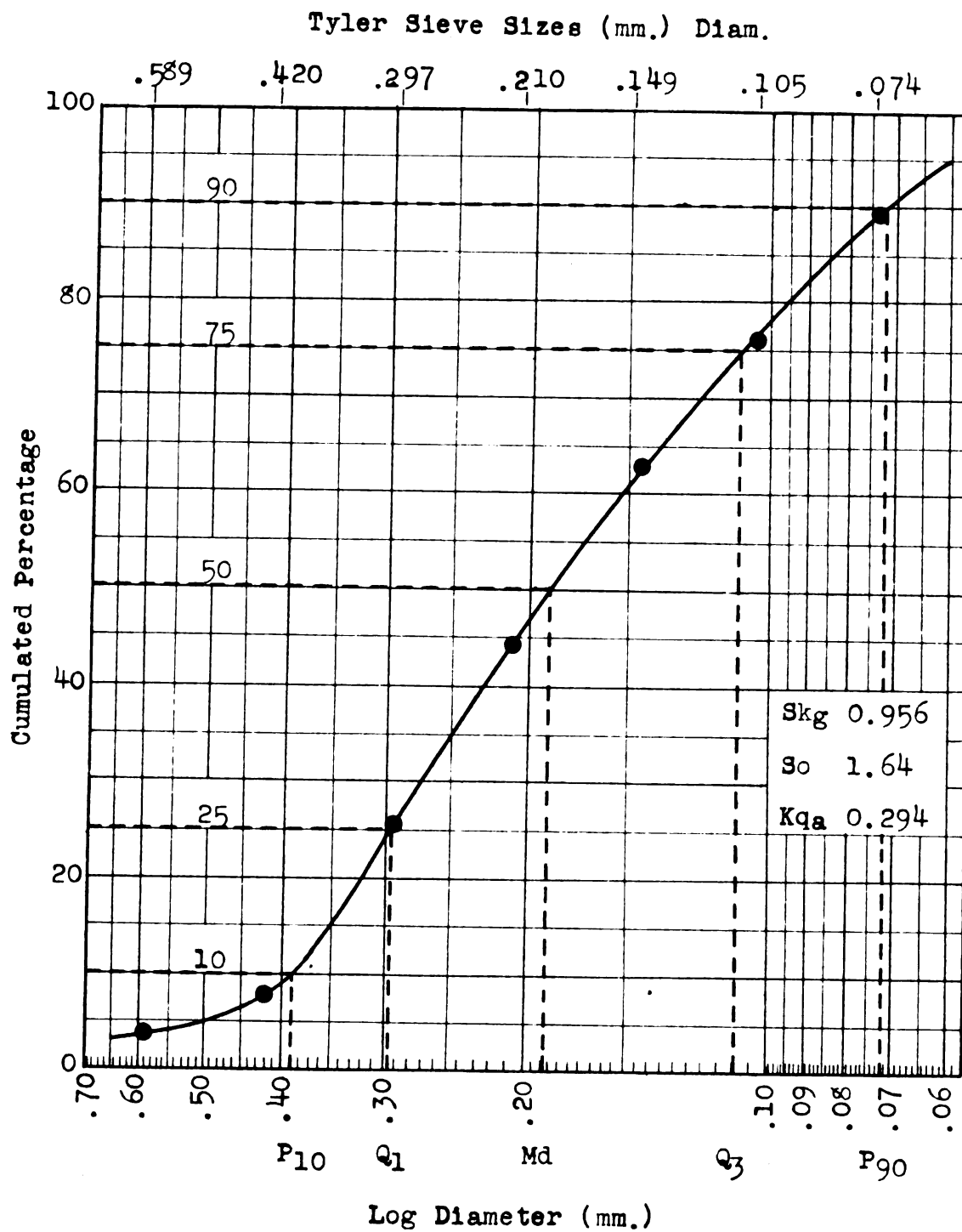
WELL #27, Sec. E

Cumulative Curve of Sieve Analysis Weights



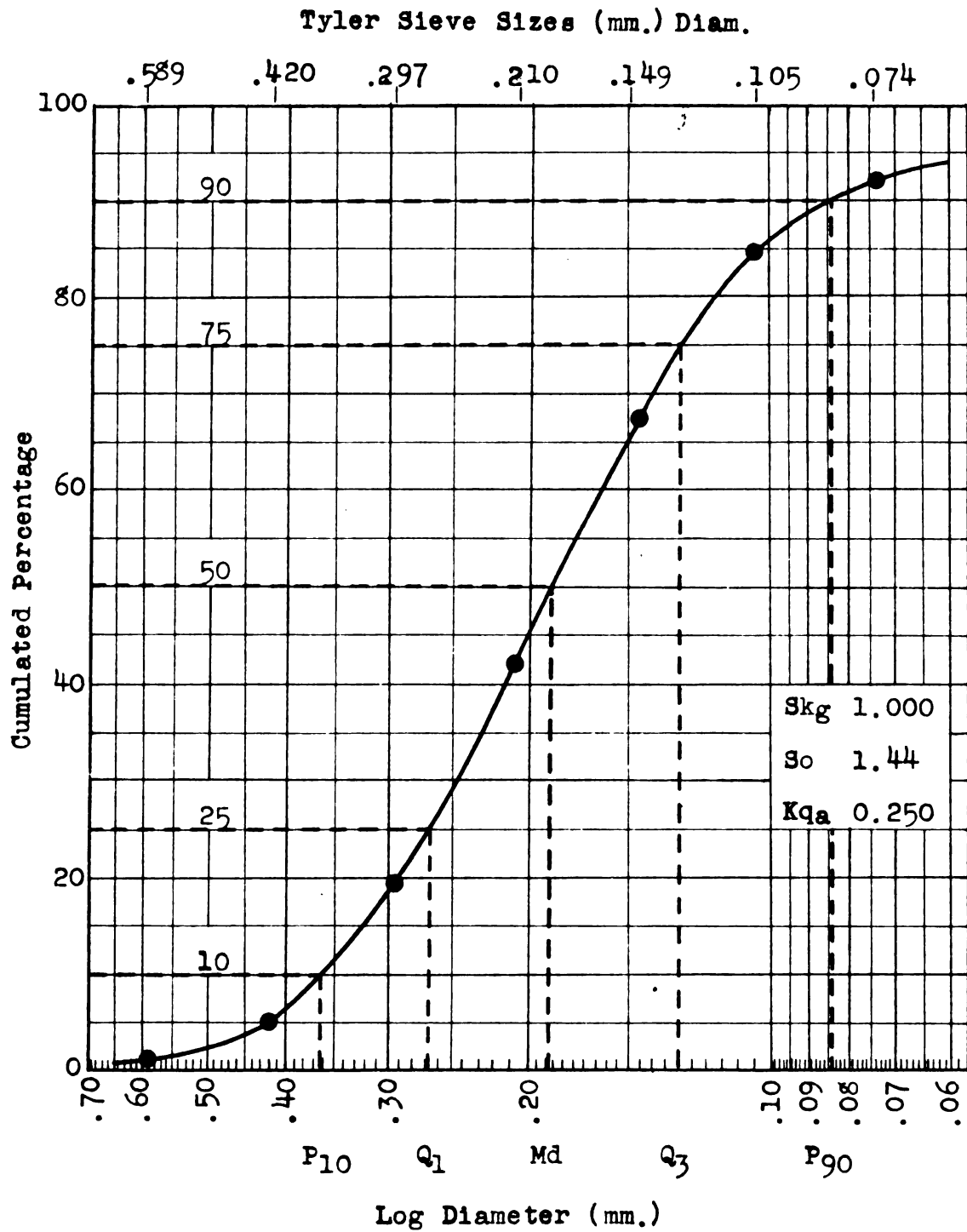
WELL #28, Sec. E

Cumulative Curve of Sieve Analysis Weights



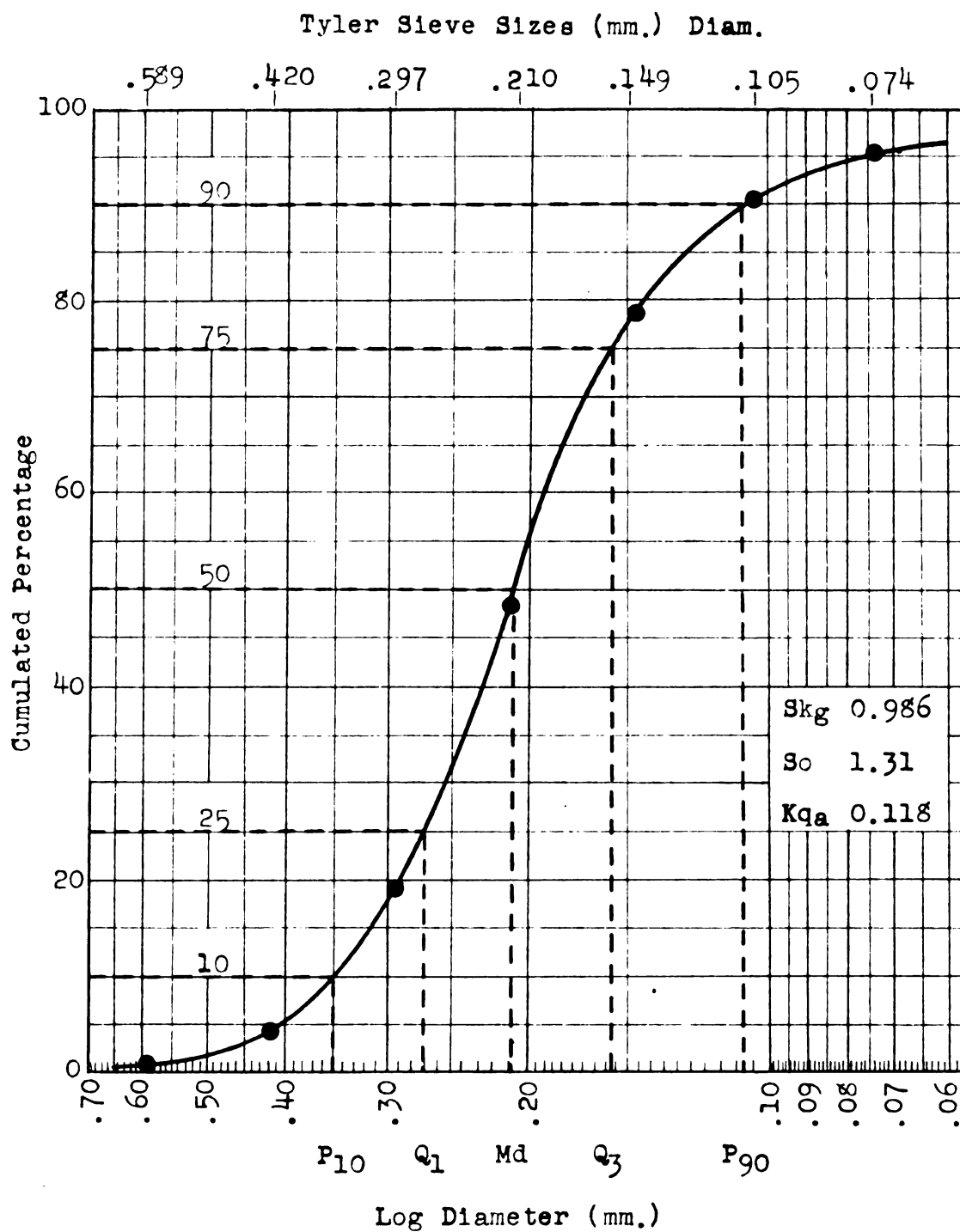
WELL #29, Sec. E

Cumulative Curve of Sieve Analysis Weights



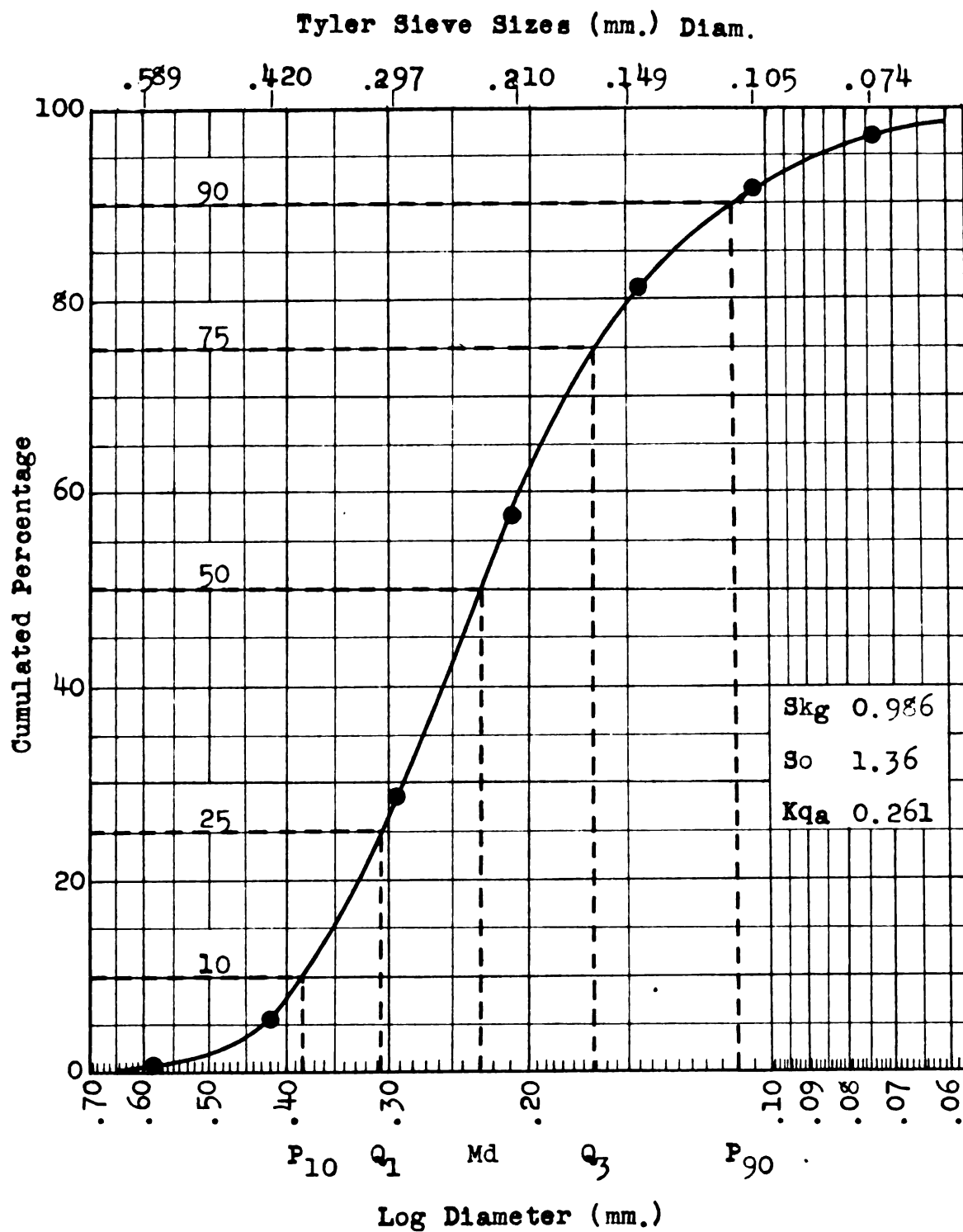
WELL #30, Sec. E

Cumulative Curve of Sieve Analysis Weights



WELL #31, Sec. F

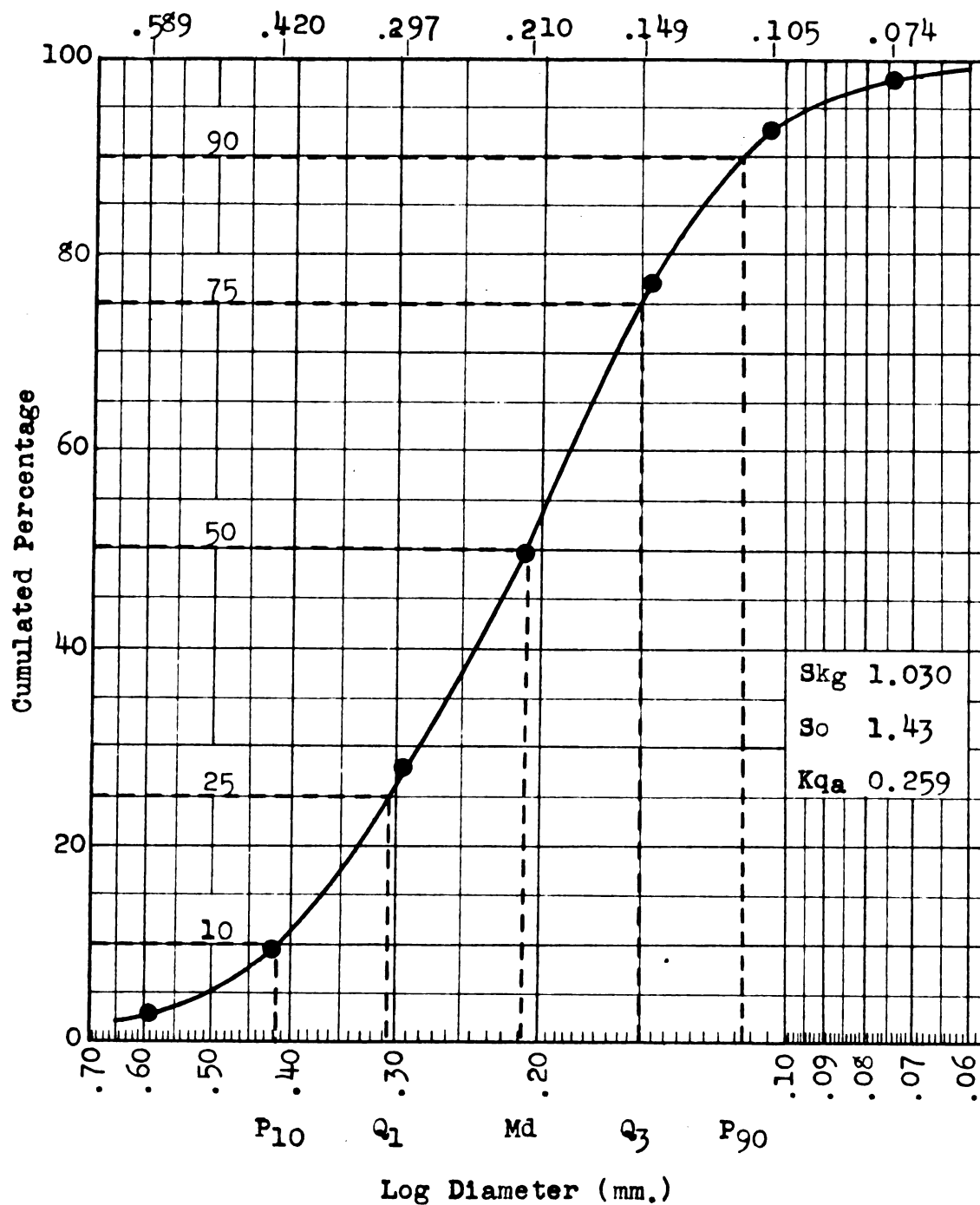
Cumulative Curve of Sieve Analysis Weights



WELL #32, Sec. F

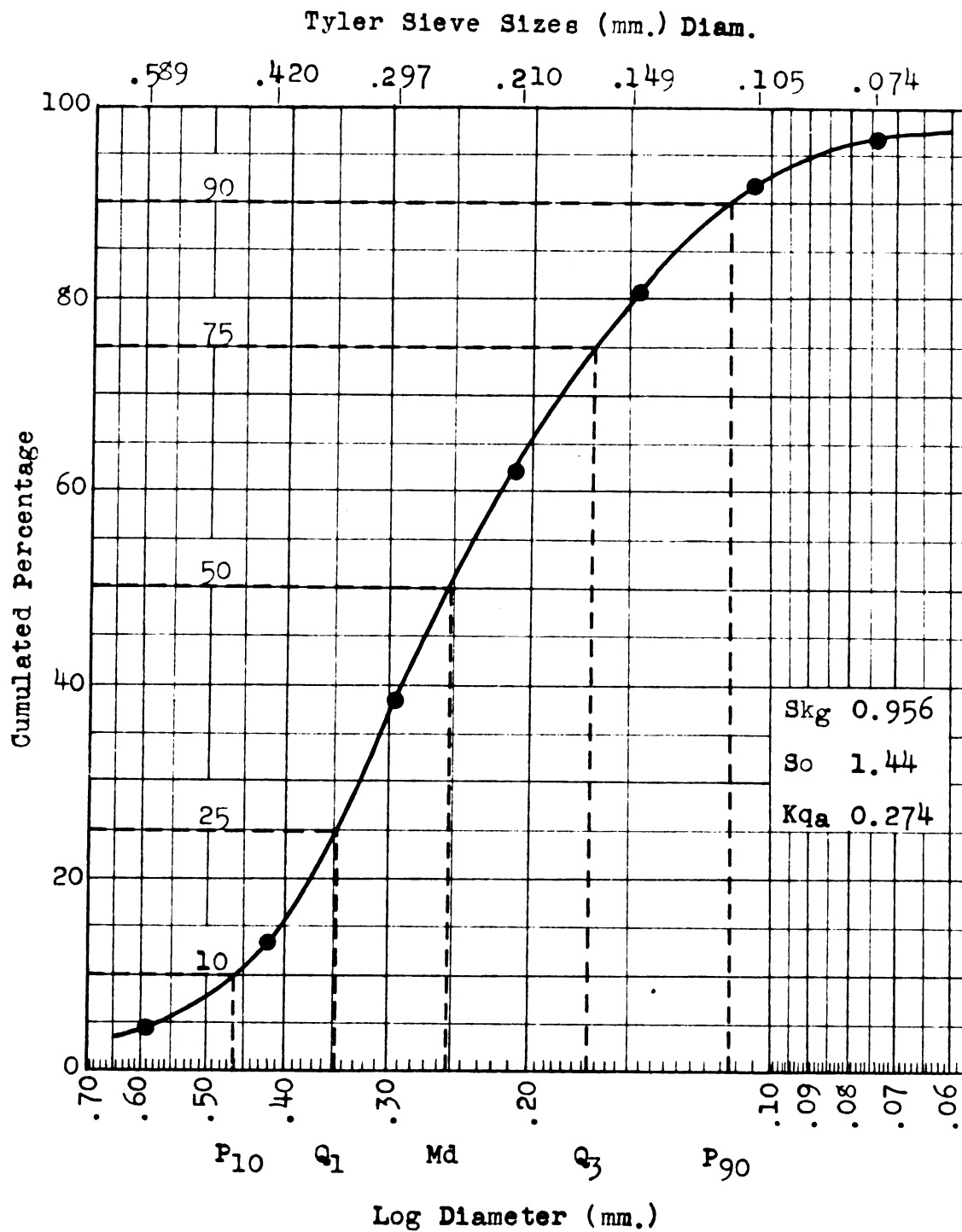
Cumulative Curve of Sieve Analysis Weights

Tyler Sieve Sizes (mm.) Diam.



WELL #33, Sec. F

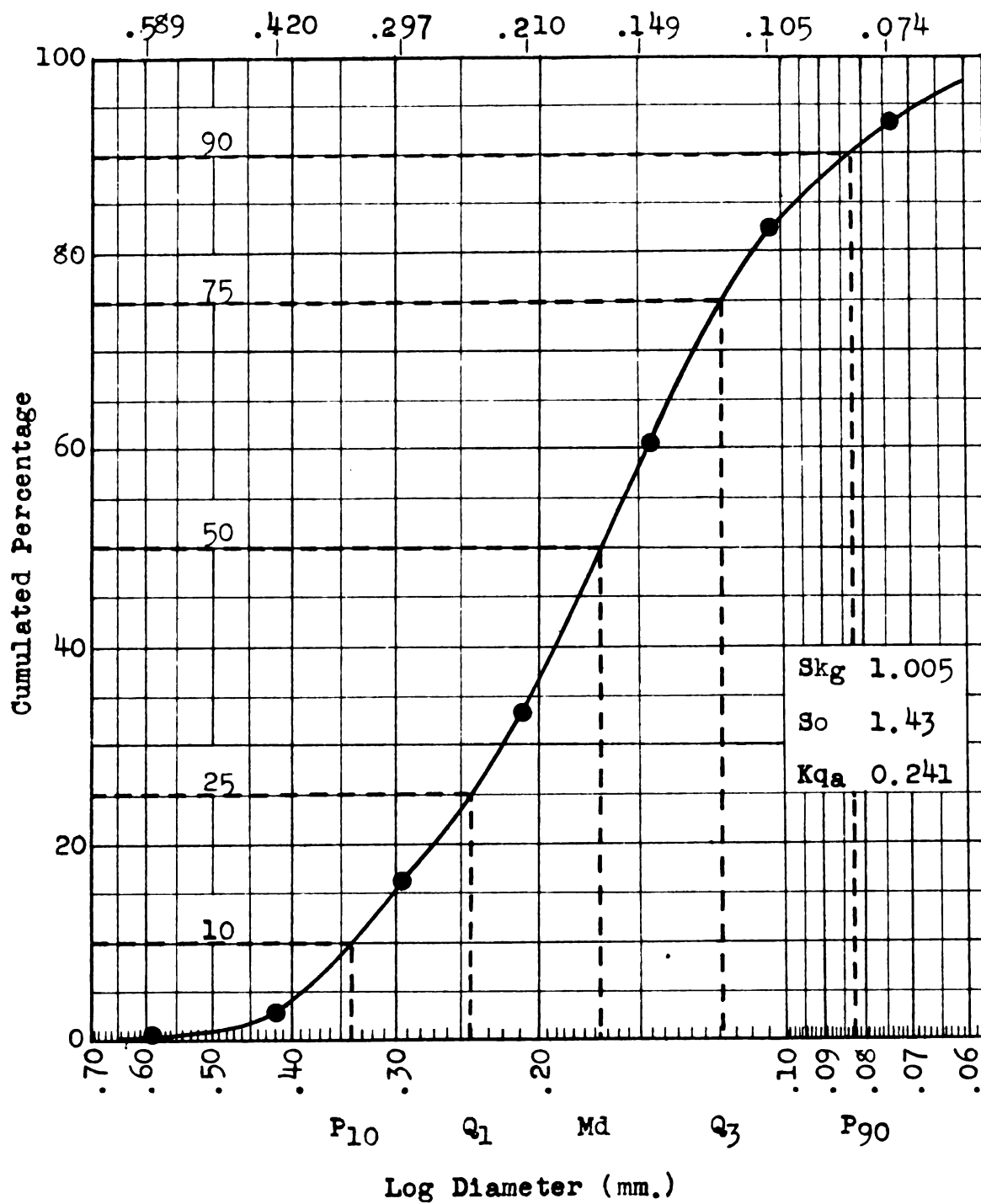
Cumulative Curve of Sieve Analysis Weights



WELL #34, Sec. F

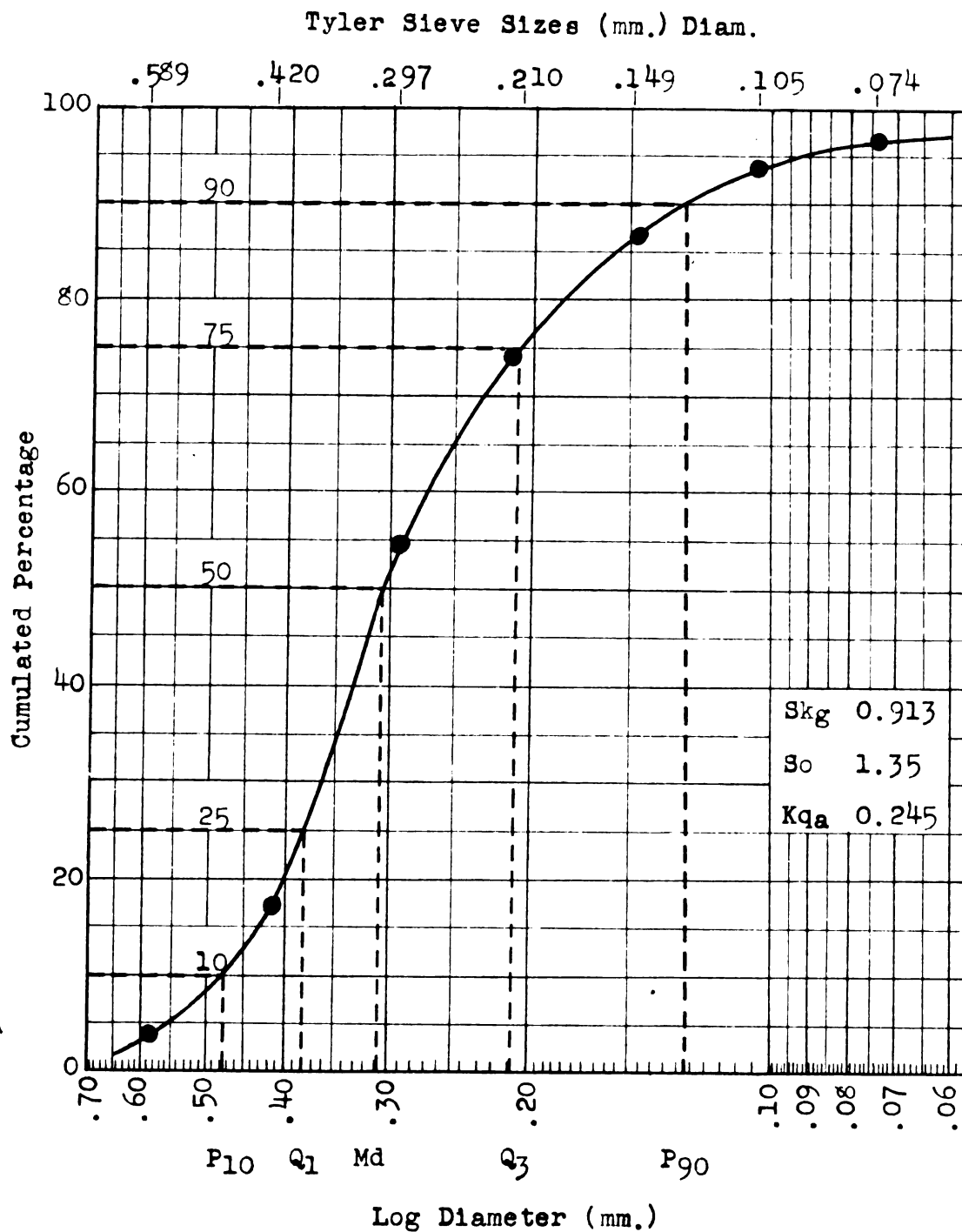
Cumulative Curve of Sieve Analysis Weights

Tyler Sieve Sizes (mm.) Diam.



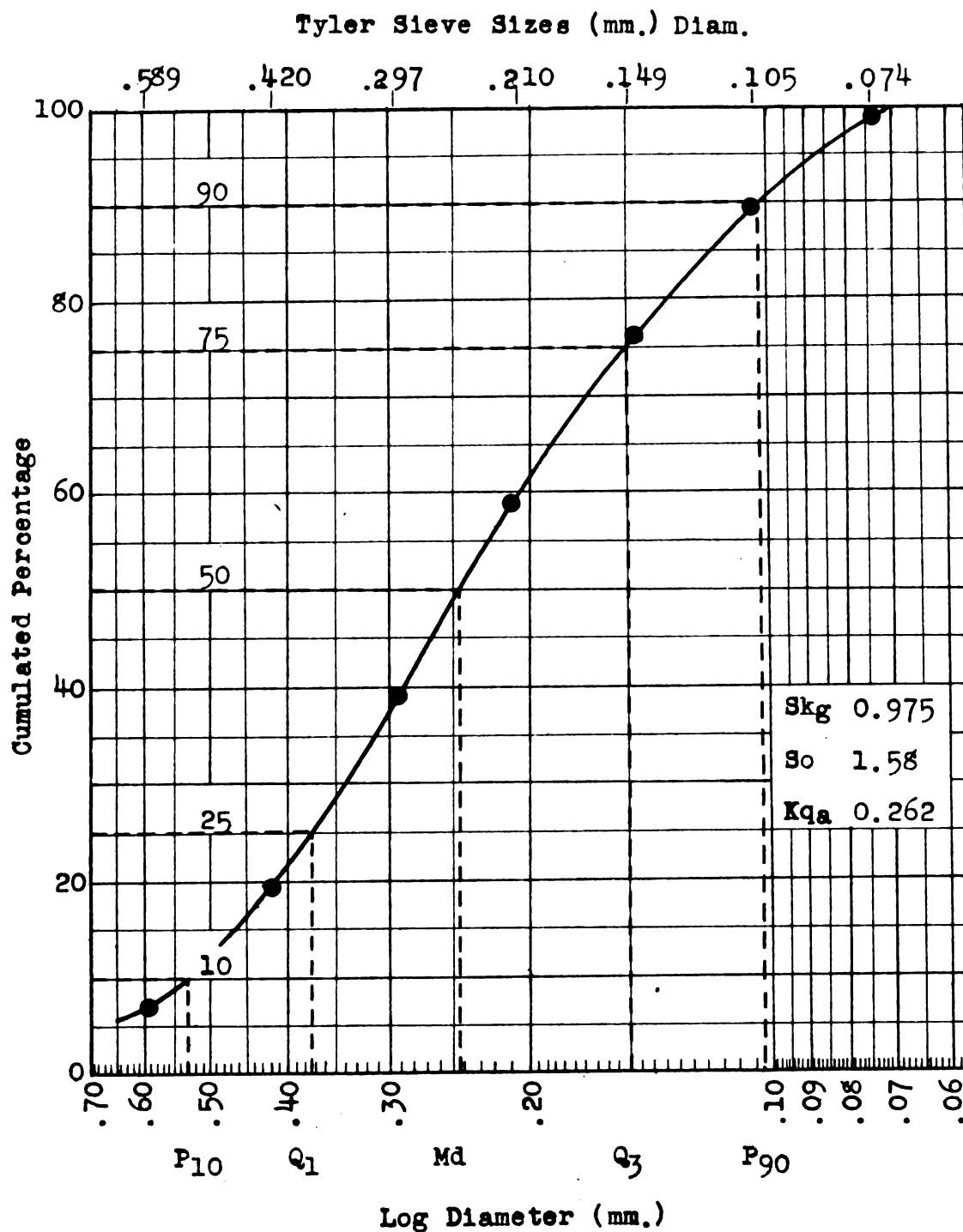
WELL #35, Sec. F

Cumulative Curve of Sieve Analysis Weights



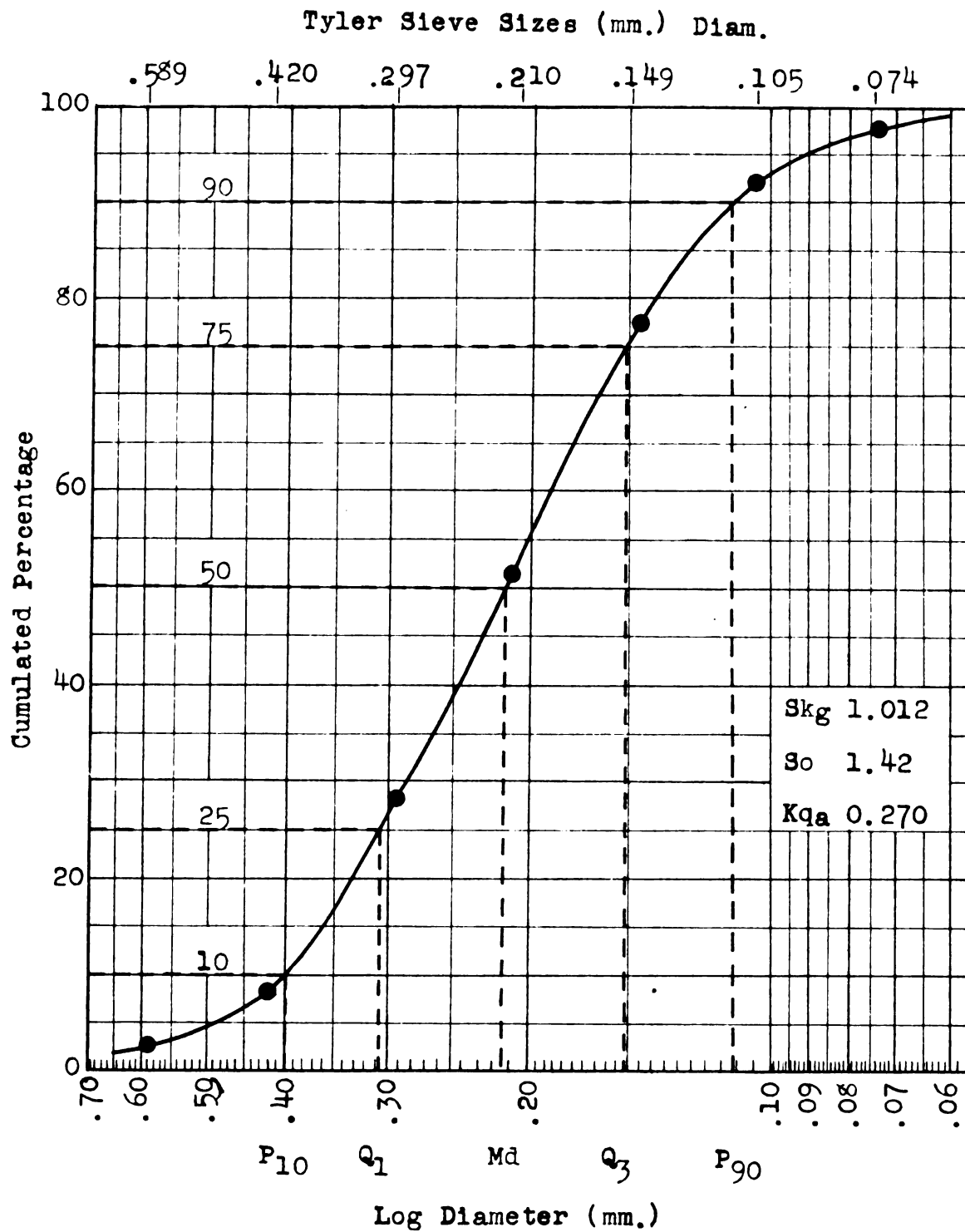
WELL #36, Sec. F

Cumulative Curve of Sieve Analysis Weights



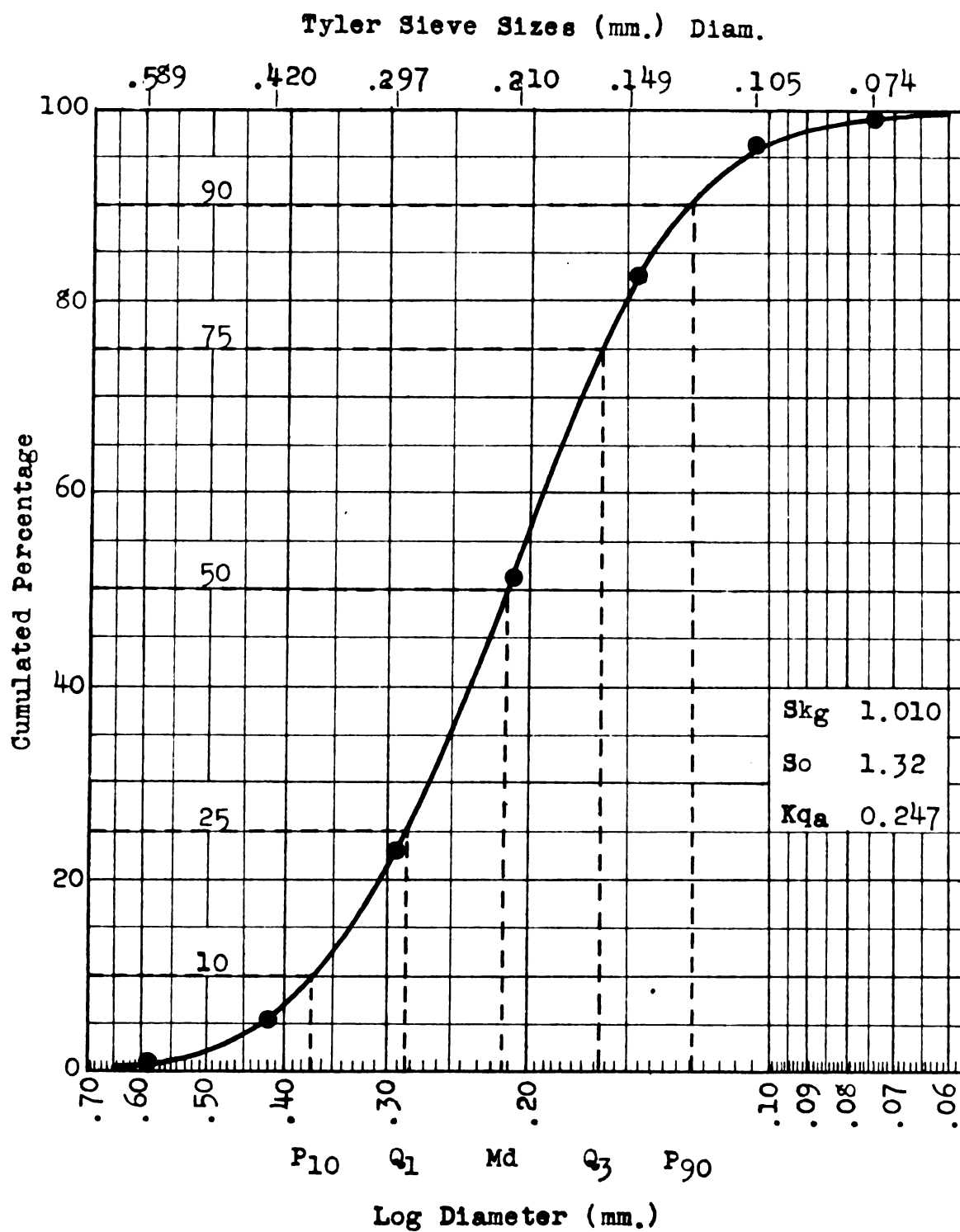
WELL #37, Sec. G

Cumulative Curve of Sieve Analysis Weights



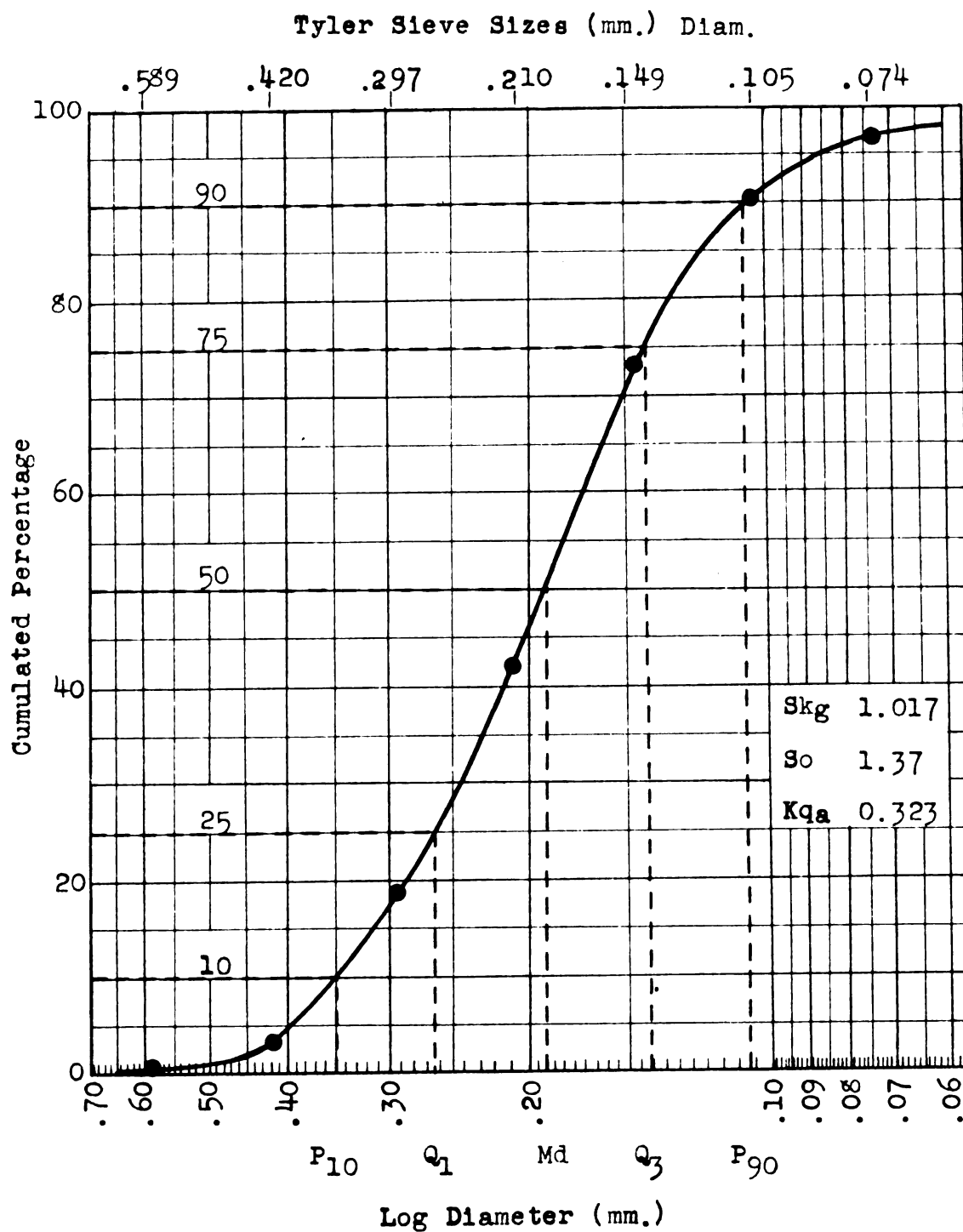
WELL #38, Sec. G

Cumulative Curve of Sieve Analysis Weights



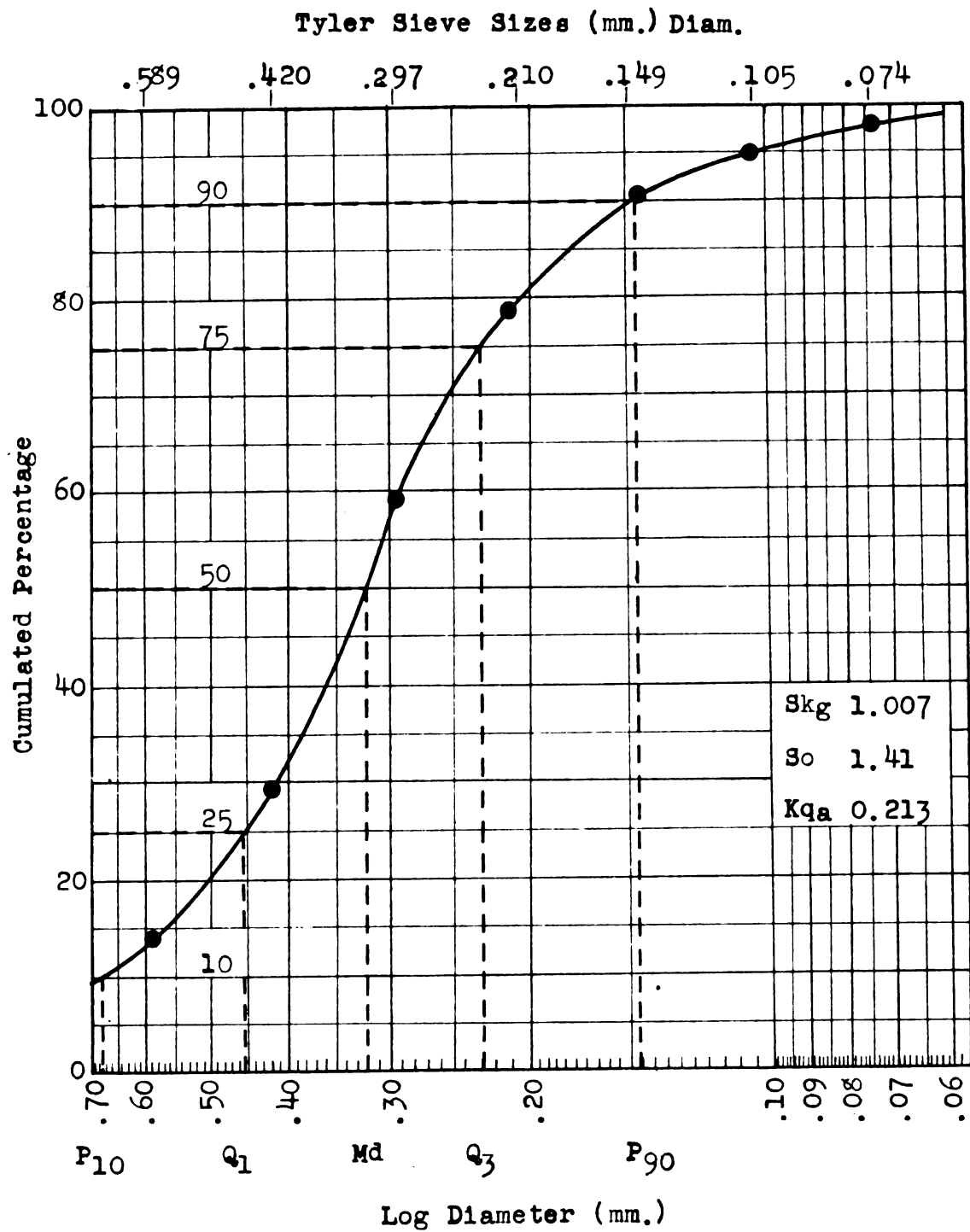
WELL #39, Sec. G

Cumulative Curve of Sieve Analysis Weights



WELL #40, Sec. G

Cumulative Curve of Sieve Analysis Weights



COMPARISON AND PRESENTATION OF DATA

Introduction

Although the various quartile terms applying to sedimentation have been defined in the preceding pages and the statistical methods and formulas for obtaining their values have been presented, the writer feels that some references showing the applications of these measurements to sedimentation should be set forth.

Krumbein (1938, p. 220) stated that "skewness is an attribute of sediments about which relatively little is known." The skewness of a sediment may result from either sampling errors, which show very noticeably, or when a symmetrical distribution is later acted upon by a transporting agent which removes only a portion of the material. Stina Gripenberg (1934) suggested that skewness may have a genetic significance in that a sediment deposited by a uniform current may increase in skewness as the material is followed along in the direction of transport. This is believed to be true in many of the areas considered in this investigation.

In discussing kurtosis, Krumbein (1938, p. 220) stated that not much is known about its significance in sediments. It appears,

however, to be related to the selective action of geological agents. The kurtosis of a curve, and especially of symmetrical curves, has a definite geometrical significance, but whether or not it may have physical or geological significance is not definitely known. No complete investigation of the aerial variation of kurtosis has been made, and virtually nothing is known of its magnitude or prevalence in sediments.

Most work done with statistical methods includes sorting, the best known of the quartile calculations. Trask (1932) defined a well-sorted sediment on the basis of two hundred analyses, as one having a "So" value less than 2.5. It should be noted that all samples used in this investigation of the Marshall formation have roundness, sphericity, and size sorting values less than 2.5 (Tables III, IV, V), and should, therefore, be considered as well-sorted sands.

It is the purpose of this section to show the relationships which are present and those which appear to be present, and to put forth the methods employed in comparing the roundness, sphericity, and size distribution values obtained in the preceding section.

TABLE V
QUARTILE CALCULATIONS FROM SIEVE ANALYSIS

Well No.	P ₁₀	Q ₁	Md	Q ₃	P ₉₀	So	Log So	Sk _g	Log Sk _g	Kq _a
1	0.276	0.196	0.135	0.106	0.085	1.36	0.134	1.069	+ .029	0.236
2	0.302	0.229	0.165	0.107	0.080	1.46	0.164	0.949	- .023	0.277
3	0.340	0.276	0.200	0.127	0.094	1.47	0.167	0.937	- .028	0.283
4	0.330	0.257	0.202	0.157	0.120	1.28	0.111	0.996	- .002	0.238
5	0.342	0.260	0.184	0.132	0.097	1.40	0.146	1.010	+ .004	0.261
6	0.346	0.282	0.215	0.154	0.109	1.35	0.131	0.971	- .013	0.270
7	0.353	0.270	0.182	0.124	0.088	1.48	0.173	1.011	+ .005	0.276
8	0.356	0.290	0.220	0.155	0.108	1.37	0.137	0.964	- .016	0.273
9	0.370	0.292	0.223	0.164	0.120	1.33	0.124	0.985	- .007	0.256
10	0.273	0.219	0.136	0.108	0.088	1.42	0.154	1.163	+ .050	0.300
11	0.357	0.287	0.213	0.144	0.097	1.41	0.149	0.956	- .020	0.275
12	0.434	0.354	0.294	0.224	0.150	1.26	0.100	0.957	- .019	0.230
13	0.320	0.259	0.200	0.133	0.082	1.39	0.143	0.929	- .032	0.265
14	0.344	0.249	0.162	0.116	0.083	1.46	0.164	1.057	+ .024	0.255
15	0.400	0.329	0.258	0.175	0.117	1.37	0.137	0.932	- .031	0.273
16	0.476	0.365	0.287	0.212	0.156	1.31	0.117	0.968	- .014	0.239
17	0.372	0.276	0.190	0.122	0.081	1.51	0.177	0.966	- .015	0.265
18	0.370	0.288	0.195	0.127	0.092	1.27	0.104	0.983	- .008	0.290
19	0.439	0.341	0.253	0.090	0.065	1.95	0.290	0.771	- .113	0.336
20	0.394	0.303	0.203	0.118	0.083	1.60	0.205	0.932	- .031	0.297

TABLE V (Continued)

Well No.	P ₁₀	Q ₁	Md	Q ₃	P ₉₀	So	Log So	Sk _g	Log Sk _g	Kq _a
21	0.360	0.251	0.179	0.130	0.094	1.39	0.143	1.010	+0.004	0.227
22	0.382	0.302	0.221	0.163	0.109	1.36	0.133	1.005	+0.002	0.255
23	0.360	0.272	0.193	0.122	0.082	1.49	0.173	0.946	-0.024	0.270
24	0.450	0.356	0.286	0.195	0.124	1.35	0.130	0.924	-0.035	0.246
25	0.372	0.289	0.200	0.134	0.097	1.47	0.167	0.984	-0.007	0.282
26	0.334	0.235	0.157	0.115	0.088	1.43	0.155	1.047	+0.020	0.244
27	0.373	0.290	0.194	0.118	0.084	1.57	0.196	0.954	-0.021	0.298
28	0.389	0.296	0.189	0.110	0.072	1.64	0.215	0.956	-0.020	0.294
29	0.362	0.269	0.187	0.130	0.084	1.44	0.158	1.000	0.000	0.250
30	0.350	0.271	0.209	0.157	0.108	1.31	0.117	0.986	-0.006	0.236
31	0.381	0.308	0.229	0.166	0.110	1.36	0.134	0.986	-0.006	0.261
32	0.417	0.307	0.208	0.150	0.113	1.43	0.155	1.030	+0.013	0.259
33	0.462	0.348	0.253	0.168	0.113	1.44	0.159	0.956	-0.020	0.274
34	0.340	0.243	0.168	0.119	0.082	1.43	0.155	1.005	+0.002	0.241
35	0.476	0.380	0.309	0.209	0.127	1.35	0.130	0.913	-0.040	0.245
36	0.530	0.374	0.243	0.150	0.103	1.58	0.199	0.975	-0.011	0.262
37	0.400	0.308	0.214	0.152	0.111	1.42	0.152	1.012	+0.005	0.270
38	0.370	0.284	0.213	0.163	0.125	1.32	0.117	1.010	+0.004	0.247
39	0.350	0.264	0.190	0.141	0.106	1.37	0.137	1.017	+0.007	0.323
40	0.675	0.454	0.320	0.229	0.146	1.41	0.149	1.007	+0.003	0.213

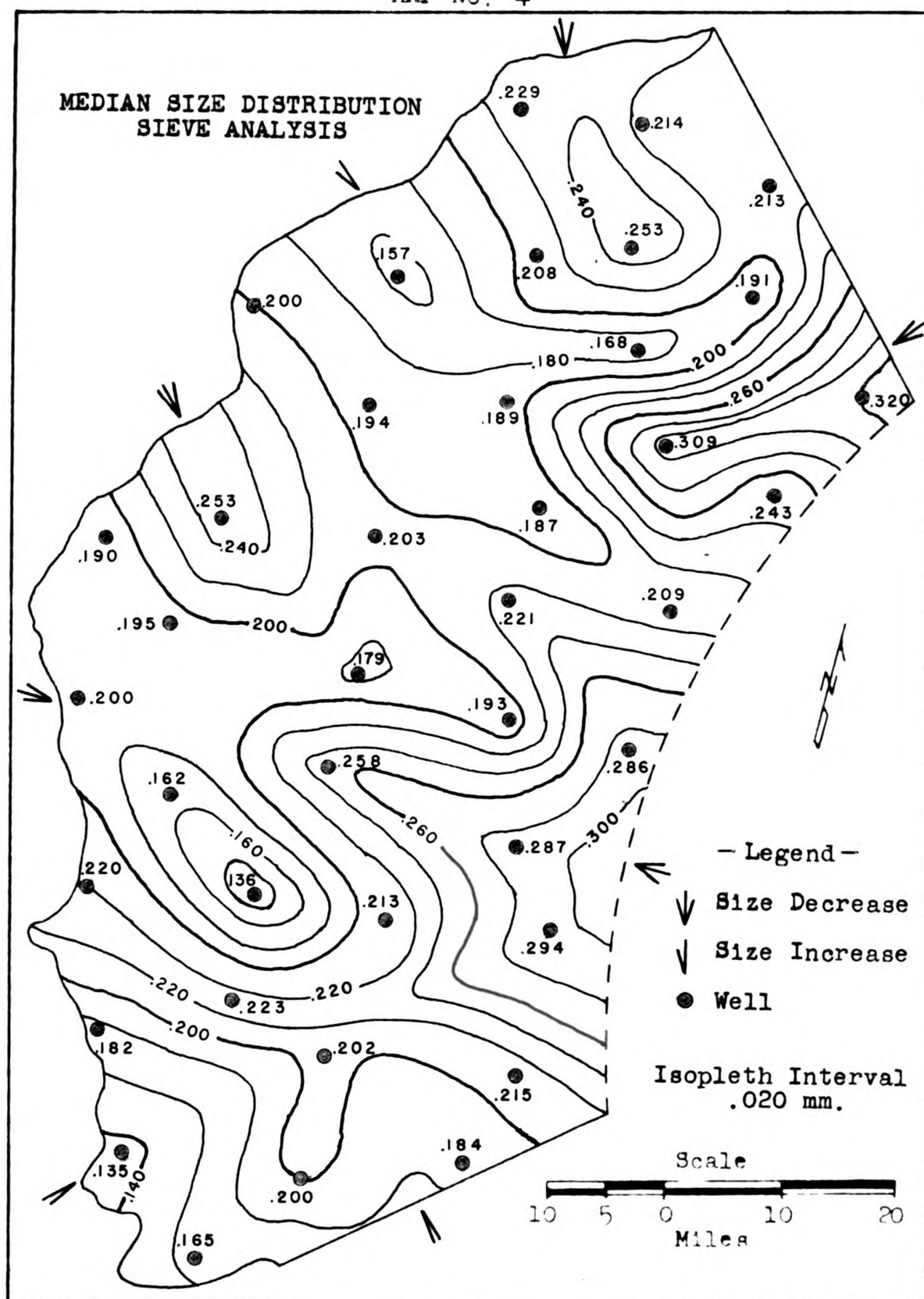
Analysis of Size Distribution

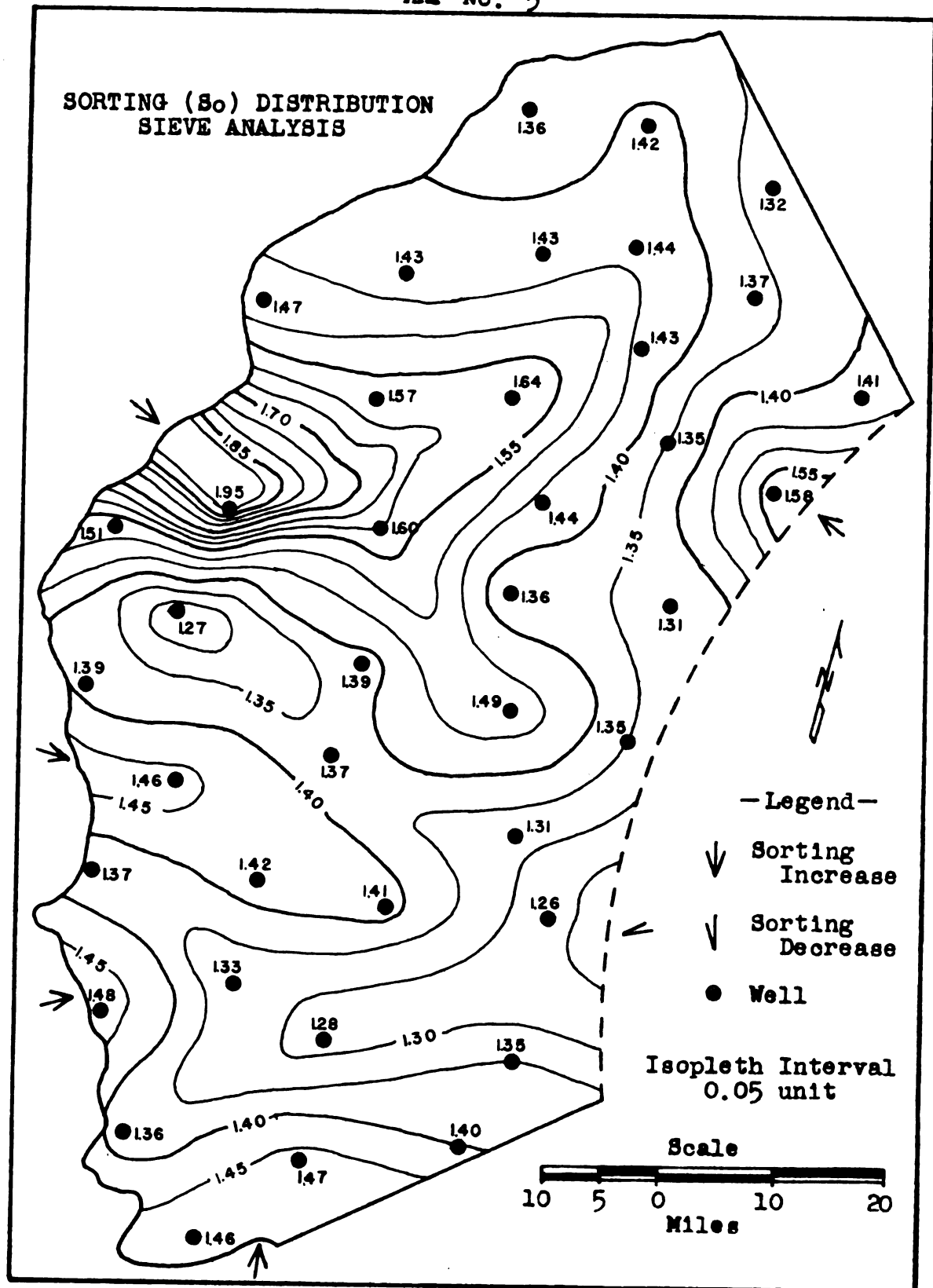
The material summarized in Table II was used in preparing the cumulative calculations presented in Table V. From Table V the values of median size, Md ; sorting, So ; skewness, Sk_g ; and kurtosis, Kq_a , were taken and plotted at their respective well locations to produce isopleth maps (Maps 4, 5, 6, 7).

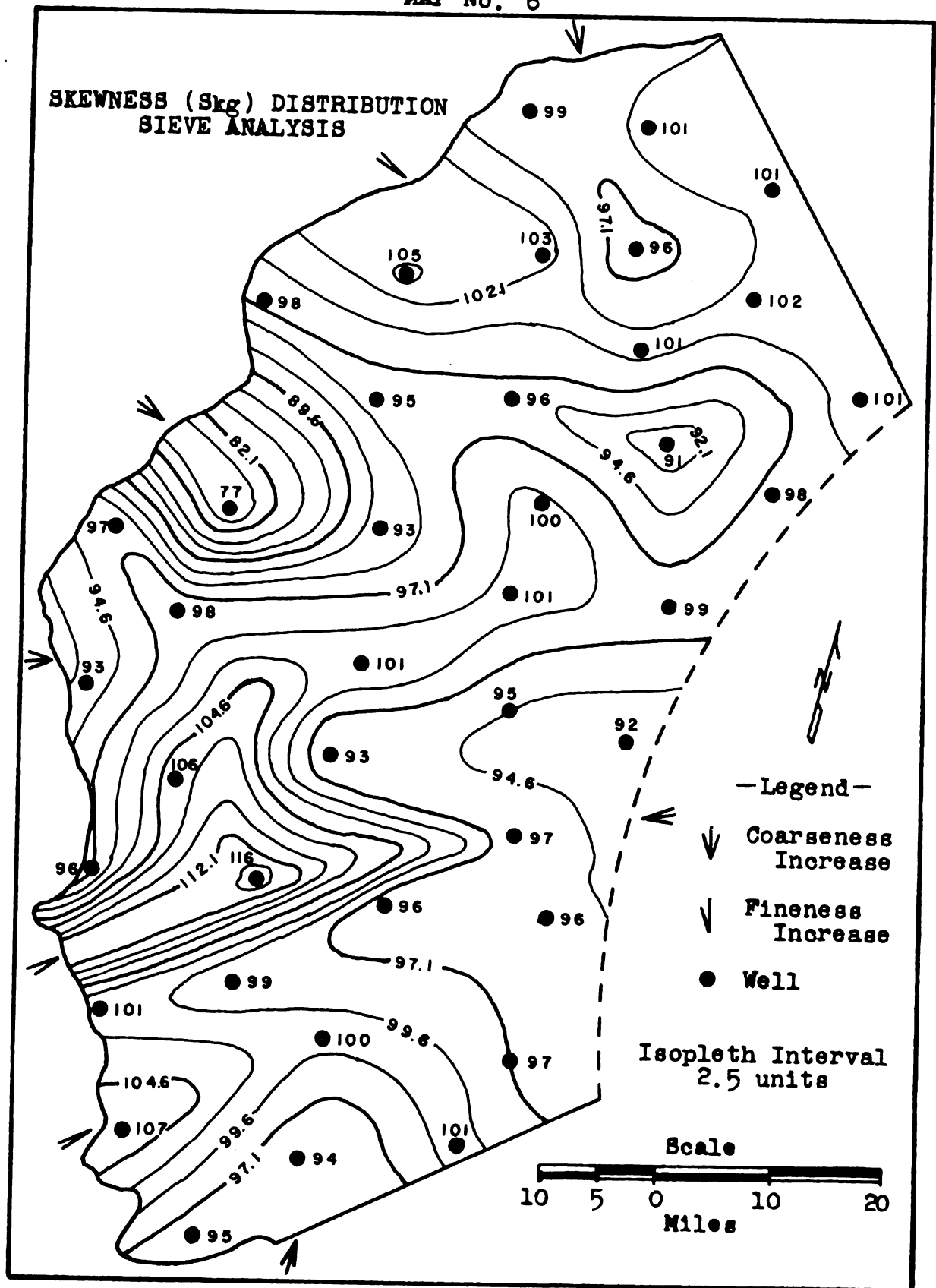
An isopleth map has been defined by Krumbein (1939, p. 587) as a map in which "lines of equal abundance (contours) are drawn through sets of numbers, such that each number is located at the point of sampling and corresponds to the magnitude of the characteristic being mapped." Trask (1930) first suggested the use of such maps, and it is recognized that any characteristic of a sediment which may be expressed as a number in a continuous range of values may be used as the basis of an isopleth map.

From the isopleth maps presented for size distribution, a definite similarity may be noted, showing that relationships between the median size, sorting, skewness, and kurtosis do exist and may be compared quantitatively. Certain relationships are believed to prevail in normal water-laid sediments. For example, it may be seen from Well No. 19 (Map 3) that the So value of 1.95 (Map 5) is higher or more poorly sorted, whereas the median size, 0.253 (Map 4), is

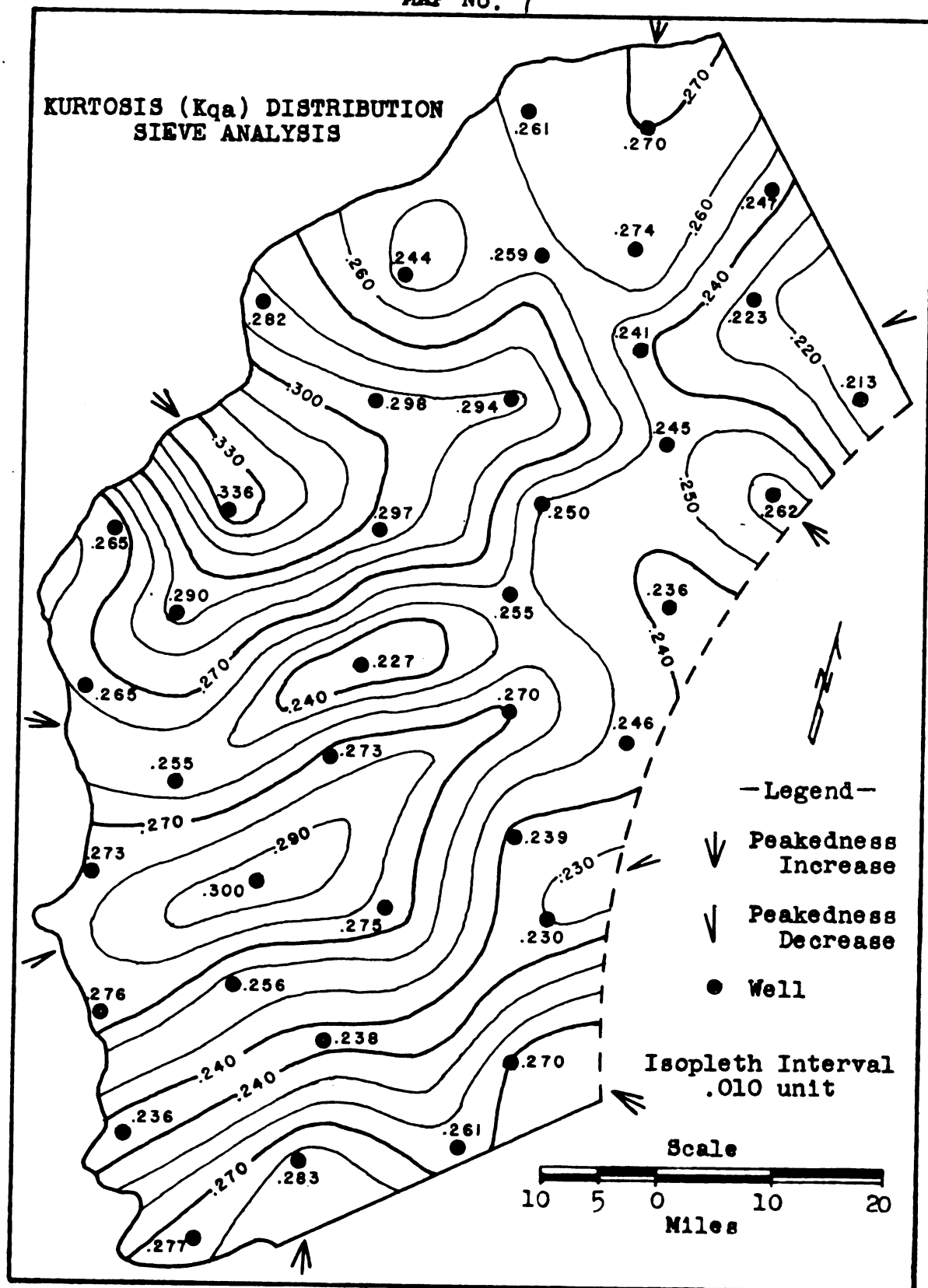
MAP No. 4







MAP No. 7



larger than at adjacent wells. Also, the Sk_g value, 0.77 (Map 6), of Well No. 19 is considerably less than one, indicating that the curve is skewed toward the smaller sizes; that is, smaller than the median. In the case of the Kq_a value of 0.336 (Map 7), peakedness of the curve is much less than in other parts of the area. As the sediment becomes better sorted, these relationships are reversed. In this same manner, comparison of other sections throughout the area of investigation may be studied.

A second method by which the size distributions may be compared is through the use of the logarithmic values of both So and Sk_g expressed in Table V. As explained on page 38, logarithmic values may be compared mathematically. For example, Well No. 12 may be said to be 2.9 times better sorted than Well No. 19, because $0.290/0.100$ equals 2.9, where the logarithmic value of sorting, " So ," for Well No. 19 equals 0.290, and for Well No. 12, equals 0.100.

In the case of skewness, it may be said that the curve for Well No. 19 is skewed 5.9 times farther toward the smaller sizes than is the curve for Well No. 12, because $0.113/0.019$ equals 5.9, where the logarithmic value of skewness, Sk_g , for the curve representing Well No. 19 equals 0.113, and for that representing Well No. 12 equals 0.019.

Still another method of comparison may be found in examining the cumulative curve from which the above numerical values have been obtained (pp. 58, 65). It will be noted by examining the curves for Well No. 19, and Well No. 12, that in the case of Well No. 19, a definite polymorphic curve is present, suggesting more than one period of deposition such as an intermittent stream might deposit. In the case of Well No. 12, on the other hand, a smooth, even curve persists, showing a continuous grading of sediments.

Another notable feature is that the areas of most prominent expression in Maps 4, 5, 6, and 7 are found around the locations of Well Nos. 3, 7, 10, 19, 20, 27, and 28. If these well numbers are also compared with their cumulative curves, it will be seen that in all cases the curves are not smooth, but show polymorphic shapes. By comparing the weight percentages listed in Table II with these curves, the exact weight percentage in each sieve size may be obtained and the resulting effect on the curves noted.

If the above three methods of comparison are now interrelated, it is possible to discover many interesting relationships which may be used in obtaining the final results. For illustration, it may be observed from the cumulative curves for Well Nos. 35 and 36 on pages 81 and 82 that the closer together the Q_1 and Q_3 lines are,

the smaller the sorting value is, or the better the sample is sorted. If these wells are then compared on the sorting map (Map 5), it will be noted that the sorting increases toward the northwest, suggesting that the material was derived from the southeast in that particular area. If the logarithmic values of sorting are now compared as on page 96, the relationship is both visible and mathematical.

Analysis of Roundness Distribution

In the analysis of roundness distributions, four methods of comparing the data secured in measuring the quartz grains are presented. The first method is by directly comparing the arithmetic averages as summarized in Table VI. In this method, however, the averages are so nearly alike that a visual comparison is of little value.

The second method of comparison may be illustrated by the histogram analysis on pages 108-117. To obtain these figures, the number of quartz grains measured between each 0.05 interval of roundness, beginning with those having a roundness of 0.100 to 0.149 and from 0.150 to 0.199, et cetera, through 0.500, were plotted in arithmetic form. Because one hundred grains of sand were measured from each well sample, each grain was equivalent to 1 per cent of

TABLE VI

ARITHMETIC AVERAGES OF ROUNDNESS AND SPHERICITY

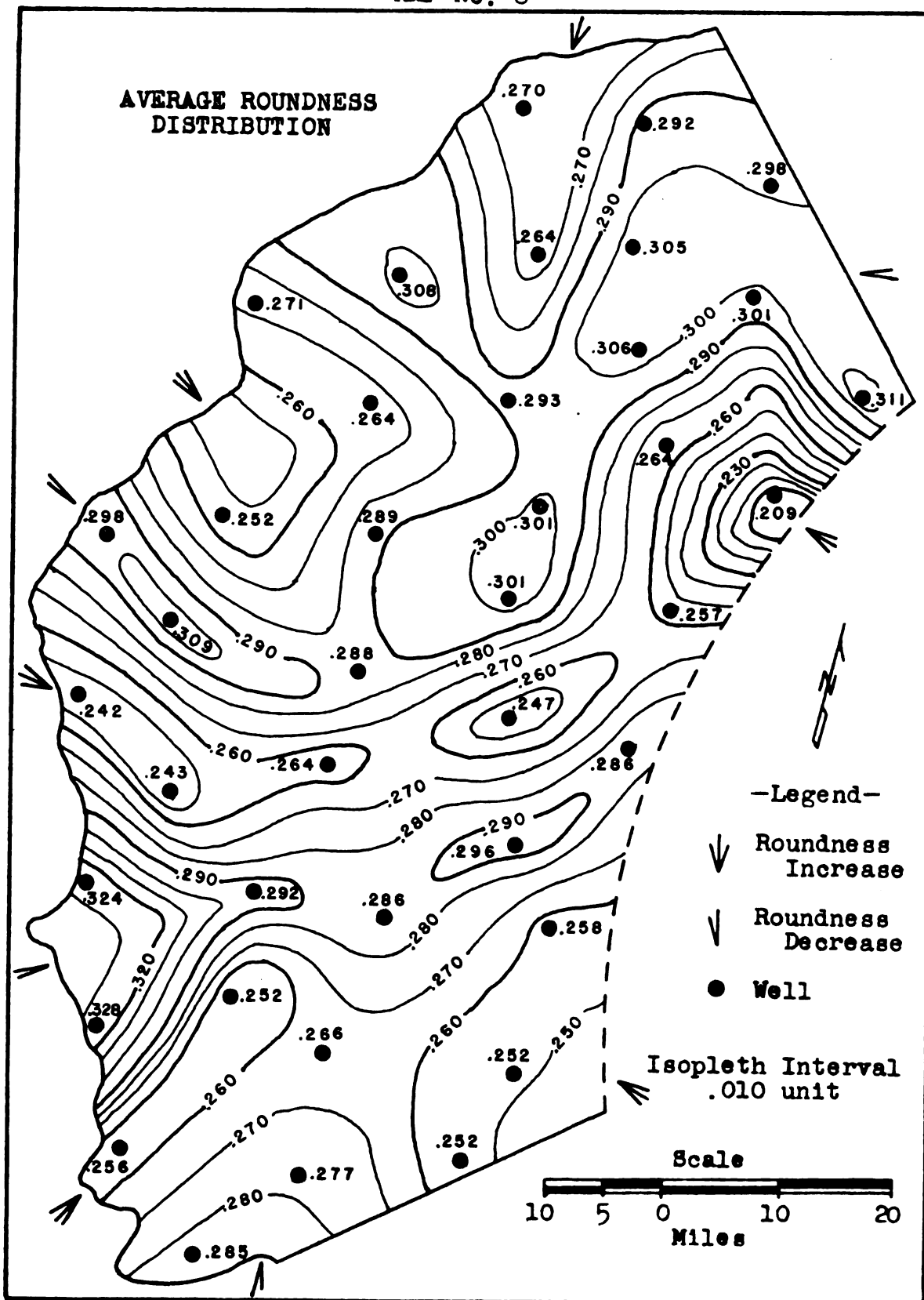
Well No.	Round- ness	Sphe- ricity	Well No.	Round- ness	Sphe- ricity
1	0.256	0.775	21	0.288	0.791
2	0.285	0.793	22	0.301	0.793
3	0.277	0.802	23	0.247	0.800
4	0.266	0.783	24	0.286	0.793
5	0.252	0.796	25	0.271	0.791
6	0.252	0.790	26	0.308	0.791
7	0.328	0.796	27	0.264	0.791
8	0.324	0.791	28	0.293	0.789
9	0.252	0.793	29	0.301	0.788
10	0.292	0.794	30	0.257	0.790
11	0.286	0.796	31	0.270	0.798
12	0.258	0.798	32	0.264	0.790
13	0.242	0.804	33	0.305	0.790
14	0.243	0.780	34	0.306	0.785
15	0.264	0.800	35	0.264	0.780
16	0.296	0.788	36	0.192	0.771
17	0.298	0.775	37	0.292	0.794
18	0.309	0.802	38	0.298	0.793
19	0.252	0.791	39	0.301	0.790
20	0.289	0.806	40	0.311	0.794

the sample. The histograms, therefore, are direct representatives of the data obtained. From these, it is possible to visualize graphically the sorting, skewness, and distribution of the sand measurements which are obtained from the quartile calculation of the cumulative curves. Features to be noted from these figures are: the interval containing the largest percentage of grains, that is, the modal class, does not, in most cases, contain the arithmetic average (Table VI), nor in many cases does it correspond to the median calculations (Table III). This represents the skewness values derived from the cumulative curves, and the modal class represents the sorting values. The writer feels that when these histograms are compared with the results obtained from the cumulative curves, the reader will gain a better understanding of these results.

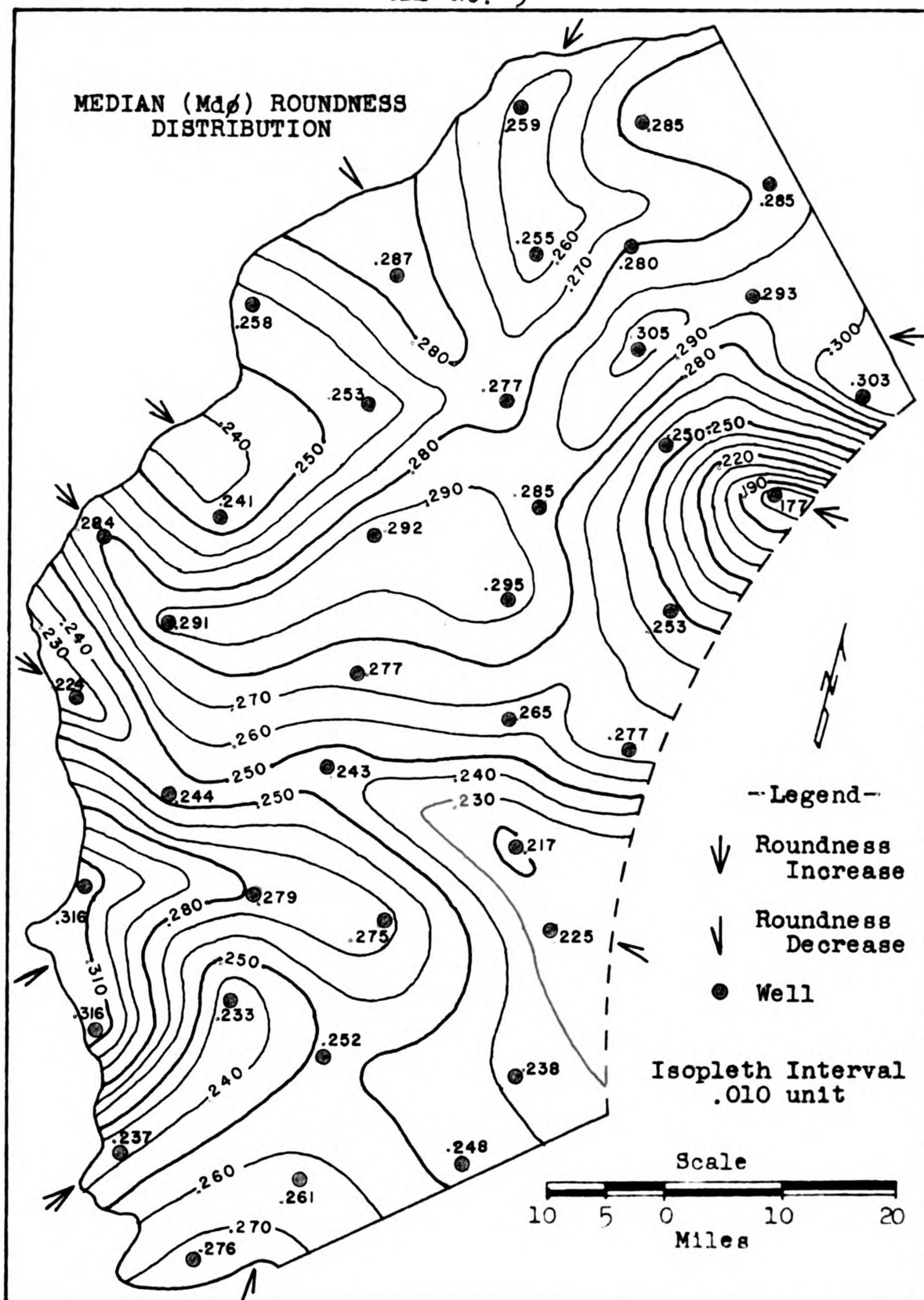
Table III is a summary of the roundness calculations taken from the cumulative curves. These curves were drawn using the phi notation as the independent variable (Figure 3), from the same data used in making the histograms. In studying the cumulative quartile calculations, important information may be obtained by comparing the quartile deviation, $QD\phi$, values. These values are taken directly from the graphs plotted according to Krumbein's phi scale, whereas the "So" values are calculated as described on page 41,

which is the same as the values obtained when the curves are plotted on semilogarithmic paper. The isopleth maps (Maps 10 and 11) plotted with $QD\phi$ and S_o values will illustrate the similarity. The same relationships exist between skewness, $Sk_g\phi$, and skewness, Sk . The logarithmic data presented for S_o and Sk are to be compared in the same manner as the logarithmic values explained in the size analysis on page 96.

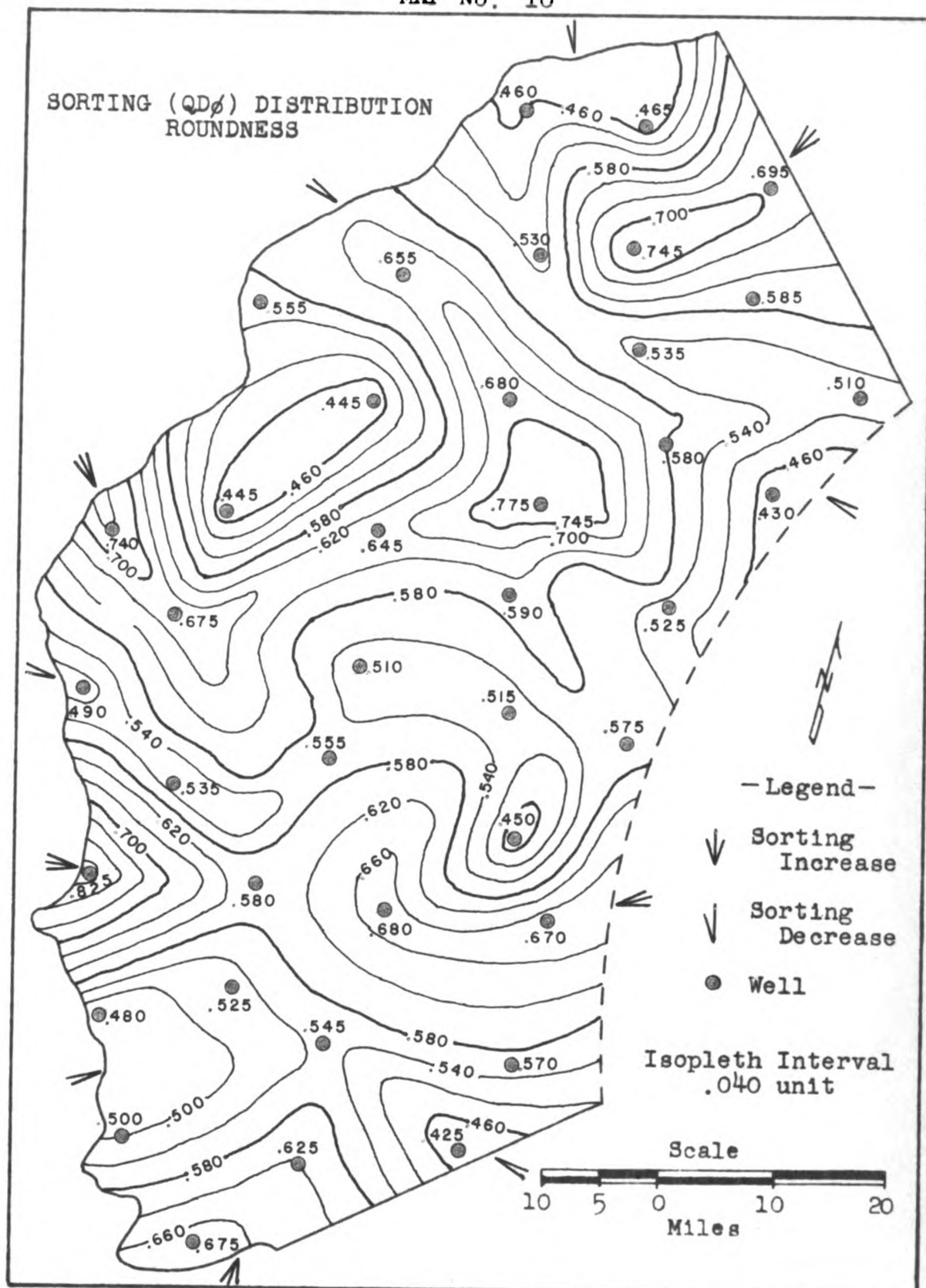
In the fourth method of comparing roundness measurements, isopleth maps have been used to represent the values derived from calculating the arithmetic averages (Map 8) and to represent the M_d , $QD\phi$, S_o , and Sk values (Maps 9, 10, 11, 12) obtained from the cumulative curves. It should be noted that in all cases these isopleth maps show the same general pattern. For example, it may be seen that Well Nos. 8 and 17 (Map 3) represent areas of sediment having a comparatively high degree of rounding (Maps 8 and 9). These same locations should now be examined on the maps representing roundness sorting (Maps 10 and 11). The same trends may be observed, and it will be seen that the sands in these areas are rather poorly sorted, in comparison to the sands in other areas such as those around Well Nos. 19 and 36. The skewness (Map 12) values should also be examined for Well Nos. 8 and 17, and the area around these



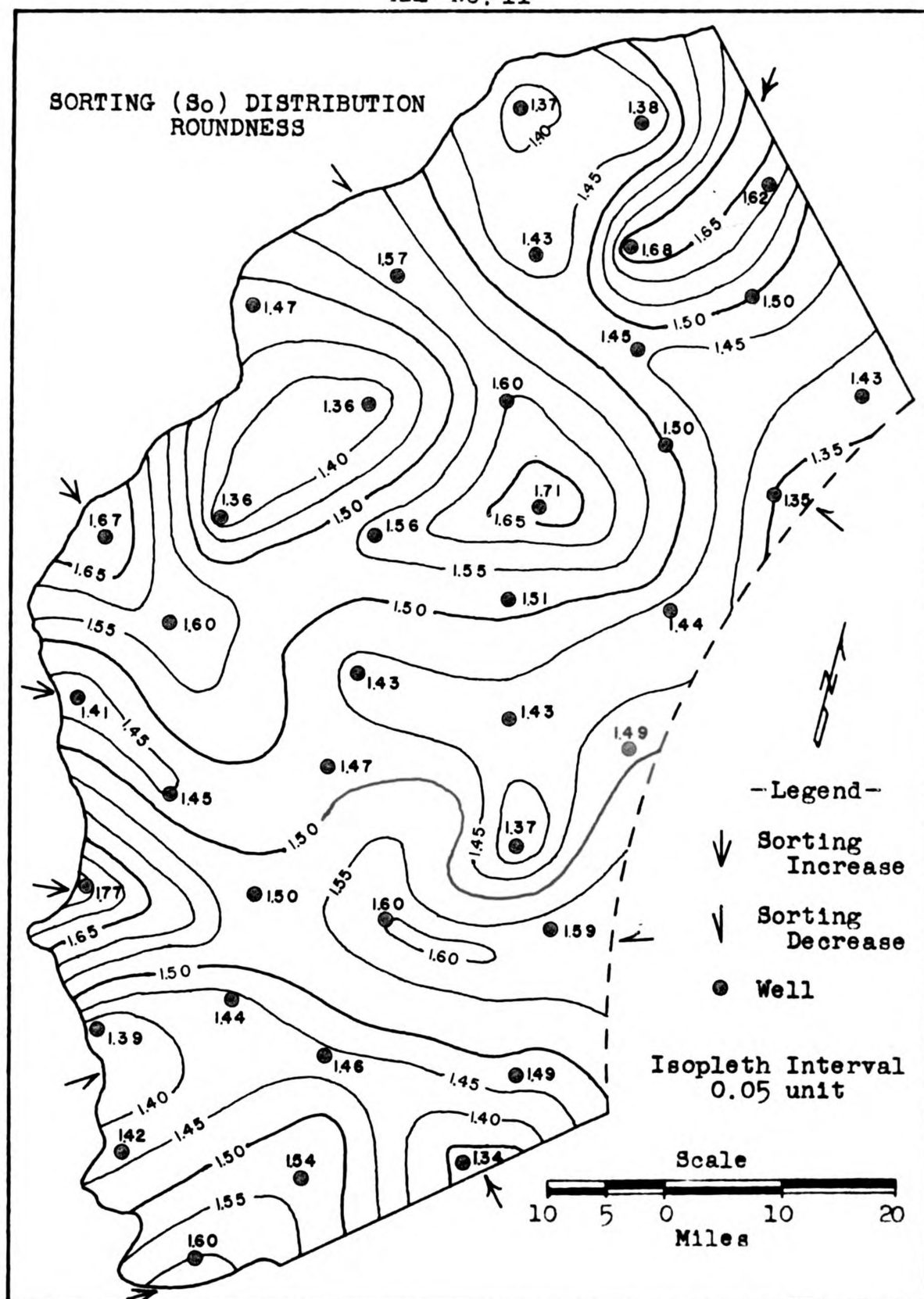
MAP No. 9

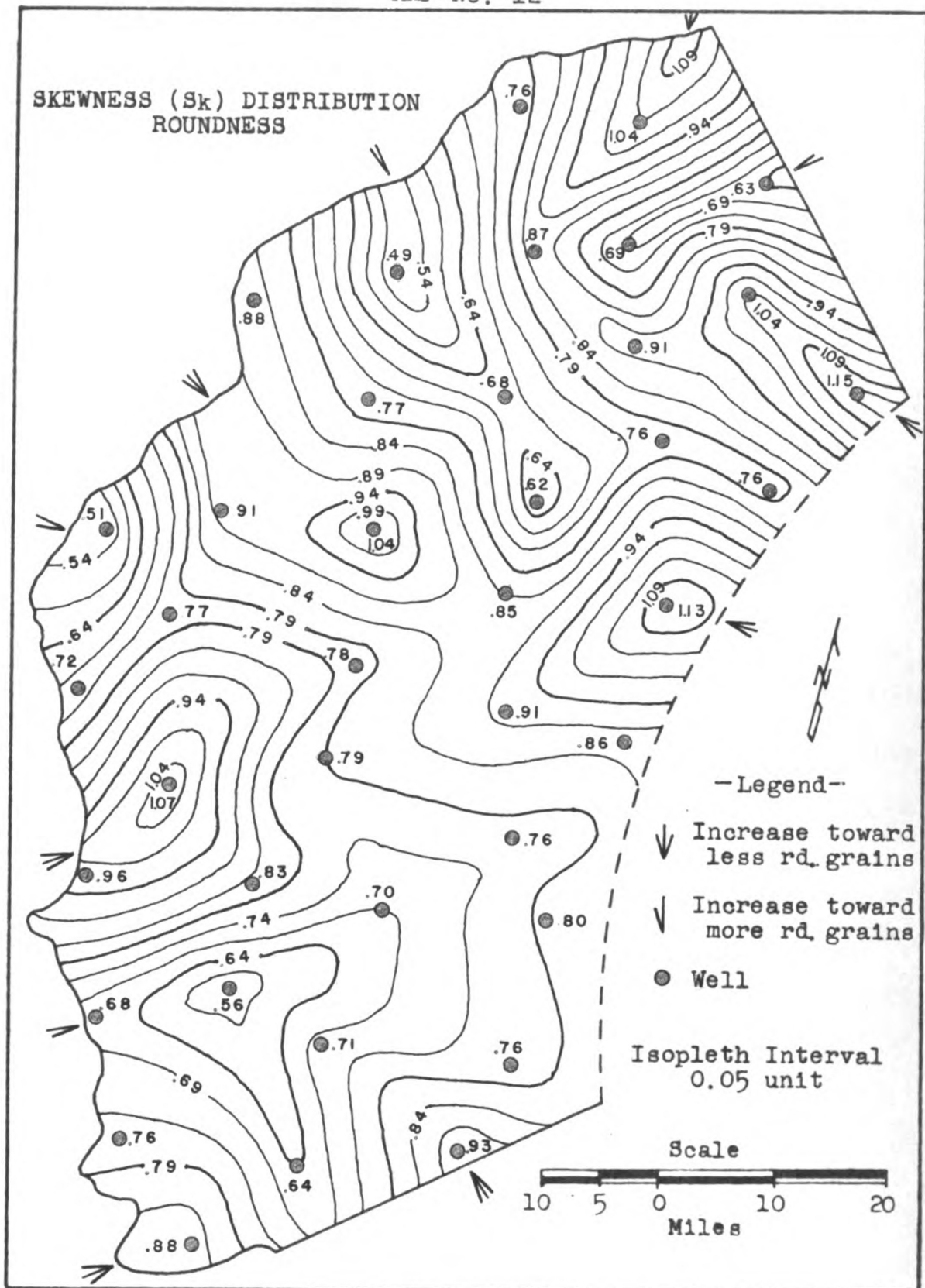


MAP No. 10



MAP No. 11



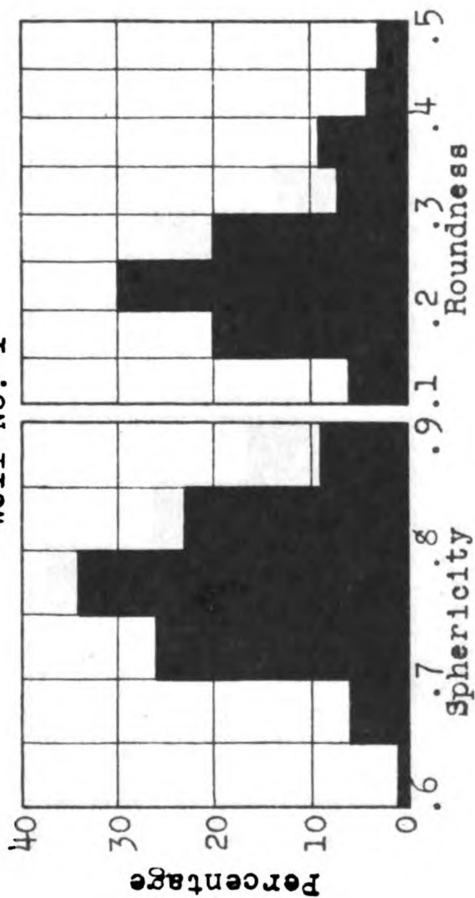


locations compared with the other isopleth maps mentioned above. From these examples, it may be seen that the average and median roundness, sorting and quartile deviation, and skewness appear, in general, to illustrate similar trends of deposition. The relationships, however, existing between these values are not, in all places, those expected in normal stream deposits. That is, many geologists take for granted that as a sand grain is transported it becomes more rounded, the sorting increases, and a graph, such as a histogram, will show the skewness of a sediment to be toward the less rounded grains as the transportation distance increases. The relationship skewness has to the histogram may be seen when the modal class is compared with the median roundness (Table III and pages 108-117). Those cases including the example given above which appear to differ from the expected results will be considered in the section on interpretation.

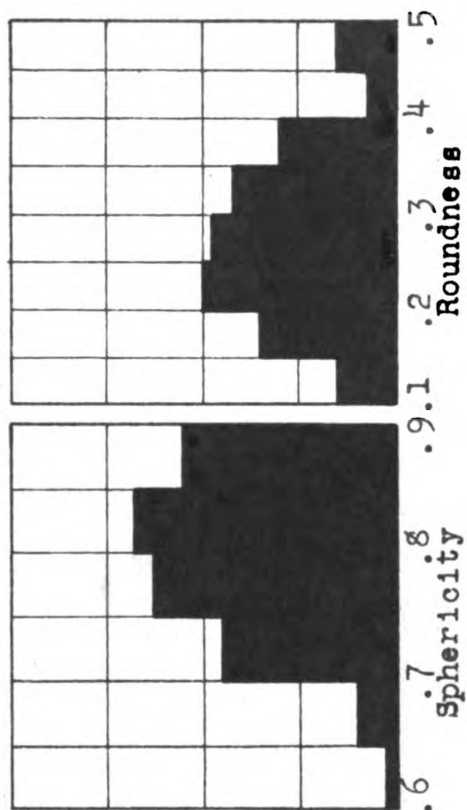
If the above-mentioned methods of comparison are now inter-related, many trends of deposition may be observed and the relationships between them noted.

HISTOGRAMS OF ROUNDNESS AND SPHERICITY DISTRIBUTION

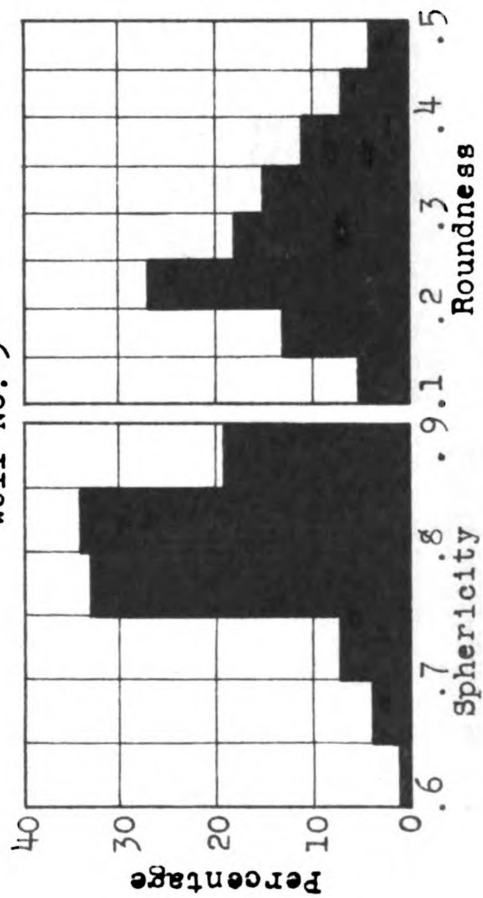
Well No. 1



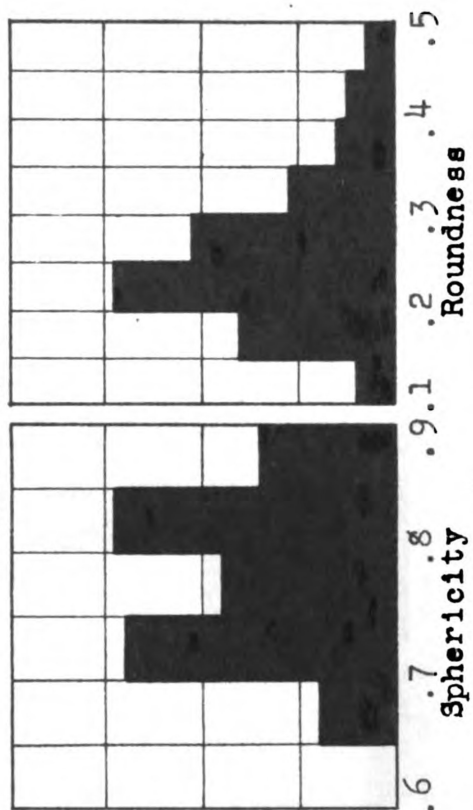
Well No. 2



Well No. 3

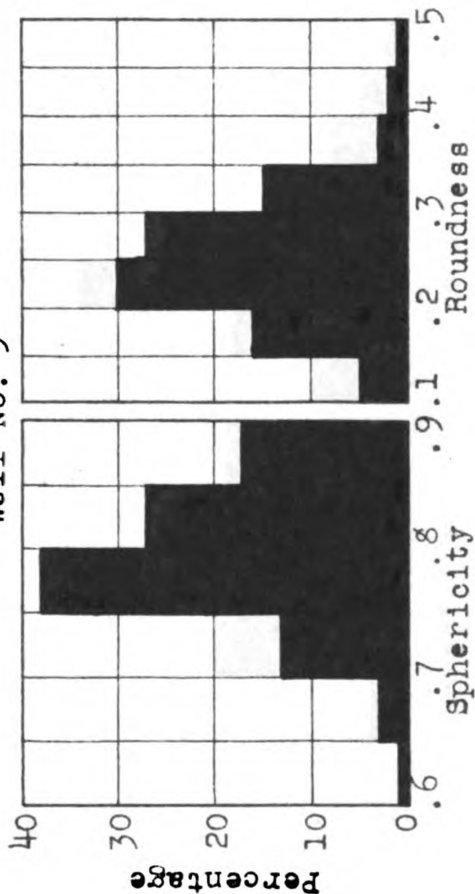


Well No. 4

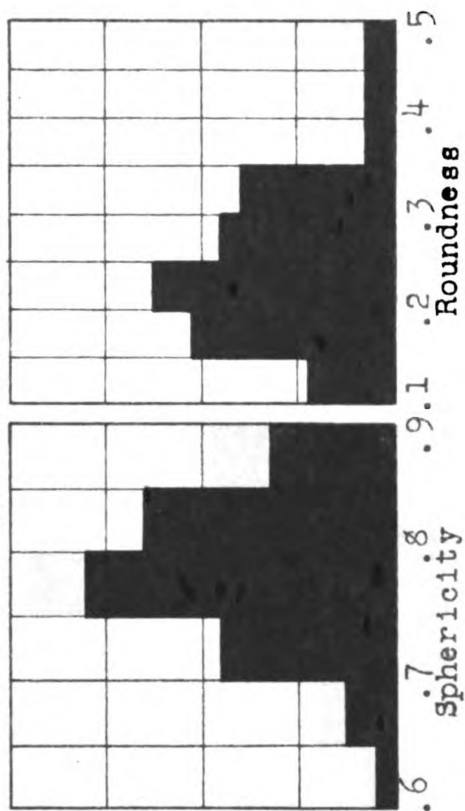


HISTOGRAMS OF ROUNDNESS AND SPHERICITY DISTRIBUTION

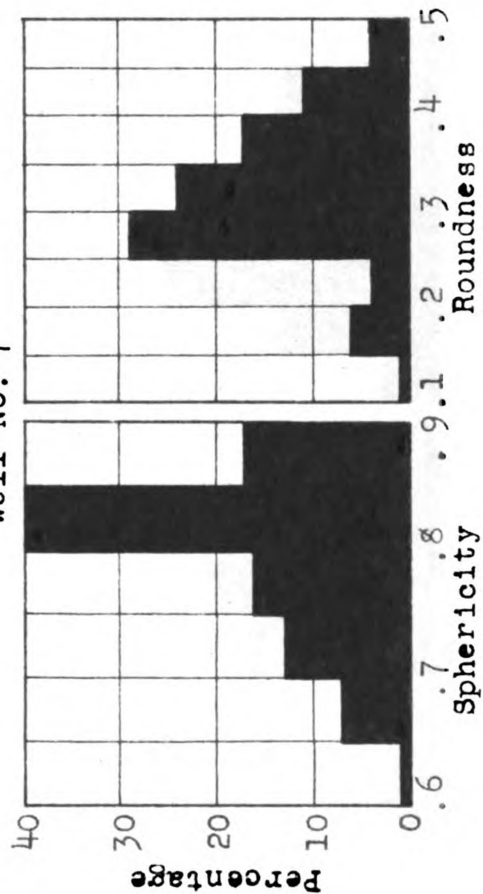
Well No. 5



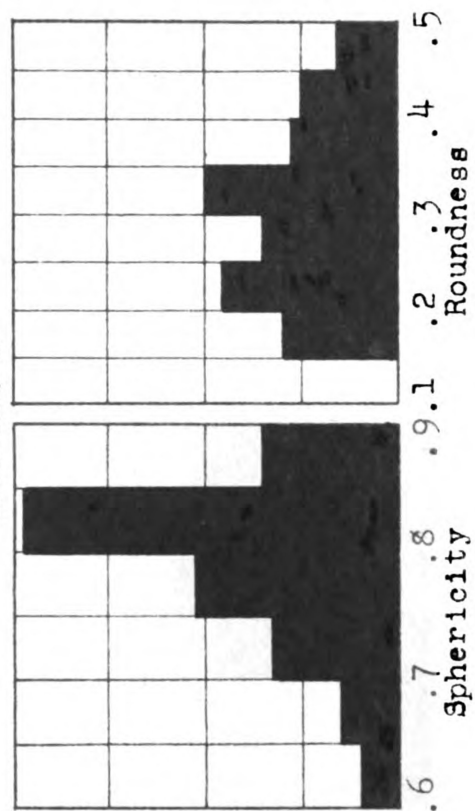
Well No. 6



Well No. 7

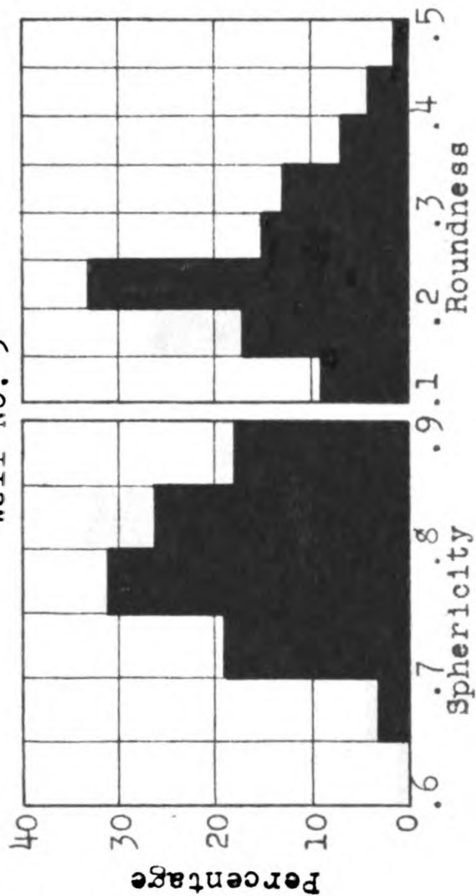


Well No. 8

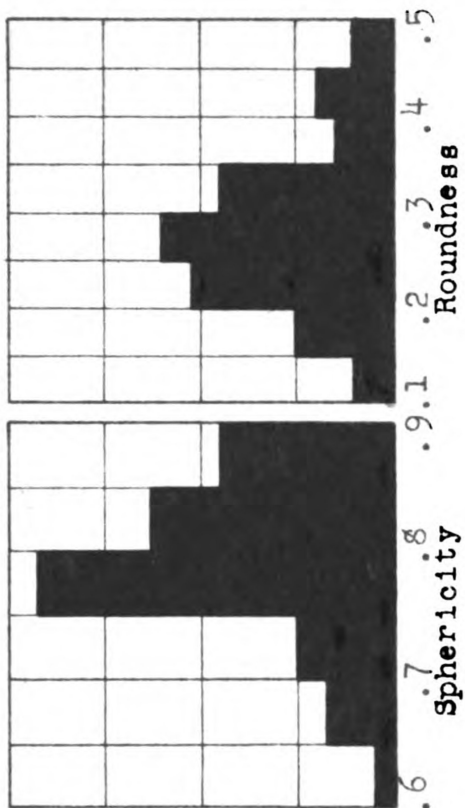


HISTOGRAMS OF ROUNDNESS AND SPHERICITY DISTRIBUTION

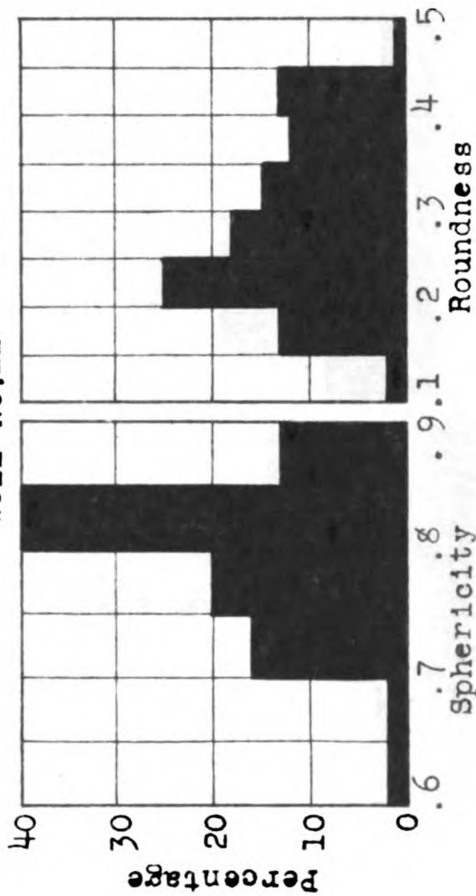
Well No. 9



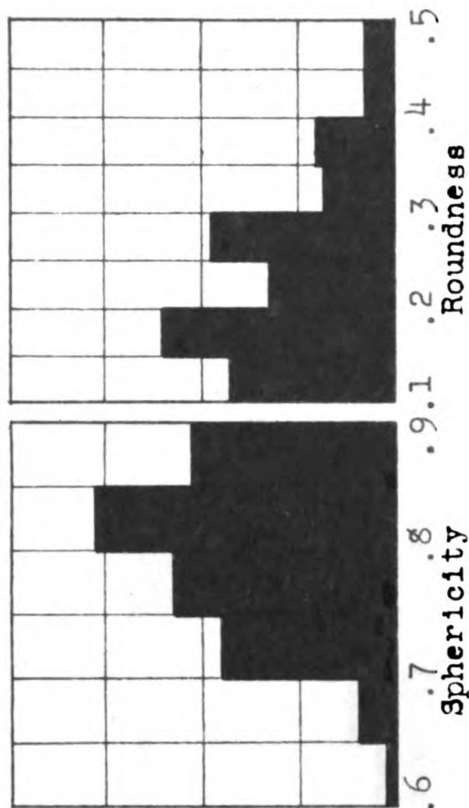
Well No.10



Well No.11

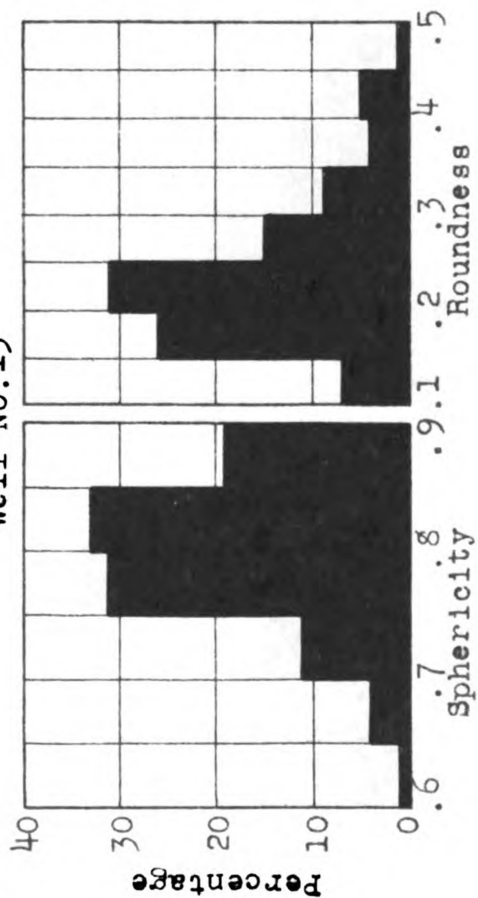


Well No.12

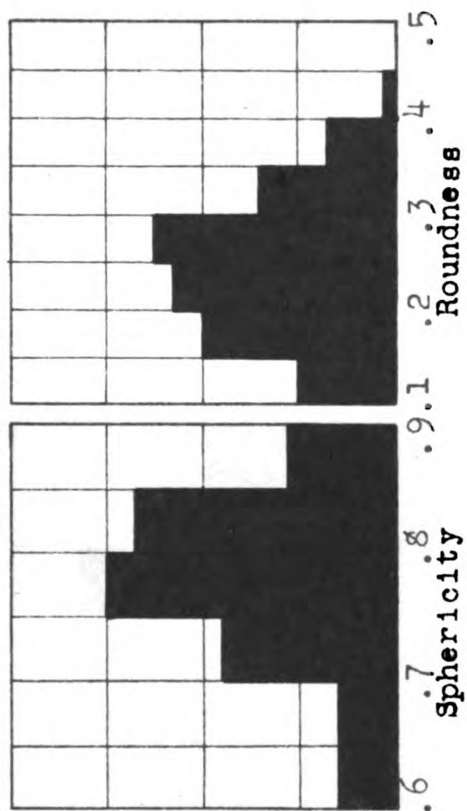


HISTOGRAMS OF ROUNDNESS AND SPHERICITY DISTRIBUTION

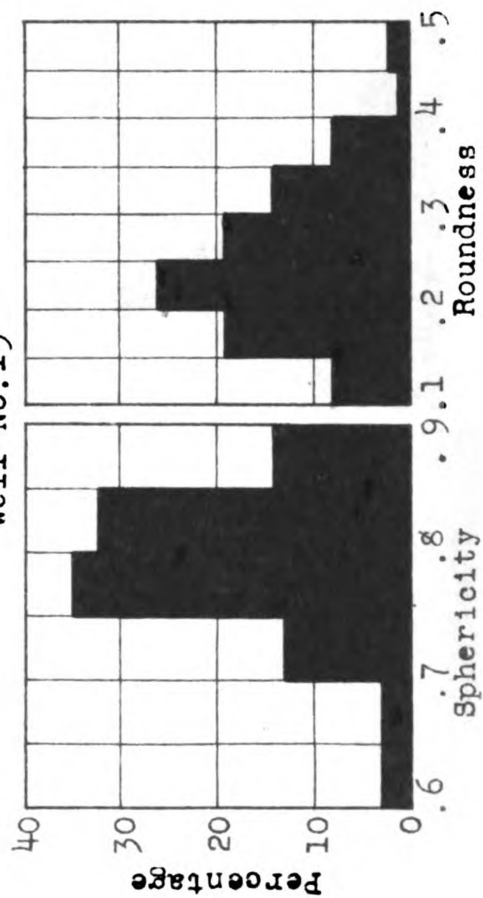
Well No.13



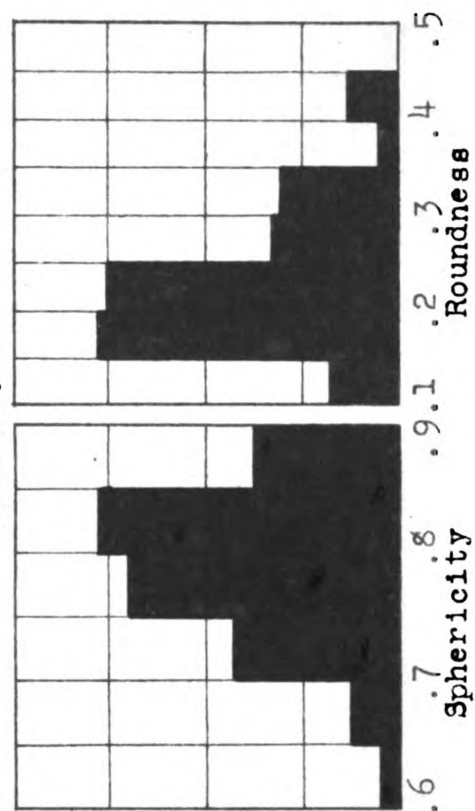
Well No.14



Well No.15

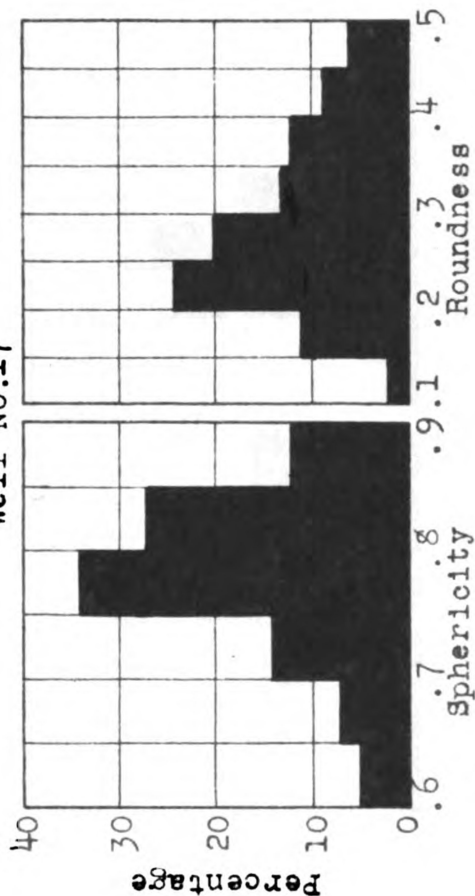


Well No.16

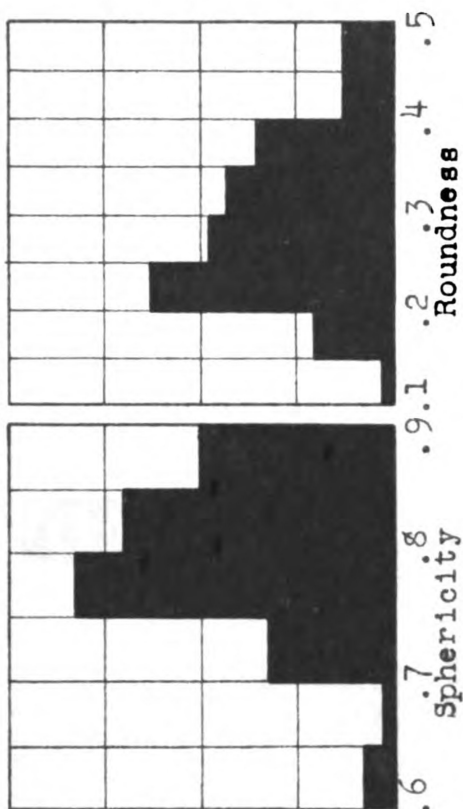


HISTOGRAMS OF ROUNDNESS AND SPHERICITY DISTRIBUTION

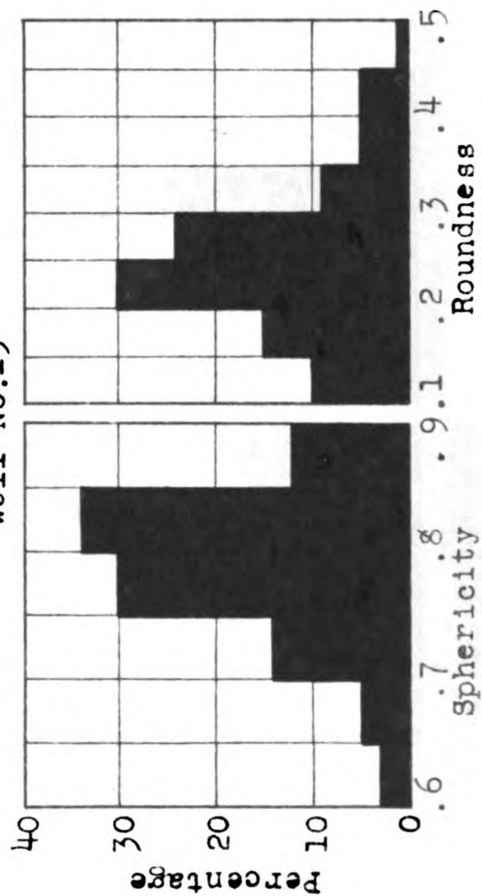
Well No.17



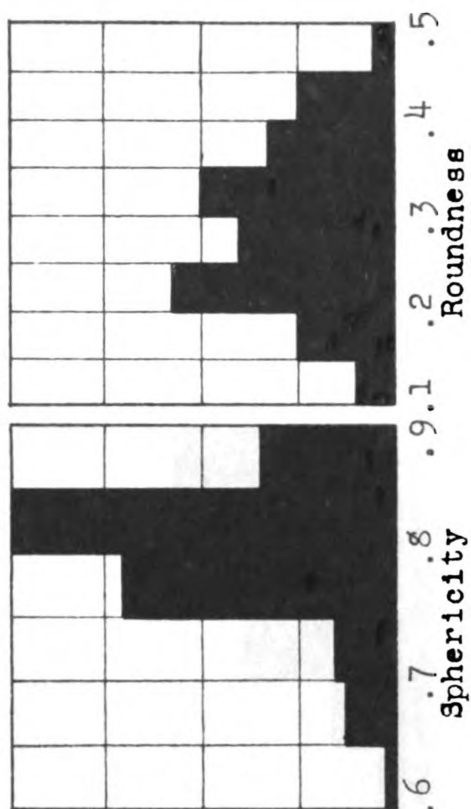
Well No.18



Well No.19

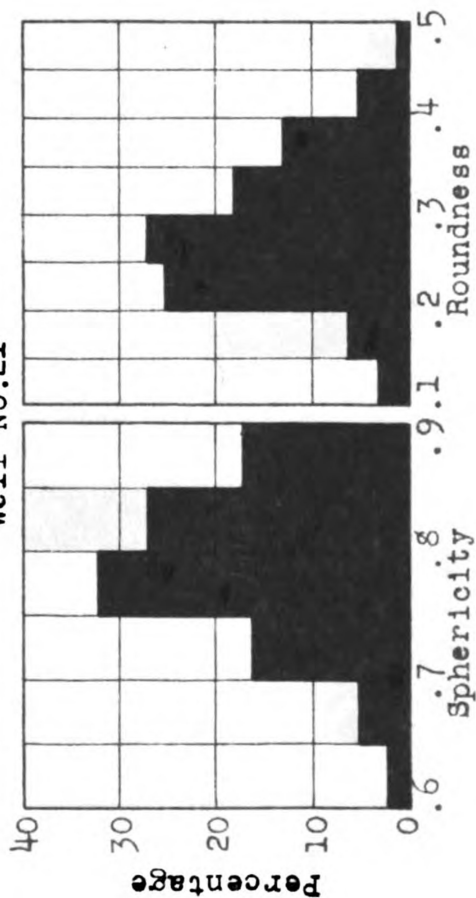


Well No.20

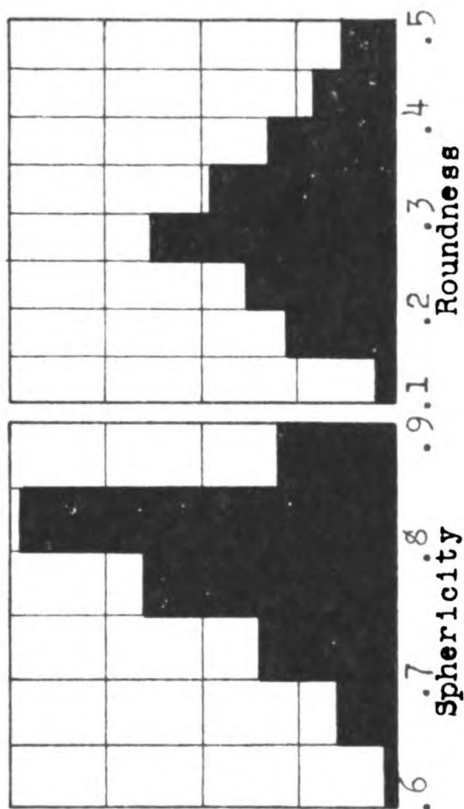


HISTOGRAMS OF ROUNDNESS AND SPHERICITY DISTRIBUTION

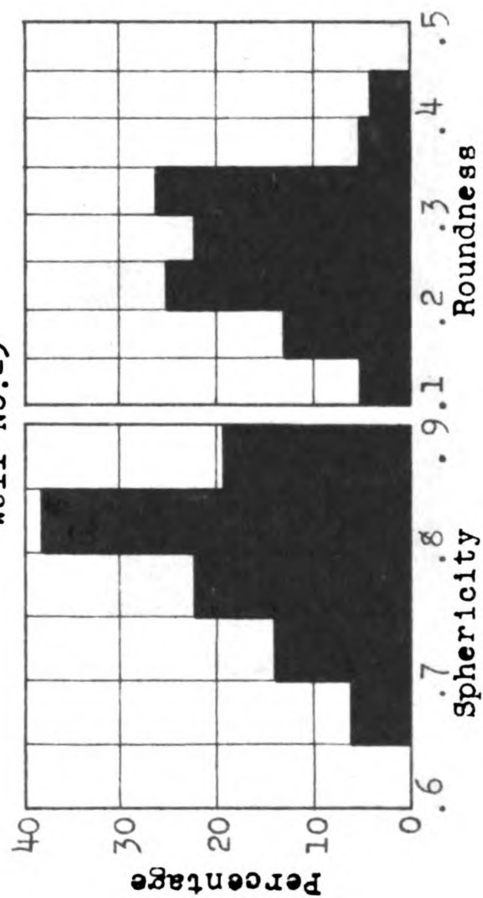
Well No.21



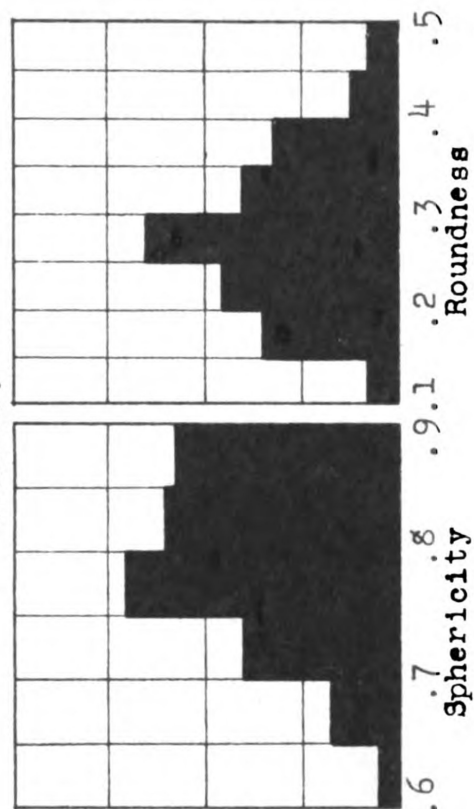
Well No.22



Well No.23

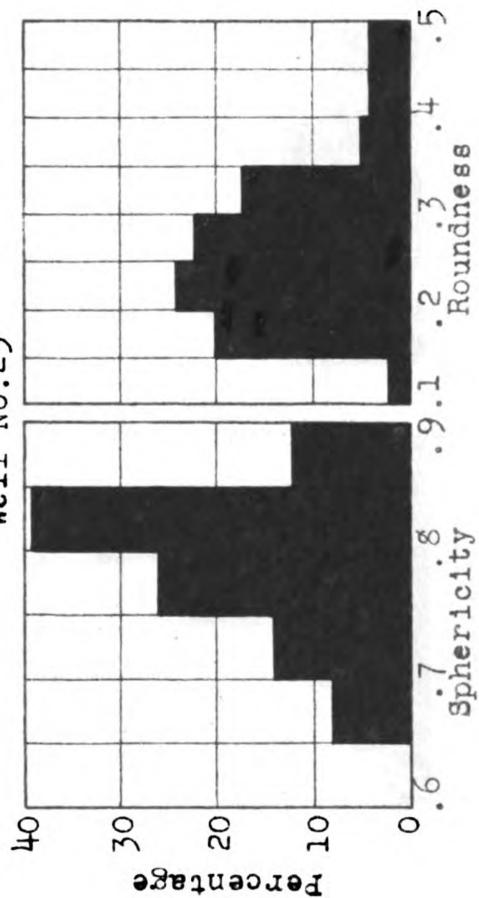


Well No.24

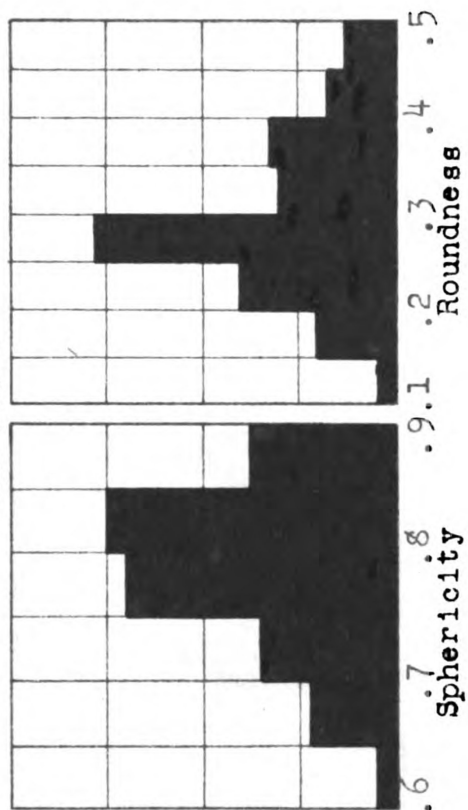


HISTOGRAMS OF ROUNDNESS AND SPHERICITY DISTRIBUTION

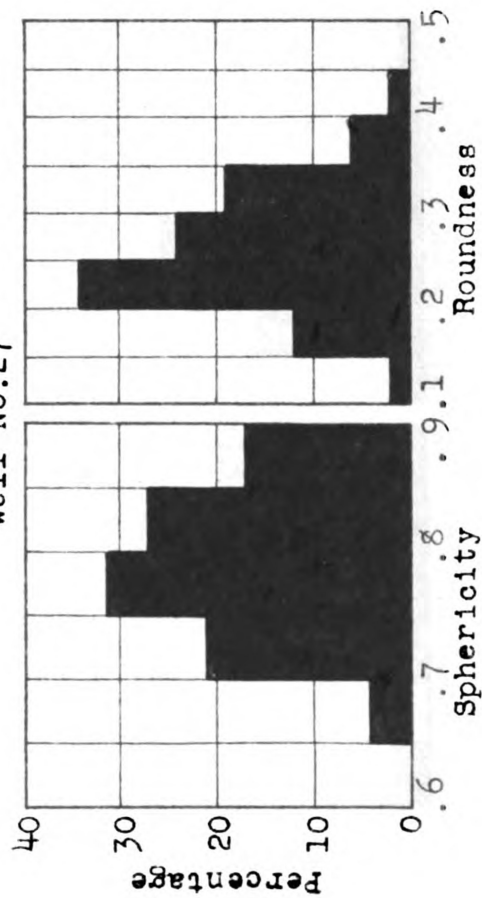
Well No.25



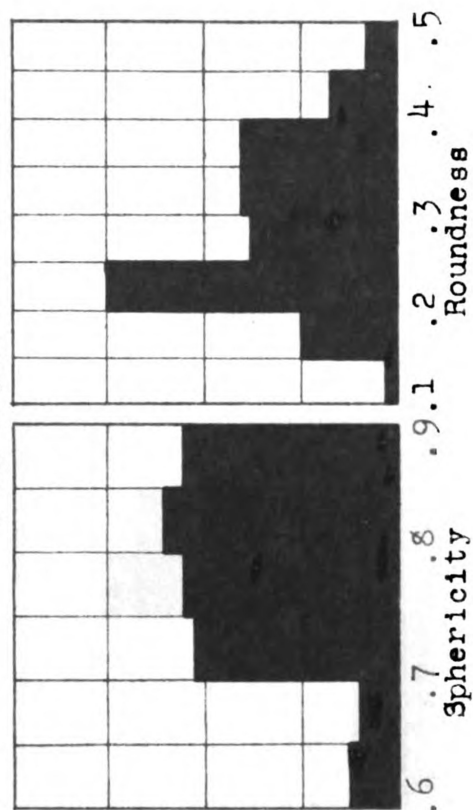
Well No.26



Well No.27

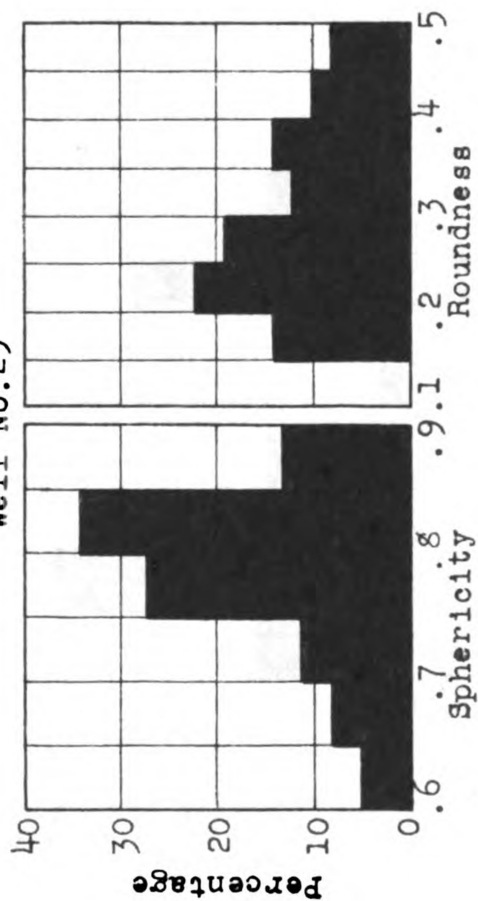


Well No.28

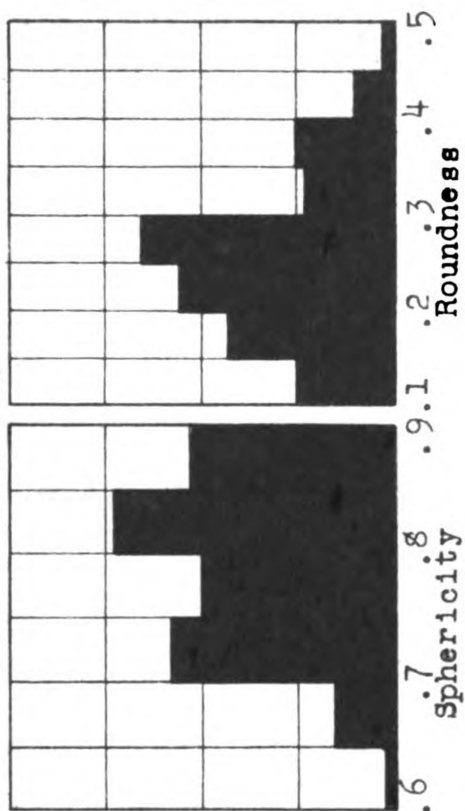


HISTOGRAMS OF ROUNDNESS AND SPHERICITY DISTRIBUTION

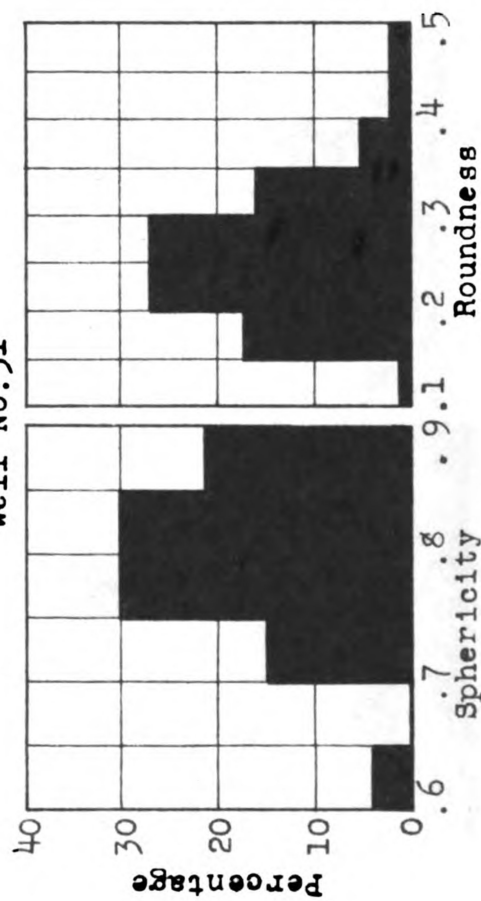
Well No.29



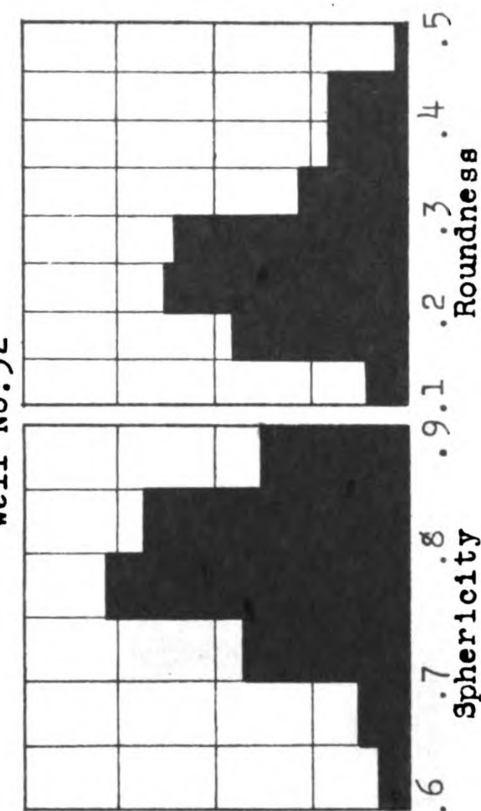
Well No.30



Well No.31

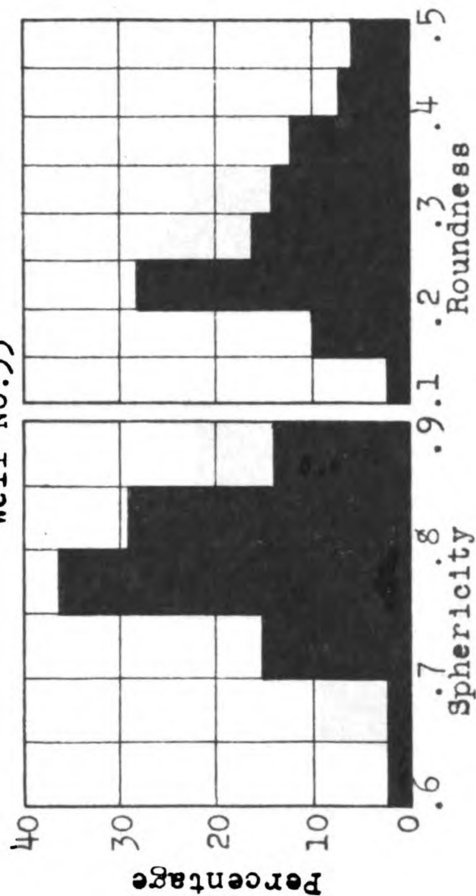


Well No.32

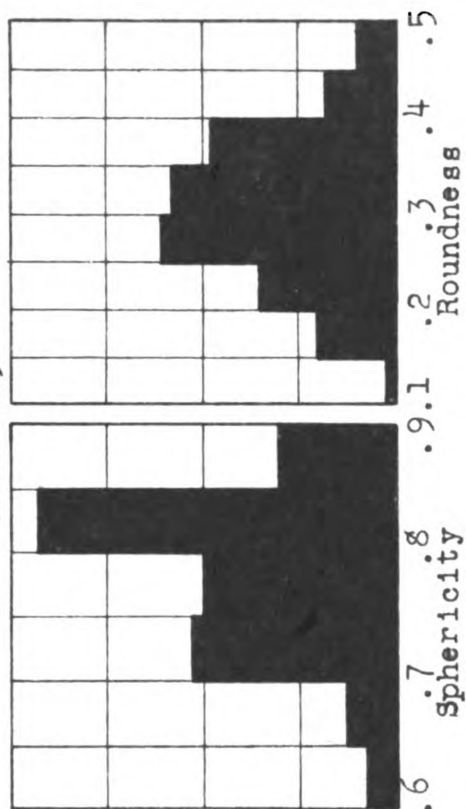


HISTOGRAMS OF ROUNDNESS AND SPHERICITY DISTRIBUTION

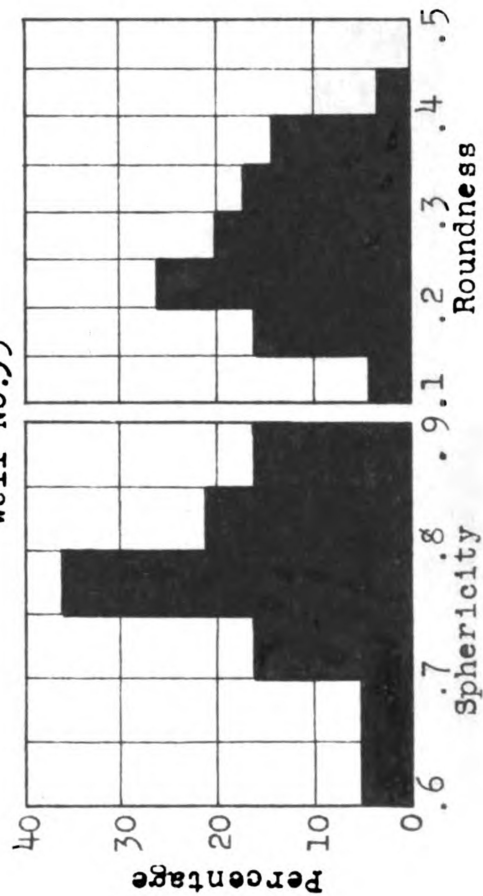
Well No.33



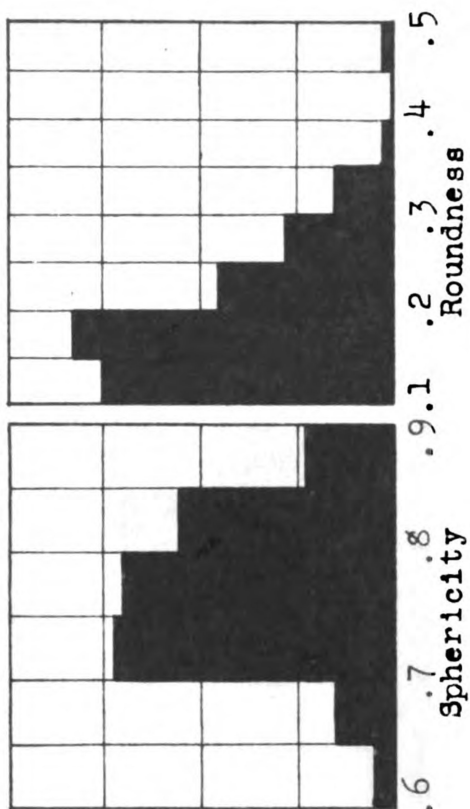
Well No.34



Well No.35

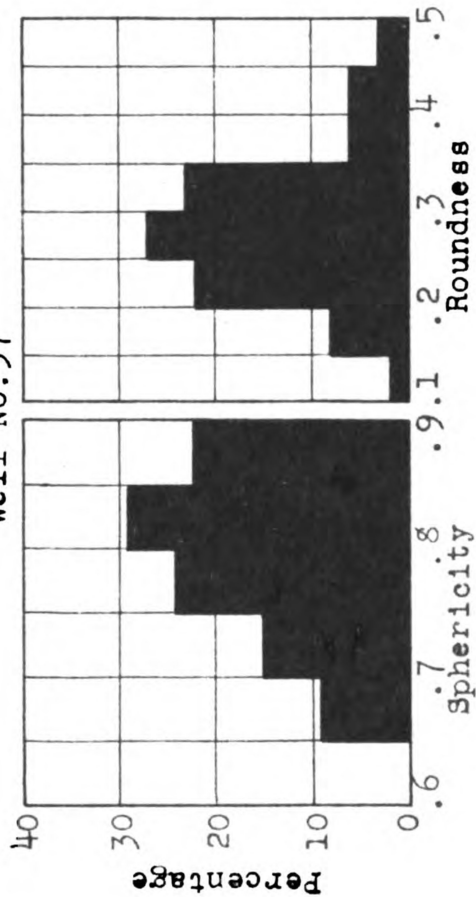


Well No.36

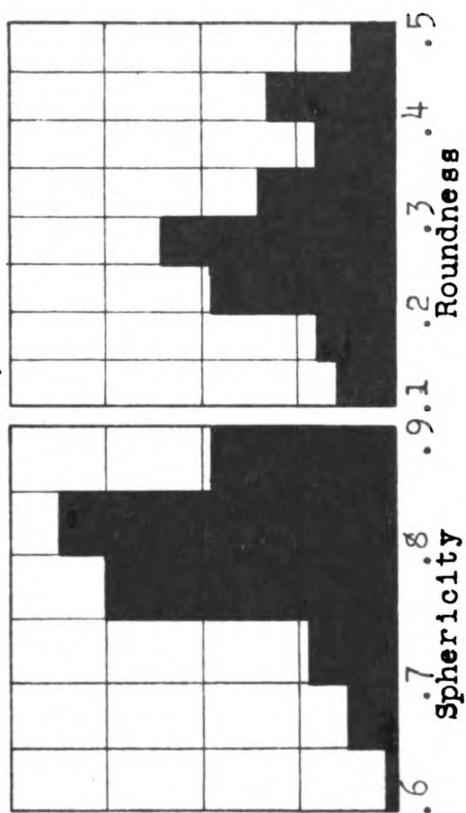


HISTOGRAMS OF ROUNDNESS AND SPHERICITY DISTRIBUTION

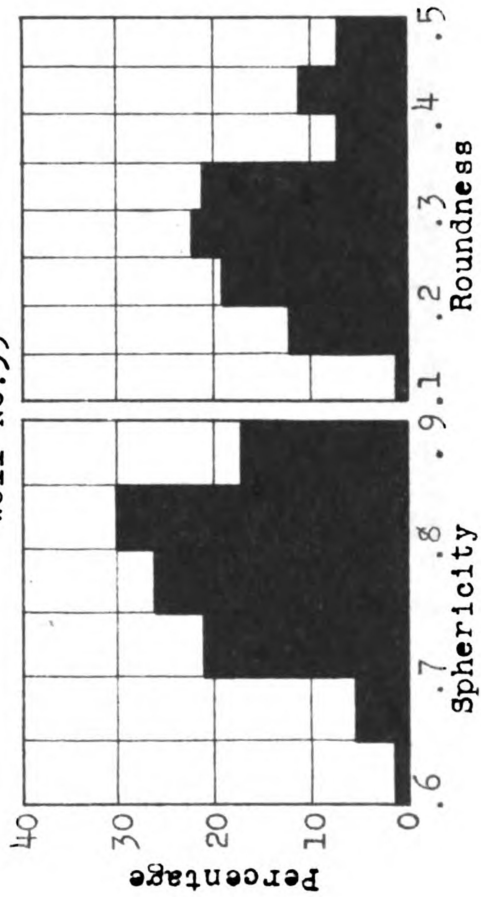
Well No.37



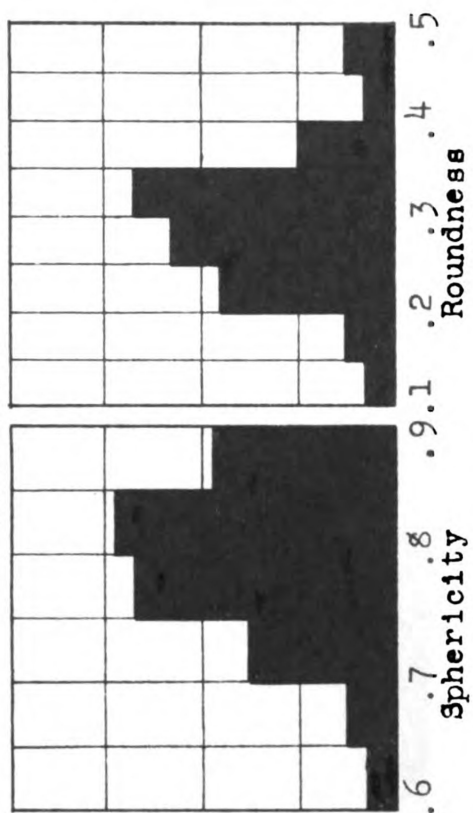
Well No.38



Well No.39



Well No.40

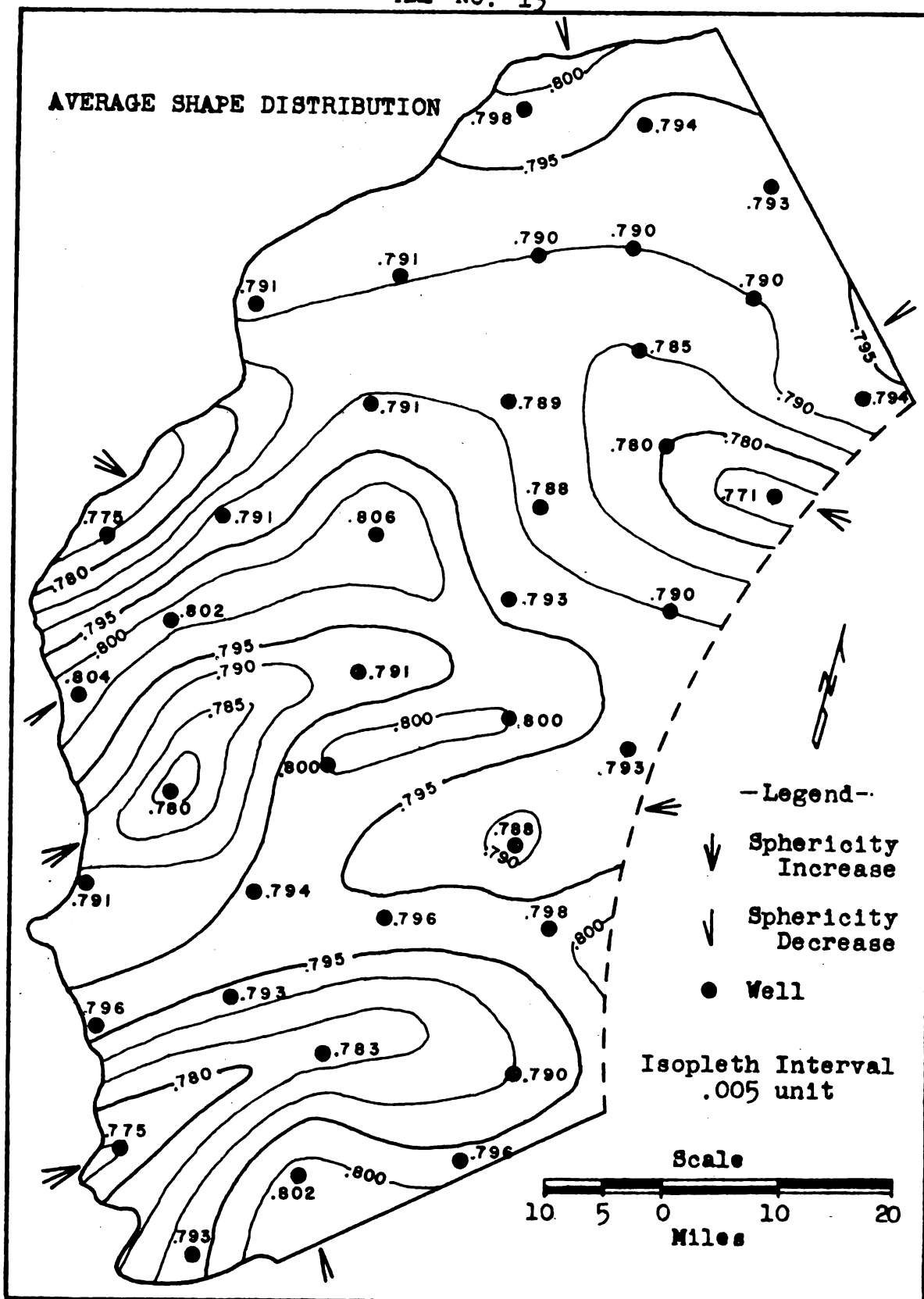


Analysis of Sphericity Distribution

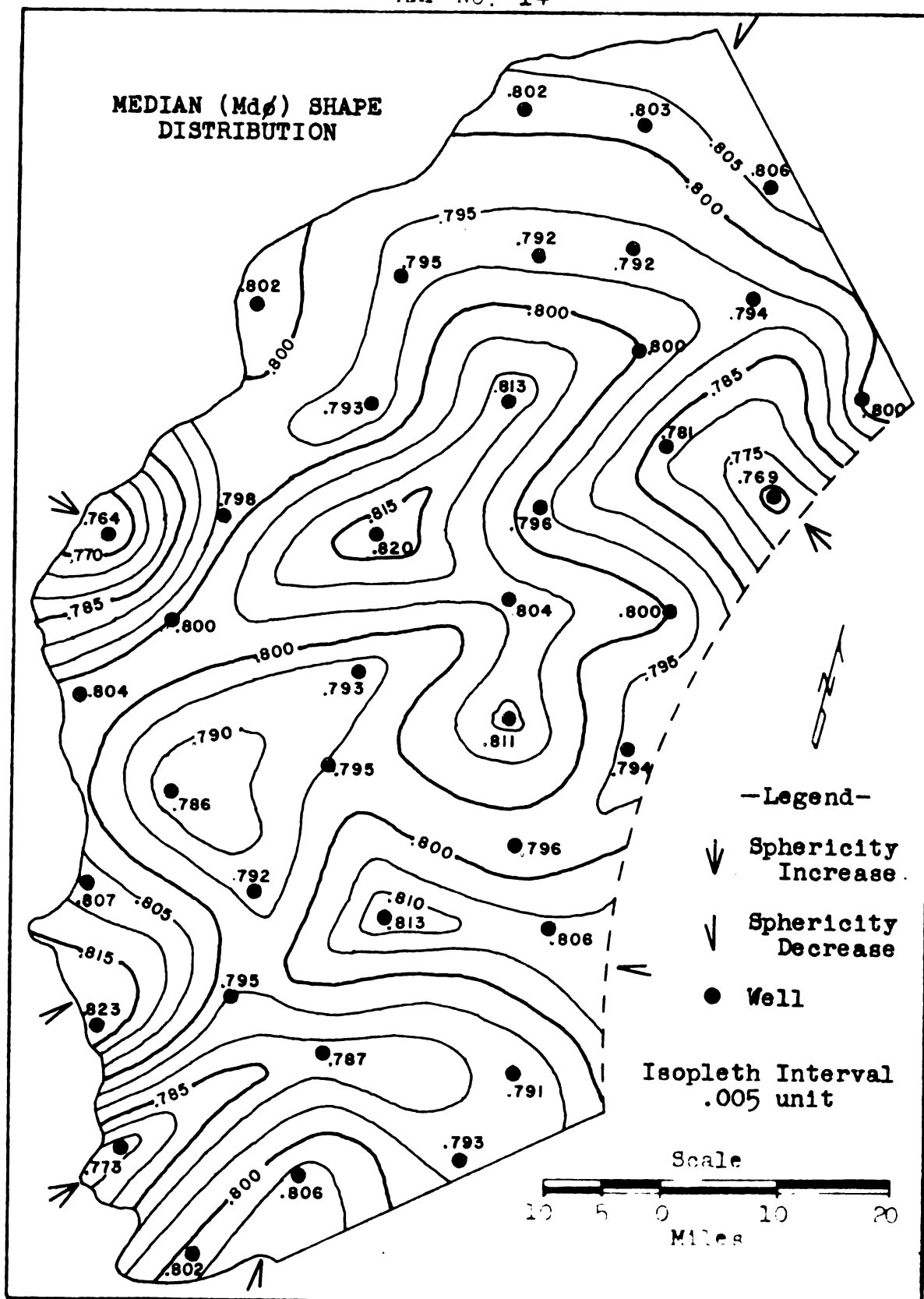
The methods by which the distributions of sphericity were analyzed are the same as those used in analyzing roundness distributions. The arithmetic averages (Table VI) again show little variation; however, when plotted as an isopleth map (Map 13), a strong similarity may be noted with the median map (Map 14). Also, as should be expected, the quartile deviation and sorting isopleth maps (Maps 15 and 16) are quite similar. Less resemblance, however, appears to be present when the first two maps and second two maps are compared. The isopleth skewness map appeared to show little resemblance to the other maps, and was therefore omitted. The areas having the most resemblance to the skewness isopleth map are found about Well Nos. 7 and 17 on the median map and in the location of Well No. 24 on the sorting and quartile deviation maps.

Table IV is a summary of the quartile calculations derived from the cumulative curves, illustrated in Figure 3; and these calculations were used in drawing the isopleth maps. Logarithmic values for S_o and S_k are included to be used in obtaining ratios of comparison.

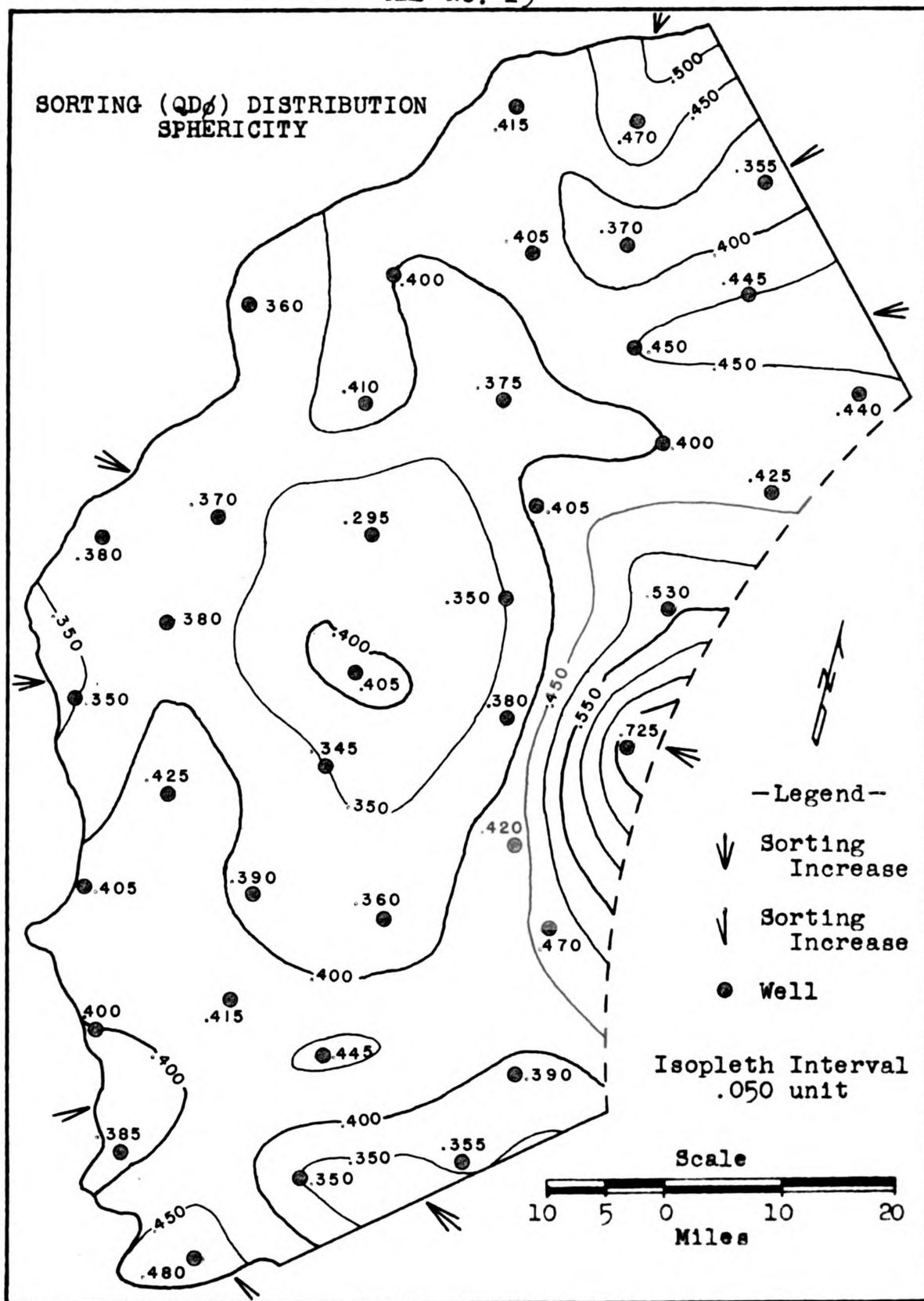
MAP No. 13

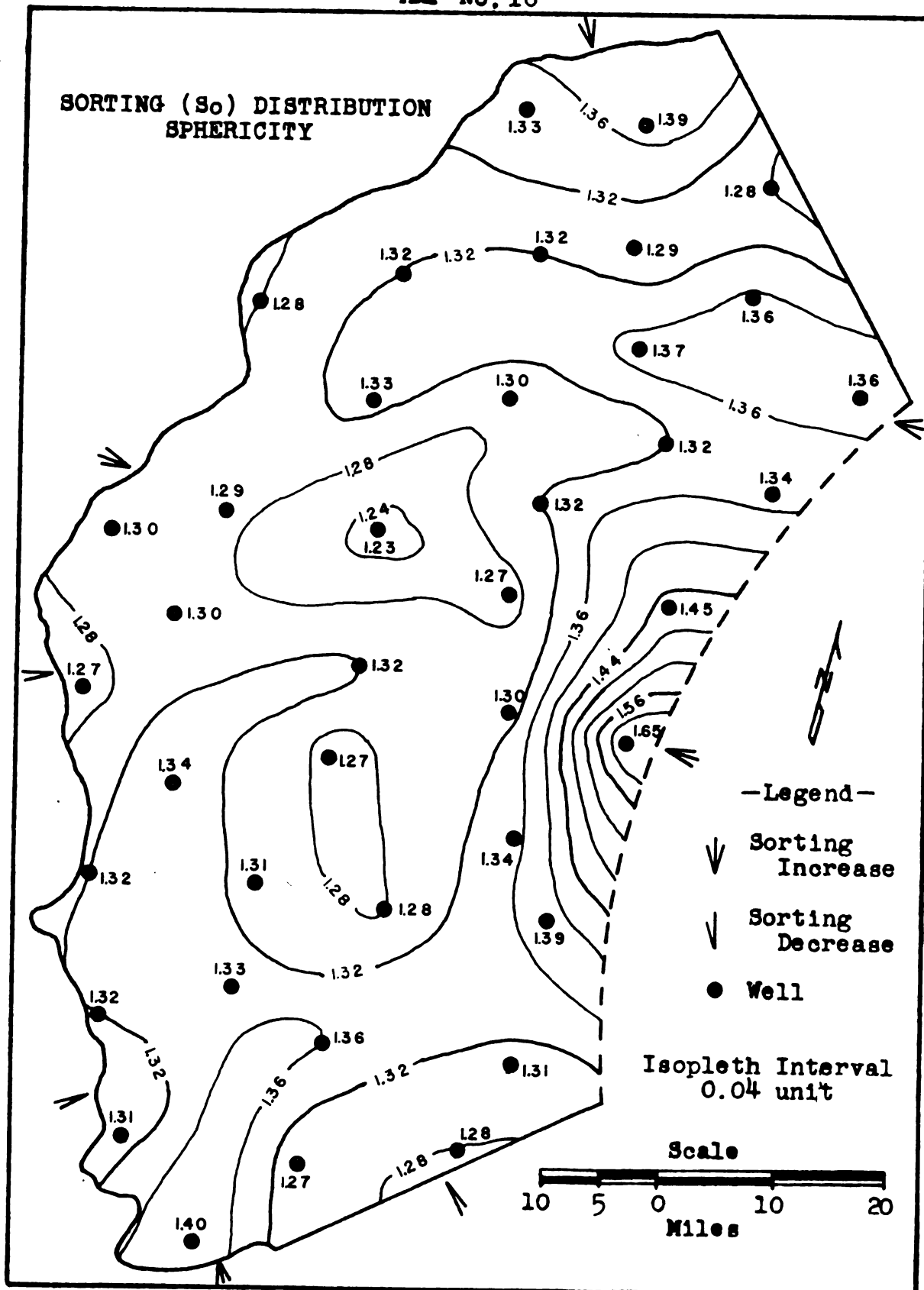


MAP No. 14



MAP No. 15





Histograms are also presented (pp. 108-117), to illustrate visually, as in the case of roundness, the sorting skewness and distribution values obtained from the cumulative curves.

The relationships believed to exist between sphericity sorting, skewness, and median size are not the same as in the case of roundness. Many geologists believe that as a grain of sand is transported, it becomes less spherical. If this is true, the degree of sorting would be expected to increase as the material becomes less spherical. By examining Table IV, it may be seen that this is not necessarily the case. If this were true, the skewness would be expected to be positive, that is, lie toward the more spherical grains as the sphericity decreases. This relationship does appear to prevail. Note Well Nos. 7 and 17 in Table IV. By comparing the modal class in the sphericity histograms with the average and median sphericity, skewness may be graphically represented. By comparing the modal class with the other sphericity intervals or classes and comparing this to the average and median sphericity, the sorting relationship may be obtained. In the case of sphericity, however, none appears to prevail.

The methods of comparing and illustrating the relationships between the sphericity quartile calculations should be used also in

comparing the relationships which may exist between the roundness and sieve analysis quartile calculations.

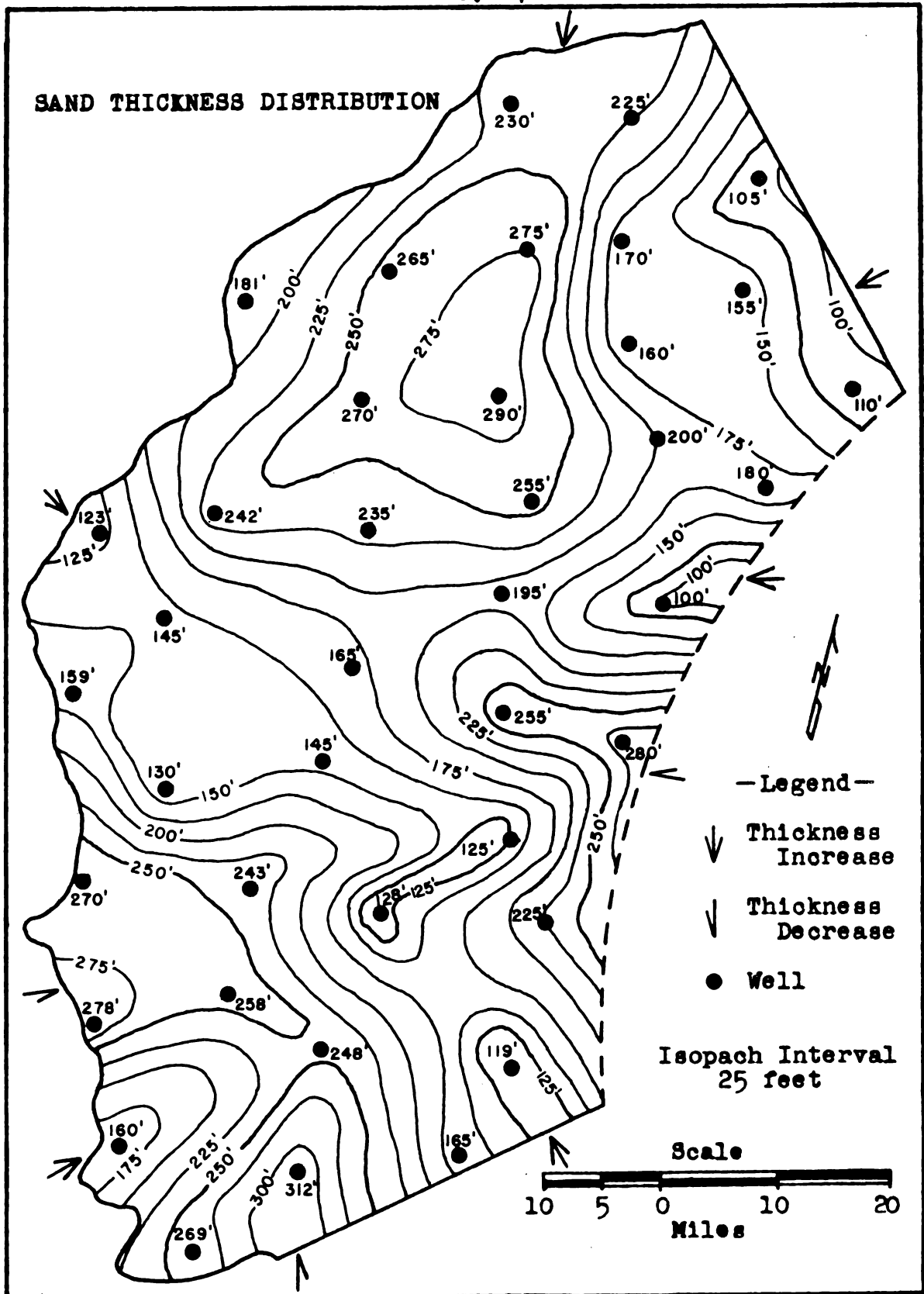
Summary Comparison

In summarizing and comparing the size, roundness, and sphericity distributions, the most valuable results are found in comparing the different isopleth maps discussed in the preceding sections.

The author feels that, in general, the isopleth maps showing size distribution (Maps 4, 5, 6, 7), roundness distribution (Maps 8, 9, 10, 11, 12), and sphericity distribution (Maps 13, 14, 15, 16) have many similar patterns and trends of deposition. An isopach map (Map 17) which has been included also appears to coincide in many areas with the above-listed maps. To best compare these maps, the localities around the following well numbers should be given special attention (Map 3): Nos. 1, 3, 5, 6, 7, 8, 12, 13, 17, 19, 24, 30, 31, 36, 37, 38, and 40. It should be noted that the areas around these wells appear to have similar depositional trends in most of the isopleth maps.

As explained on page 96, the extent of the differences between the quartile calculations of each sample may be determined mathematically by figuring the ratios of their logarithmic values. A visual comparison, in most cases, however, is all that is required.

SAND THICKNESS DISTRIBUTION



In making comparisons between the different isopleth maps, certain relationships between the quartile calculations, such as median size, sorting, skewness, and kurtosis are considered by most authorities to prevail. These characteristics have been illustrated in the preceding pages. In similar manner, certain relationships should exist between roundness, sphericity, and size distribution. These relationships, however, are not agreed upon by most geologists, and little information is available to prove which relationships are correct. For example, some geologists believe that as a sediment is transported, the size decreases, and the roundness and sphericity increase. Krumbein (1945, p. 1241) has shown this relationship with abrasion curves of limestone fragments. Other geologists disagree with this viewpoint and consider that, as a sediment is transported, the size decreases, the roundness increases, but the sphericity decreases. The type of evidence which supports this group is given by R. L. Erickson (1948, p. 23). In this investigation both an increase and a decrease in the median sphericity (Map 14) appear in different locations as the material is transported. The author believes in the case of deposits studied from a large body of water, such as the ocean or a large lake, that many relationships exist between the results derived from the different sedimentary methods of study.

The author also believes that those areas which appear to have a reverse relationship from what is expected, have so only because the type of geologic action being considered is the one produced by streams. Stream action is not the only geologic action to be considered in a study such as this, and if it were, even then different relationships between the sedimentary values should be expected. This is true because of the different factors existing in stream transportation, such as the turbulence and velocity of the currents. In this study the apparent reversals of relationships may be seen to exist between roundness and distance of transportation in the same areas where sphericity appears to show reverse characteristics. An example of reverse relationships will be seen by examining Wells 7 and 8 on Maps 9 and 14. It will be noted that the material probably was carried toward the east, and becomes less rounded and less spherical. If this had been ordinary stream deposition, with the material rolled along the stream bed, one would expect to find the more rounded and more spherical material carried toward the east. Depositional areas, such as the example just given, which do not agree with the expected results considered on the previous pages, are designated on the isopleth maps with half-arrowhead symbols. The trends, expressing expected depositional relationships, developed by traction in stream transportation, are pointed out with full-arrowhead symbols.

INTERPRETATIONS

Method of Deposition

To best explain why different relationships exist between the roundness, sphericity, and size distributions, and to show why one sediment, for example, is more rounded, while another is less rounded, the following information is included:

The principal method in determining how a sediment is laid down is to examine the various sorting values within the sediment; that is, the sphericity, roundness, and size sorting values. According to R. D. Russell (1939, p. 33), the most important factors involved in sorting are the size, shape, and specific gravity of the particles, and the velocity, degree of turbulence, viscosity, and specific gravity of the transporting agent. In general, it is the degree of sorting shown by a sediment, that indicates the character and effectiveness of the sorting agent. Therefore, by analyzing the degree of sorting and considering the methods by which a sediment is sorted, extremely helpful information may be obtained for determining the agent involved and the conditions of deposition in that area. By considering the different ways in which a sediment is sorted, it is possible to

understand why different relationships exist between the values presented from the various sedimentary methods of analysis.

Shape of Sand Grains

The shape of sand particles may be sorted in two ways as shown by Wadell (1932). One way is, if the movement of a grain is by suspension, the grains having a lower sphericity value will tend to concentrate down current. In this case, the grains which possess lower sphericity also have greater surface areas in relation to their volume, and therefore remain in suspension longer than the more spherical grains. If, however, the grains are moved dominantly by rolling, the more spherical grains will be transported farther, because they will roll more easily than the flatter grains, which have less sphericity. From these two types of movement, it may be seen that although grains being rolled by stream action are more common, the relationship of degree of sphericity to distance may either increase or decrease as a stream deposits sediments into a basin. It should be noted that whichever case prevails is dependent upon the velocity, viscosity, and other factors of the transporting medium. However, as a stream enters a standing body of water, its velocity and viscosity decrease, and the material is rolled from then on, thus causing the more spherical particles to be deposited farther from the shore.

If now, as G. R. MacCarthy (1933) has shown, the material is caught in suspension and moved along a beach by longshore currents, the sorting again will show an increase, but the median sphericity will show a progressive decrease in the direction of movement in the same manner as do the flatter particles being carried by the stream currents. Therefore, when considering a beach, R. E. Landon's (1930) research which shows that spherical pebbles are less stable than flat ones, is conceivable only when the direction of transportation is considered. The author wishes to point out that in 1930 when these facts were presented, very little data were available relating to the behavior of beach currents. At the present time, seasonal fluctuations of the material on beaches is believed to take place. It is therefore possible that Landon's samples were taken during the summer months when the currents were moving dominantly toward the beach.

Another geologic agent which is considered to affect the sorting by sphericity is the wind. MacCarthy (1935) has discovered that the material present in dune sands shows a higher degree of sphericity than the material found in the adjacent beach sands from which they were derived. This he ascribed to selective transportation by rolling of the more spherical grains.

Rounding of Sand Grains

Though sphericity and roundness are distinctly different properties of a sediment, Russell (1937) has shown that a rough relationship exists between the two, especially in those minerals with poor cleavage, such as quartz. Samples having a higher mean roundness usually have a higher mean sphericity than do angular grains. This is due primarily to sorting, and not abrasion. Russell (1939, p. 41) also stated that in order for a sand to have its roundness increased by abrasion, either in streams or open water currents, there must not be an abundant amount of coarse material present, even when transportation is by traction. From this evidence, Russell concludes that the most favorable sites for the rounding of sand grains are in areas of sand concentration. These areas are most commonly related to dunes and sand beaches.

Effect of Grain Size

P. Marshall's (1929) studies of beach gravels have led him to conclude that the relationships of roundness and sphericity and the laws by which they are sorted depend, in addition, on the various agents of transportation, the factors controlling them, and upon the size of the material being considered. He stated that the largest fragments

at any particular locality, if worn by abrasion, tend to become flat with rounded edges when they are above one-half inch in diameter. If below that size, they become more spherical.

Summary Interpretation

The evidence presented in this summary explains how sand grains become sorted according to roundness, sphericity, and size, and how various modes of transportation affect these properties in sediments. If this evidence is acceptable, it will be possible to explain the different relationships which appear in this investigation. As stated previously, those areas and trends of deposition designated on the isopleth maps by full-arrowhead symbols shall be considered as having been deposited by streams where the currents were such that the material in transport was rolled along the stream bottom by traction. In such areas, it should be noted that the median roundness (Map 9) and median sphericity (Map 14) increase as the material is deposited into the basin. The sorting values decrease, showing that the sand becomes better sorted (Maps 5, 11, 16) as the sediment is transported. The median size also decreases (Map 4). The skewness values either increase or decrease, depending upon the method of analysis represented (Maps 6 and 12); that is, whether the median values increase or decrease.

The best place to illustrate deposition will be seen by examining the trends in the location of Well Nos. 17, 18, and 19. Other examples of this type of deposition may be present in the northeast and northwest portions of the area.

In considering the trends which on some of the isopleth maps appear to have reverse relationship from those just considered, the evidence given in the earlier part of this section should be kept in mind. For example, the trend of deposition found around Wells 7 and 8 may be caused either from an old beach where the material was extensively worked over by wave action, by wind, or by stream action with currents strong enough to move the sand in suspension. In either case, the sand appears to have been moved in suspension because, as may be seen on Maps 9 and 14, the median roundness and sphericity decrease toward the east. Wave action is given support by the large north-south area involved between Well Nos. 7 and 8, and also by the east-west shape of the trend (Map 9). It should also be noted that in this same area the sorting increases toward the east (Maps 5 and 11). A similar pattern may be noted in the southern part of the area in the vicinity of Wells 2 and 3.

Another type of relationship may be found by examining the southeast part of the area, the eastern part of segments A, B, and

C (Map 3). In this area, the sphericity decreases while the roundness increases and the grain size decreases. Conditions of deposition in this locality may have been due to wave action and currents which moved the material by saltation in a to-and-fro motion, although, in time, toward the west. If this were true, the less-spherical material may have been carried partly in suspension and partly in contact with the bottom, in such a manner that material became more rounded and less spherical. At the same time, the currents may have decreased in power, due to a shrinking sea, and therefore the material was sorted according to size.

By examining the isopach map (Map 17), additional proof may be seen that the various trends of deposition, described previously, did exist. In comparing these trends with the other isopleth maps, it will be seen that in the areas believed to have been deposited by stream action, the sands become thicker as the material is carried into the basin. This increase and decrease in sand thickness will be explained more clearly when the history of deposition is presented in the conclusion.

In the examples given in this interpretation, those trends being considered all appear to show direct evidence of being deposited from an area above water level or very close to it. By examining the

various isopleth maps it may be seen that many of these trends of deposition appear to form pockets of sediment toward the center of the area. Note the central parts of the isopleth maps, segments D, E, and F (Map 3). These pockets have been shown by F. P. Shepard (1948) to be characteristic of offshore deposition, and are believed to be due to the action of currents and residual topographic features present on the ocean bottom.

CONCLUSION

From a study of the isopleth maps and the interpretations of the data present, it may be concluded that the environmental pattern of a sandstone may be determined by the use of statistical and mechanical methods of analysis. However, it should be realized that the interpretation of evidence and the relationships existing between the various statistical methods of analysis are the most important factors in determining the conditions of deposition during a specific interval of time.

The writer has found that, although the methods used in obtaining statistical results of roundness, shape, and size distribution are well known, information regarding the interpretation of these results and the relationships existing between them is extremely meager and lacking. At this time many erroneous concepts of offshore deposition exist. For illustration, according to Shepard (1948, p. 150), "the idea that sediments grade outward across the shelf from coarse near shore to fine at the outer edge has become so much of a geologic dogma, that it has been slow to yield ground."

Sequence of Events

The Coldwater basin of deposition was an area of marine sedimentation in which mud and carbonate materials were deposited in the deeper and quieter waters covering the western part of Michigan (Monnett, 1948, p. 682).

At the beginning of Marshall deposition, there appears to have been a crustal movement in both the Michigan basin and the adjacent lands. Although many of the surrounding highland areas may have been uplifted, the one most affecting Marshall sediments was probably the rejuvenation of the Wisconsin arch. The fine red sandstone lenses, found mostly in the lower part of the Marshall formation, are considered to be the first sands from the west to be deposited on the Coldwater shales. This change in the type of sediments deposited in western Michigan marks the beginning of Marshall deposition.

During the early part of Marshall deposition, vast amounts of sand were carried into the sea by numerous streams in each area indicated on the isopleth maps. These large amounts of sand were carried into the interior of the basin (Map 17), where they were shifted about and deposited over the sea floor, with the thickest accumulations in the low areas and the thinnest on the topographically high areas. Distribution by wave action may have been important.

By the middle of Marshall deposition what had previously been a large depositional basin throughout the Coldwater period was a shallow sea having an irregular floor, the greater part of which was subjected to wave and current action.

As the sea receded, wave action became stronger, and in many areas where stream deposition was limited, material may have been carried by wave action toward shore, where, as the sea retreated, this material was picked up and reworked by the wind to form dunes. D. W. Johnson (1925, p. 93) has shown that, where wave action increases, it is likely that sand moves toward shore from considerably greater depths.

The areas to the west of the basin continued to rise, and the climate became arid or semiarid. Continued aridity and evaporation of the shallow sea waters resulted in further restriction of the Marshall sea until the area within the basin, which may have been uplifted at the beginning of the Marshall period, became exposed. This uplifted arch, extending into the basin, east of the area investigated in this study, is also believed to be present by Kropschot (1953, p. 53). He described this uplifted area as a rejuvenation of the Kankakee arch. Kropschot believed this structure to extend in a north-south direction into the Michigan basin. From the material presented in

this investigation and illustrated on the isopleth maps, trends of sedimentation suggesting stream deposition appear to come from an eastern source which may be explained by this rejuvenated structure.

Toward the end of Marshall deposition, it is possible that the environment had become very arid throughout the area of deposition as well as in the adjacent land areas. Streams in diminishing numbers continued to drain the Wisconsin highland to the west. During the initial stage of deposition of the Michigan formation, streams carried the sand intermittently into the depositional basin. Finally the volume of the streams became so reduced that they were unable to carry sand into the area. Mud and precipitates became the primary deposits, and the Marshall period came to a close.

REFERENCES

- Cook, C. W. (1914), "Brine and Salt Deposits of Michigan," Mich. Geol. and Biol. Survey, Pub. 15, Geol. Ser. 12, p. 64.
- Erickson, R. L. (1948), "A Petrographical Investigation of the Longitudinal Deposition within the Mason Esker Relative to its Origin," Unpublished Master's Thesis, Dept. of Geology and Geography, Mich. State College, p. 23.
- Gripenberg, S. (1934), "A Study of the Sediments of the North Baltic and Adjoining Seas," Fennia, vol. 60, no. 3, p. 200.
- Hobbs, R. A. (1949), "The Application of Roundness and Sphericity Measurements to Sub-Surface Samples of the Marshall Formation of Western Michigan," Unpublished Master's Thesis, Dept. of Geology and Geography, Mich. State College, pp. 1-36.
- Johnson, D. W. (1925), Shore Processes and Shoreline Development, John Wiley and Sons, New York, p. 93.
- Kelley, T. L. (1924), Statistical Methods, London, p. 77.
- Kropschot, R. E. (1953), "A Quantitative Sedimentary Analysis of the Mississippian Deposits in the Michigan Basin," Unpublished Master's Thesis, Dept. of Geology and Geography, Mich. State College, pp. 25-53.
- Krumbein, W. C. (1936), "Application of Logarithmic Moments to Size Frequency Distribution of Sediments," Jour. Sed. Petrology, vol. 6, no. 1, pp. 35-47.
- Krumbein, W. C. (1939), "Recent Marine Sediments," Am. Assoc. Petrol. Geol., Tulsa, Oklahoma, pp. 559-91.
- Krumbein, W. C. (1941), "Measurement and Geological Significance of Shape and Roundness of Sedimentary Particles," Jour. Sed. Petrology, vol. 11, no. 2, pp. 64-72.

- Krumbein, W. C. (1945), "Recent Sedimentation and the Search for Petroleum," Am. Assoc. Petrol. Geol. Bull., vol. 29, no. 9, pp. 1233-61.
- Krumbein, W. C., and F. J. Pettijohn (1938), Manual of Sedimentary Petrography, Appleton-Century-Crofts, New York.
- Krumbein, W. C., and L. L. Sloss (1951), Stratigraphy and Sedimentation, W. H. Freeman and Co., San Francisco, pp. 70-85, 186-195.
- Landon, R. E. (1930), "An Analysis of Beach Pebble Abrasion and Transportation," Jour. Geol., vol. 38, pp. 437-46.
- MacCarthy, G. R. (1933), "The Rounding of Beach Sands," Am. Jour. Sci., 225, pp. 205-24.
- MacCarthy, G. R. (1935), "Eolian Sands: A Comparison," Am. Jour. Sci., 230, pp. 81-95.
- Marshall, P. (1929), "Beach Gravels and Sands," Trans. and Proc. New Zealand Inst., 60, part 2, pp. 324-65.
- Monnett, V. B. (1948), "Mississippian Marshall Formation of Michigan," Am. Assoc. Petrol. Geol. Bull., vol. 32, pp. 629-87.
- Perry, R. C. (1951), "An Investigation of the Effects of Sphericity and Roundness on the Permeability of Unconsolidated Sediments," Unpublished Master's Thesis, Dept. of Geology and Geography, Mich. State College, p. 10.
- Pirtle, G. W. (1932), "Michigan Structural Basin and its Relationship to Surrounding Areas," Am. Assoc. Petrol. Geol. Bull., vol. 16, pp. 145-152.
- Riley, N. A. (1941), "Projection Sphericity," Jour. Sed. Petrology, vol. 11, pp. 94-97.
- Rominger, C. (1876), "Geology of Lower Peninsula," Mich. Geol. Survey Div., vol. 3, no. 1, p. 98.

- Russell, R. D. (1939), "Effects of Transportation on Sedimentary Particles," Am. Assoc. Petrol. Geol., Tulsa, Oklahoma, pp. 33-47.
- Russell, R. D., and R. E. Taylor (1937), "Roundness and Shape of Mississippi River Sands," Jour. Geol., vol. 45, pp. 225-67.
- Schmitt, G. T. (1949), "A Petrographic Investigation of the Relationship of Deposition of Sediments in a Group of Esker's Related to the Charlotte Till Plain," Unpublished Master's Thesis, Dept. of Geology and Geography, Mich. State College, p. 47.
- Shepard, F. P. (1948), Submarine Geology, Harper and Brothers, New York.
- Stearns, M. D. (1933), "The Petrology of the Marshall Formation of Michigan," Jour. Sed. Petrology, vol. 3, no. 3, pp. 99-112.
- Trask, P. D. (1930), "Mechanical Analysis of Sediments by Centrifuge," Econ. Geology, vol. 25, pp. 581-99.
- Trask, P. D. (1932), Origin and Environment of Source Sediments of Petroleum, Houston, Texas, pp. 67ff.
- Wadell, H. (1932), "Volume, Shape, and Roundness of Rock Particles," Jour. Geol., vol. 40, pp. 443-51.
- Wadell, H. (1934), "Shape Determinations of Large Sedimentary Rock-Fragments," Pan-Am. Geol., vol. 61, pp. 187-220.
- Wadell, H. (1935), "Volume, Shape and Roundness of Quartz Particles," Jour. Geol., vol. 43, pp. 250-80.
- Wentworth, C. K. (1922), "The Shape of Beach Pebbles," U. S. Geol. Survey, Prof. Paper 131-C, pp. 75-83.

ROOM USE ONLY.

JUN 23 58

ROOM USE ONLY

~~SECRET~~ 10

MICHIGAN STATE UNIV. LIBRARIES



31293010137176